UNIVERSITY OF AMSTERDAM

UvA-DARE (Digital Academic Repository)

A search for dark matter produced in association with a dark Higgs boson decaying into a Higgs boson pair in 3b or 4b final states using pp collisions at √s = 13 TeV with the ATLAS detector

ATLAS Collaboration

DOI
10.1007/JHEP09(2025)067

Publication date
2025

Document Version
Final published version

Published in
Journal of High Energy Physics

License
CC BY

Link to publication

Citation for published version (APA):
ATLAS Collaboration (2025). A search for dark matter produced in association with a dark Higgs boson decaying into a Higgs boson pair in 3*b* or 4*b* final states using *pp* collisions at √s = 13 TeV with the ATLAS detector. *Journal of High Energy Physics*, *2025*(9), Article 067. https://doi.org/10.1007/JHEP09(2025)067

General rights
It is not permitted to download or to forward/distribute the text or part of it without the consent of the author(s) and/or copyright holder(s), other than for strictly personal, individual use, unless the work is under an open content license (like Creative Commons).

Disclaimer/Complaints regulations
If you believe that digital publication of certain material infringes any of your rights or (privacy) interests, please let the Library know, stating your reasons. In case of a legitimate complaint, the Library will make the material inaccessible and/or remove it from the website. Please Ask the Library: https://uba.uva.nl/en/contact, or a letter to: Library of the University of Amsterdam, Secretariat, P.O. Box 19185, 1000 GD Amsterdam, The Netherlands. You will be contacted as soon as possible.

UvA-DARE is a service provided by the library of the University of Amsterdam (https://dare.uva.nl)

Download date:14 sep 2026

Published for SISSA by Springer

Received: *July 4, 2025*
Accepted: *August 6, 2025*
Published: *September 8, 2025*

A search for dark matter produced in association with a dark Higgs boson decaying into a Higgs boson pair in $3b$ or $4b$ final states using pp collisions at $\sqrt{s} = 13$ TeV with the ATLAS detector

The ATLAS collaboration

E-mail: atlas.publications@cern.ch

Abstract: A search is performed for dark matter particles produced in association with a resonant pair of Higgs bosons using 140 fb^{-1} of proton-proton collisions at a centre-of-mass energy of 13 TeV recorded by the ATLAS detector at the Large Hadron Collider. This signature is expected in some extensions of the Standard Model predicting the production of dark matter particles, and is interpreted in terms of a dark Higgs model containing a Z' mediator in which the dark Higgs boson s decays into a pair of Higgs bosons. The dark Higgs boson is reconstructed through final states with at least three b-tagged jets, produced by the pair of Higgs boson decays, in events with significant missing transverse momentum consistent with the presence of dark matter. The observed data are found to be in good agreement with Standard Model predictions, constraining scenarios with dark Higgs boson masses within the range of 250 to 400 GeV and Z' mediators up to 2.3 TeV.

Keywords: Higgs Physics, Hadron-Hadron Scattering

ArXiv ePrint: 2507.02175

Open Access, © The Authors.
Article funded by SCOAP^3.

https://doi.org/10.1007/JHEP09(2025)067

JHEP09(2025)067

Contents

1 Introduction **1**

2 ATLAS detector **4**

3 Data and Monte Carlo simulations **4**

4 Event reconstruction **6**

5 Analysis strategy **7**
- 5.1 Event selection 7
- 5.2 Higgs boson reconstruction 9
- 5.3 Neural network classifier 9

6 Background estimation **12**

7 Systematic uncertainties **14**

8 Statistical interpretation **15**

9 Results **16**

10 Conclusion **20**

The ATLAS collaboration **30**

JHEP09(2025)067

1 Introduction

The existence of dark matter (DM) is widely supported by astrophysical evidence [1–4] including galactic rotation velocities of stars [5–7], gravitational lensing [8–10] and precise measurements of the cosmic microwave background [11, 12]. There is no suitable candidate in the Standard Model (SM), thus its particle nature and interactions remain key open questions in particle physics, motivating many beyond-the-SM (BSM) scenarios.

Complementary approaches are seeking evidence of dark matter particles. These include searches for direct detection of DM scattering from electrons or nuclei [13–18]; indirect searches for the product of DM annihilation or decay [19–24]; gravitational, astrophysical and cosmological probes [25, 26]; and searches for evidence of dark matter production at colliders [27–29] with particle detectors such as the ATLAS experiment [30] at the Large Hadron Collider (LHC) [31].

Collider particle physics experiments have advantages in this endeavour — they are sensitive across a wide range of types and masses of proposed DM candidates, and have the potential to characterise their interactions, making them complementary to other types of searches. One class of DM candidates is stable, electrically neutral, weakly interacting massive

particles (WIMPs), motivated by the observation that a candidate with interactions and mass of the order of the weak scale would reproduce the observed relic density [32] via the freeze-out mechanism: a paradigm known as the *WIMP miracle* [33]. Consequently colliders could be a natural place to find evidence for WIMP DM under well-controlled experimental conditions.

At colliders, it is assumed that dark matter interacts via *mediator* particles, which interact with both DM and SM particles. New mediator particles can be searched for directly, via their decay into SM particles, or may decay into DM. DM produced at colliders would not interact with the detector, and its presence must be inferred by an imbalance in the total momentum in the plane perpendicular to the collision axis. This quantity is the missing transverse momentum, with magnitude denoted $p_{\mathrm{T}}^{\mathrm{miss}}$ (or $E_{\mathrm{T}}^{\mathrm{miss}}$). Some visible radiation X must also be present to create this imbalance, creating what is known as an $X + p_{\mathrm{T}}^{\mathrm{miss}}$ signature.

This paper presents a search for dark matter produced in association with a new scalar mediator, which decays into a resonant pair of SM Higgs bosons. The decay of each Higgs boson (h) into two b-quark-initiated jets, results in a resonant $hh(\rightarrow b\bar{b}b\bar{b}) + p_{\mathrm{T}}^{\mathrm{miss}}$ signature. This signature, of large $p_{\mathrm{T}}^{\mathrm{miss}}$ consistent with the presence of DM and two Higgs bosons, is sensitive to many DM models with extended Higgs sectors or heavy (pseudo-)scalar mediators [34, 35].

To optimise and interpret the results of the search, a *dark Higgs* model is used [36]. Motivated by the Higgs mechanism for electroweak symmetry breaking in the SM, this model explains massive fermionic dark matter (χ) through a similar mass generation mechanism in the dark sector, positing a *dark Higgs* boson, (s). Such a weak-scale dark Higgs boson, interacting through mixing with the SM Higgs boson, will decay analogously to an SM Higgs boson of that mass. Thus the primary decays are into a pair of b-quarks at lower masses ($m_s < 150\,\mathrm{GeV}$), with diboson decays (WW, ZZ, hh) dominating at higher masses. Decays of s into a top quark pair can occur at low rate, whilst decays into the dark matter particles may be dominant, if kinematically allowed. An independent motivation for these models is an improved ability to reproduce the observed relic density, due to the presence of additional annihilation channels featuring the dark Higgs boson, such as $\chi\chi \rightarrow ss$, with subsequent decay of s into SM particles. This avoids the over-population common in simple or simplified models with weak-scale mediators [27]. Thus the relic density depends primarily upon the coupling between DM and s, whose SM couplings can be small, and hard to observe with traditional collider DM signatures.

The specific implementation of this model uses a two-mediator dark Higgs DM scenario, containing the dark Higgs boson, identified through its decay into hh, a new broken U(1)$'$ symmetry yielding an additional massive spin-1 Z' mediator, and a Majorana fermion DM candidate. The model parameters are the DM particle mass m_χ; the Z' mass $m_{Z'}$; the dark Higgs boson mass m_s; the Z' coupling with quarks g_q and with the DM candidate g_χ; and the mixing angle θ between the SM and dark Higgs bosons, which should be small to enable reproduction of the relic density and consistency with measurements of the Higgs boson. The dominant $q\bar{q} \rightarrow Z' \rightarrow s\chi\chi$ signal diagram for the large Z' masses explored in this paper can be found in figure 1.

A signal region is defined requiring significant $p_{\mathrm{T}}^{\mathrm{miss}}$ and at least three hadronic jets identified to contain b-hadrons (b-tagged jets). The dominant SM background processes in these regions are top quark pair production with additional radiation and Z boson production

JHEP09(2025)067

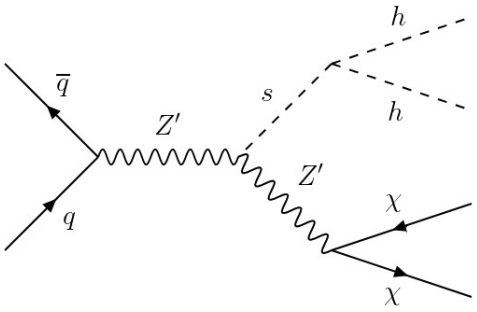

Figure 1. Representative signal diagram for resonant $q\bar{q} \to Z' \to s\chi\chi$ production with the dark Higgs boson decay $s \to hh$.

with multiple additional jets, where the Z boson decays invisibly into neutrinos. Production of W bosons and single top quarks contribute sub-dominantly. Control regions (CRs) are defined to constrain the yields of these processes in a partly data-derived approach. A neural network (NN) is trained to improve the sensitivity through greater discrimination of signal from background processes whilst preserving the shape of the invariant mass distribution of the reconstructed di-Higgs system which is fit in the analysis.

Searches in similar final states have been made for supersymmetric particle cascades in which a pair of new heavy particles decay producing multiple b-quark jets and $p_{\mathrm{T}}^{\mathrm{miss}}$, either from heavy gluino or squark decay cascades [37, 38] or electroweakino decays via the emission of Higgs bosons [39, 40]. The symmetric topology and lack of connection between the four b-quarks differs significantly from the resonant hh topology targeted in this paper. Searches for dark Higgs bosons have been made in the bb signature by the ATLAS Collaboration [41], and in WW final states by the ATLAS [42, 43] and CMS [44] Collaborations. The bb signature is sensitive to $30 < m_s < 150\,\mathrm{GeV}$, with WW sensitive from $m_s = 150\,\mathrm{GeV}$ and growing weaker with increasing m_s, motivating the exploration of the hh decay for larger m_s values.

There is complementary sensitivity from spin-1 mediator searches compatible with the Z' mediator present in the standard benchmark model used to facilitate comparisons between signatures and experiments. Care is needed in translating them into the Majorana DM dark Higgs model, but limits from dijet searches [27] are strong and place powerful constraints on TeV-mass Z' mediators, assuming the assumptions underlying the simplified models are fully realised in a more complete model, which may not be the case. Generally, the balance of the resonant and $p_{\mathrm{T}}^{\mathrm{miss}}$ signatures depends strongly upon the choice of the couplings g_q and g_χ, and the model is not strongly constrained. Reprodution of the observed relic density tends to favour larger g_χ values [36, 41], emphasising the importance of the $X + p_{\mathrm{T}}^{\mathrm{miss}}$ signatures.

The paper is organised as follows: section 2 describes the ATLAS detector, whilst section 3 details the collision data and simulation used in the analysis. Section 4 documents the object reconstruction and event selections used. The analysis strategy is outlined in section 5, before section 6 explains how background processes are estimated. The systematic uncertainties evaluated on data and simulations are detailed in section 7, and the statistical treatment of the data in section 8. The analysis results are reported in section 9; section 10 provides a conclusion.

JHEP09(2025)067

2 ATLAS detector

The ATLAS experiment [30] at the LHC is a multipurpose particle detector with a forward-backward symmetric cylindrical geometry and a near 4π coverage in solid angle.[1] It consists of a tracking inner detector (ID) surrounded by a thin superconducting solenoid providing a 2 T axial magnetic field, electromagnetic and hadronic calorimeters, and a muon spectrometer. The inner tracking detector covers the pseudorapidity range $|\eta| < 2.5$. It consists of silicon pixel, silicon microstrip, and transition radiation tracking detectors. Lead/liquid-argon (LAr) sampling calorimeters provide electromagnetic (EM) energy measurements with high granularity within the region $|\eta| < 3.2$. A steel/scintillator-tile hadronic calorimeter covers the central pseudorapidity range ($|\eta| < 1.7$). The endcap and forward regions are instrumented with LAr calorimeters for EM and hadronic energy measurements up to $|\eta| = 4.9$. The muon spectrometer surrounds the calorimeters and is based on three large superconducting air-core toroidal magnets with eight coils each. The field integral of the toroids ranges between 2.0 and 6.0 T m across most of the detector. The muon spectrometer includes a system of precision tracking chambers up to $|\eta| = 2.7$ and fast detectors for triggering up to $|\eta| = 2.4$. The luminosity is measured mainly by the LUCID-2 [45] detector, which is located close to the beampipe. A two-level trigger system is used to select events [46]. The first-level trigger is implemented in hardware and uses a subset of the detector information to accept events at a rate below 100 kHz. This is followed by a software-based trigger that reduces the accepted event rate to 1.25 kHz on average depending on the data-taking conditions. A software suite [47] is used in data simulation, in the reconstruction and analysis of real and simulated data, in detector operations, and in the trigger and data acquisition systems of the experiment.

3 Data and Monte Carlo simulations

The proton-proton collisions analysed were collected by the ATLAS detector between 2015 and 2018, at a centre-of-mass energy of $\sqrt{s} = 13$ TeV and a 25 ns inter-bunch spacing. They correspond to an integrated luminosity of 140 fb^{-1}, with an uncertainty of 0.83% [48] obtained using the LUCID-2 detector [45] for the primary luminosity measurements, complemented by measurements using the inner detector and calorimeters, after requiring all detector systems to be recording good quality data [49].

Unprescaled $p_{\mathrm{T}}^{\mathrm{miss}}$ triggers were used [50] to select events for the analysis. The $p_{\mathrm{T}}^{\mathrm{miss}}$ thresholds ranged from 70 GeV to 110 GeV, for a $p_{\mathrm{T}}^{\mathrm{miss}}$ definition in which muons are treated as invisible. The offline $p_{\mathrm{T}}^{\mathrm{miss}}$ selection, which does not treat muons as invisible, was kept more stringent than the trigger-level requirement to ensure that trigger efficiencies are constant.

Dark Higgs Monte Carlo (MC) simulated events were generated, as detailed in table 1, using consistent parameter choices with other analyses [41–44] and simplified dark matter models: the dark matter mass m_χ is fixed at 200 GeV, its coupling constant is set as $g_\chi = 1$,

[1] ATLAS uses a right-handed coordinate system with its origin at the nominal interaction point (IP) in the centre of the detector and the z-axis along the beam pipe. The x-axis points from the IP to the centre of the LHC ring, and the y-axis points upwards. Polar coordinates (r, ϕ) are used in the transverse plane, ϕ being the azimuthal angle around the z-axis. The pseudorapidity is defined in terms of the polar angle θ as $\eta = -\ln\tan(\theta/2)$ and is equal to the rapidity $y = \frac{1}{2}\ln\left(\frac{E+p_z}{E-p_z}\right)$ in the relativistic limit. Angular distance is measured in units of $\Delta R \equiv \sqrt{(\Delta y)^2 + (\Delta\phi)^2}$.

JHEP09(2025)067

Physics process	Generator (ME)	Parton shower (PS)	Order in $\alpha_s(+\alpha_{EW})$	Tune	PDF (ME)	PDF (PS)
Dark Higgs signals	MadGraph5_aMCNLO 2.9.9 [65]	Pythia 8.307 [66]	LO	A14 [67]	NNPDF2.3LO [63]	NNPDF2.3LO
$Z(\to \nu\nu)+$jets	Sherpa 2.2.1 [68, 69]	Sherpa[2.2.1]	NNLO [70]	Sherpa default [71]	NNPDF[3.0NNLO] [72]	NNPDF 3.0NNLO
$W(\to \ell\nu)+$jets	Sherpa 2.2.1	Sherpa 2.2.1	NNLO	Sherpa default	NNPDF 3.0NNLO	NNPDF 3.0NNLO
Diboson	Sherpa 2.2.1	Sherpa 2.2.1	NLO	Sherpa default	NNPDF 3.0NNLO	NNPDF 3.0NNLO
Triboson	Sherpa 2.2.14	Sherpa 2.2.14	NLO	Sherpa default	NNPDF 3.0NNLO	NNPDF 3.0NNLO
$t\bar{t}$	Powheg Box v2 [73–76]	Pythia 8.230 [77]	NNLO+NNLL [78]	A14	NNPDF[3.0NLO] [72]	NNPDF2.3LO
Single top	Powheg Box v2	Pythia 8.230	NLO [79, 80]	A14	NNPDF 3.0NLO	NNPDF2.3LO
ttW/ttZ	MadGraph5_aMCNLO 2.3.3	Pythia 8.210	NLO	A14	NNPDF 3.0NLO	NNPDF2.3LO
Four-top	MadGraph5_aMCNLO 2.2.2	Pythia 8.186 [62]	NLO	A14	NNPDF2.3LO	NNPDF2.3LO
ttH	Powheg Box v2	Pythia 8.230	NLO	A14	NNPDF 3.0NLO	NNPDF2.3LO
VH	Pythia 8.186	Pythia 8.186	NNLO+NLO [81–87]	A14	PDF4LHC15NLO [88]	PDF4LHC15NLO

Table 1. Simulated event samples with the corresponding matrix element and parton shower generators, cross-section order in α_s (and α_{EW} where corrections are available) used to normalise the event yield, underlying-event set of tuned parameters and the generator PDF sets used. The abbreviation (N)NLO stands for (next-to-)next-to-leading-order, and NNLL stands for next-to-next-to-leading-logarithm.

the coupling between the SM quarks and the Z' is fixed at $g_q = 0.25$ [51, 52] and the mixing angle between the SM and dark Higgs bosons is set to $\sin\theta = 0.01$. Samples of MC simulated events are generated for 106 mass points covering a range of $m_{Z'}$ and m_s values. To consider the region where the Z' is heavy enough to decay into two dark matter particles and is light enough to have a sufficient production cross-section for sensitivity, $420\,\text{GeV} < m_{Z'} < 3300\,\text{GeV}$ is chosen. The range $251\,\text{GeV} < m_s < 435\,\text{GeV}$ is chosen to probe the region where s is heavy enough to decay into two SM Higgs bosons and light enough that the decay into two dark matter particles in this benchmark is not overwhelming. Larger DM masses will have generally smaller Z' and s production cross-sections, with $s \to \chi\chi$ decays becoming dominant at larger m_s and a different predicted relic density. For all generated signal events, the detector response is simulated [53] using a fast parametrised simulation of the calorimeters [54], and the full Geant4 [55] simulation for the other sub-detectors.

The dominant SM background processes are $t\bar{t}$ production with additional radiation, and $Z(\to \nu\nu)+$jets. Subdominant background processes are single top (Wt) production and $W(\to \ell\nu)+$jets. Smaller background processes include other multi-top processes hereinafter grouped as $t\bar{t}+X$ (ttW, ttZ, ttH, four-top production), and diboson (WW, WZ, ZZ) production. Triboson production and VH production were also considered and found to be negligible. All SM processes are modelled using MC simulations, processed through a full simulation of the ATLAS detector [53] based on Geant4 [55]. All samples used (signal and SM) are listed in table 1 along with the relevant parton distribution function (PDF) sets used for the matrix element (ME) and parton shower (PS), the configuration of underlying-event and hadronisation parameters (tune), and the cross-section order in α_s (and α_{EW} where corrections are available) used to normalise the event yields for these samples. Further information about the ATLAS simulations of $t\bar{t}$, single top, multi-boson and vector-boson plus jets processes can be found in refs. [56–60]. The decays of bottom and charm hadrons were simulated using the EvtGen 1.6.0 program [61] for the samples not generated with Sherpa. The effect of pile-up in the same and neighbouring bunch crossings was modelled by overlaying the simulated hard-scattering event with inelastic proton-proton events generated with Pythia 8.186 [62] using the NNPDF2.3LO leading-order PDF set [63] and the A3 set of tuned parameters [64]. The MC samples were reweighted so that the distribution of the average number of interactions per bunch crossing reproduces the observed distribution in the data.

JHEP09(2025)067

The $t\bar{t}$ processes are categorised based on the true flavour content of the jets in the events. An event is labelled as $t\bar{t}+ \geq 1b$ if three or more jets are associated with b-hadrons. Events with two b-jets and at least one c-hadron are labelled as $t\bar{t}+ \geq 1c$ while all remaining events are categorised as $t\bar{t}$ + light.

4 Event reconstruction

For the particle candidate objects used in this analysis, two distinct categories are defined. These differ in the stringency of their reconstruction requirements, and have different uses in the analysis. `Baseline` objects are used to construct the events' $p_{\mathrm{T}}^{\mathrm{miss}}$. After this, an overlap removal procedure is applied to deal with potential ambiguities between particle candidates. Finally `Signal` objects are defined with additional reconstruction requirements, which are used for the analysis region selections.

All events are required to have a primary vertex. Primary vertices are reconstructed from at least two charged-particle tracks with transverse momentum $p_{\mathrm{T}} > 0.5\,\mathrm{GeV}$, measured in the ID [89]. The hard-scatter vertex is defined as the primary vertex with the largest sum of squared track momenta.

Hadronic jets are reconstructed from particle flow objects [90], using the anti-k_t algorithm [91, 92] with a radius parameter of $R = 0.4$. These are calibrated using a multi-step procedure as outlined in ref. [93]. `Baseline` jets are required to have $p_{\mathrm{T}} > 20\,\mathrm{GeV}$ and $|\eta| < 2.8$ to be considered in the analysis. To suppress jets originating from pile-up, a Jet Vertex Tagger (`JVT`) is used; this is a likelihood-based algorithm described in ref. [94]. `Baseline` jets with $20 < p_{\mathrm{T}} < 60\,\mathrm{GeV}$ and $|\eta| < 2.4$ are required to satisfy a selection on the `JVT` with a 0.90–0.96 probability of correctly identifying hard-scatter jets depending on the p_{T}. Outside of this p_{T} range, no `JVT` requirement is applied. `Signal` jets are formed from the `Baseline` jets which pass the overlap removal procedure, and are additionally required to satisfy an increased p_{T} requirement of 25 GeV.

For both `Baseline` and `Signal` jets, those likely to originate from a b-quark are identified using a deep neural network-based algorithm (`DL1r`) [95]. This is applied to jets with $p_{\mathrm{T}} > 20\,\mathrm{GeV}$ and $|\eta| < 2.5$, with a 77% probability to identify jets containing b-hadrons, as measured in MC simulations of $t\bar{t}$ processes. The algorithm has a probability of 0.5% (18%) of misidentifying light-flavour (charm) jets, as determined in a sample of simulated $t\bar{t}$ events. The b-tagging efficiencies in simulated events are corrected to match those measured in data [96–98].

`Baseline` electrons (muons) are required to have $|\eta| < 2.47$ ($|\eta| < 2.7$) and $p_{\mathrm{T}} > 8\,\mathrm{GeV}$, and to satisfy the `Loose` likelihood-based identification working point defined in ref. [99] (`Medium` identification working point as defined in ref. [100]). `Signal` electron and muon candidates are defined to place a stringent veto on events with any prompt leptons, to reduce SM backgrounds, and `Signal` muons are used in the estimate of the Z-boson background. These are required to fulfil the following additional requirements and the overlap removal procedure must be passed. The significance of the transverse impact parameter d_0 must obey $d_0/\sigma(d_0)$ less than 5 (3), for electrons (muons). `Signal` electrons are required to satisfy the `Loose` isolation working point of ref. [99] to reduce contamination from semileptonic hadron decays and jets misidentified as electrons. `Signal` muons are required to satisfy

JHEP09(2025)067

the `Tight` isolation working point of ref. [100] to reduce contamination from semileptonic heavy flavour and hadron decays.

The overlap removal procedure is applied to `Baseline` electrons (e), muons (μ) and jets (j). Individual overlap removals are done in the following sequence of steps, in which objects are considered at a given step only if they were not removed in a previous step. Firstly, if a muon shares an ID track with an electron, the electron is removed. Secondly, if $\Delta R(j, e) < 0.2$ the jet is removed. For any surviving jets, if $\Delta R(j, e) < \min(0.4,\, 0.04 + 10\,\text{GeV}/p_{\text{T}}^{e})$, the electron is removed. Penultimately, if $\Delta R(j, \mu) < 0.2$ or the muon ID track is ghost associated[2] with the jet, then the jet is removed if the jet has less than three associated tracks with $p_{\text{T}} > 0.5\,\text{GeV}$. Finally, for any surviving jets, if $\Delta R(j, \mu) < \min(0.4, 0.04 + 10\,\text{GeV}/p_{\text{T}}^{\mu})$, the muon is removed.

The missing transverse momentum ($\boldsymbol{p}_{\text{T}}^{\text{miss}}$) of the event is defined as the negative vector sum of the $\boldsymbol{p}_{\text{T}}$ of all selected and calibrated `Baseline` physics objects in the event before the overlap removal procedure, with an extra term added to account for soft energy in the event which is not associated with any of the selected objects. This soft term is calculated from inner detector tracks matched to the primary vertex. The magnitude of the missing transverse momentum vector is denoted $p_{\text{T}}^{\text{miss}}$. The `Loose` $p_{\text{T}}^{\text{miss}}$ working point is used, as defined in ref. [101]. The object-based $p_{\text{T}}^{\text{miss}}$ significance ($\mathcal{S}(p_{\text{T}}^{\text{miss}})$), defined in ref. [101], is also used in the analysis. This is an estimate of how genuine the $p_{\text{T}}^{\text{miss}}$ in the event is, originating from neutrinos or potential dark matter candidates, in contrast to 'fake' $p_{\text{T}}^{\text{miss}}$ originating from the finite detector acceptance and resolution, pile-up and object mismeasurement. It is calculated by dividing the $p_{\text{T}}^{\text{miss}}$ by a measure of its resolution, built from the resolutions of the objects from which the $p_{\text{T}}^{\text{miss}}$ is constructed.

5 Analysis strategy

5.1 Event selection

The signal is characterised by large $p_{\text{T}}^{\text{miss}}$ from the DM particle production and substantial hadronic activity from $s \to hh$ decays resulting in four b-quark jets with an invariant mass consistent with m_s. Events considered for the search must fulfil a set of 'preselection' requirements summarised in table 2. To target the signal's final state, events are required to contain no `Signal` leptons (n_{leptons}) and between four and seven `Signal` jets (n_{jets}), at least three of which must be b-tagged. The loose upper requirement on n_{jets} reduces backgrounds with many additional jets, including top quark processes. Requiring the events' $p_{\text{T}}^{\text{miss}}$ to be greater than 200 GeV ensures the selected trigger is fully efficient over the complete data-taking period, and effectively targets the high $p_{\text{T}}^{\text{miss}}$ signature for the range of DM masses considered. To reduce background contributions from QCD multijet processes, $\Delta\phi_{\text{min}}^{4j}$ — the minimum azimuth between any of the event's four highest p_{T} jets and the $\boldsymbol{p}_{\text{T}}^{\text{miss}}$— is required to be greater than 0.4. The variable $m_{\text{T,min}}^{b}$, defined as:

$$m_{\text{T,min}}^{b} = \min_{1 \le i \le 3} \sqrt{(p_{\text{T}}(b_i) + p_{\text{T}}^{\text{miss}})^2 - (p_{\text{x}}(b_i) + p_{\text{x}}^{\text{miss}})^2 - (p_{\text{y}}(b_i) + p_{\text{y}}^{\text{miss}})^2},$$

[2] Ghost association consists of repeating the anti-k_t jet clustering process with the addition of 'ghost' versions of the muon's track with the same direction but infinitesimal p_{T}. A muon is ghost-associated if it is contained within the re-clustered jet.

JHEP09(2025)067

Variable	Requirement
n_{leptons}	0
n_{jets}	$[4, 7]$
$n_{b\text{-jets}}$	≥ 3
$p_{\text{T}}^{\text{miss}}$ [GeV]	> 200
$\Delta\phi_{\text{min}}^{4j}$	> 0.4
$m_{\text{T,min}}^{b}$ [GeV]	> 80
$\mathcal{S}(p_{\text{T}}^{\text{miss}})$	> 7
m_{T}^{4b} [GeV]	> 300

Table 2. Definition of the event preselection requirements, used to select the final states of interest.

where i indexes the three highest-p_{T} b-tagged jets in the event, has an approximate upper bound at the mass of a particle with decay products including a b-tagged jet and $p_{\text{T}}^{\text{miss}}$, such as a semileptonic top quark decay in which the lepton is not reconstructed. It is thus generally smaller for SM background processes than the signal. The optimal event requirement was found to be $m_{\text{T,min}}^{b}$ larger than 80 GeV. To reduce backgrounds with fake $p_{\text{T}}^{\text{miss}}$ such as QCD multijet processes, events must have a $\mathcal{S}(p_{\text{T}}^{\text{miss}})$ greater than 7. Finally, the transverse mass of the di-Higgs system and $p_{\text{T}}^{\text{miss}}$ must exceed 300 GeV to target events consistent with a heavy Z' decay.

To discriminate further between the signals and SM backgrounds, an NN classifier is used, as detailed in section 5.3, which produces a probability score for events ranging from 0 (highly background compatible) to 1 (highly signal compatible). For all the search regions in the analysis, the events' NN output score is required to be greater than 0.95 to maximise sensitivity to the dark Higgs signals whilst keeping sufficient event yields to maintain the clear resonant peak signature expected in the signal in the di-Higgs invariant mass (m_{hh}). For the dark Higgs model this corresponds to the reconstructed m_s, and has a resonance peak in its distribution.

Two sets of search regions are defined in table 3, which both exploit m_{hh} to distinguish the signals from the SM backgrounds. Firstly, a binned signal region (`SR`), optimised for sensitivity to the dark Higgs signal resonances, is used to test the signal hypotheses in multi-bin profile likelihood fits over m_{hh}. The m_{hh} distribution is binned with the set of lower edges: $[100, 200, 250, 300, 350, 400, 450, 500, 700]$ GeV, with the final bin ending at 900 GeV. The binning is chosen to reflect the mass resolution of the dark Higgs signal and there are no yields in data or MC simulation above 900 GeV. The overall acceptance times efficiency for the dark Higgs signals to enter the `SR` varies from 1.5% to 6.9% across the parameter space considered. Secondly, a set of single bin regions (`DRa-DRg`) is used to perform individual discovery fits testing the SM-only hypothesis and set limits on the possible number of BSM events with this detector signature. These are each defined in a given range of m_{hh}. These overlapping regions are chosen to cover a range of possible BSM particle masses, contain sufficient expected event yields, and reflect the expected mass resolution. Whilst the $4b$ final state is the most sensitive at preselection level, the larger event samples in the $3b$ regions benefit most from the NN discrimination, such that both contribute and a categorisation in b-tagged jet multiplicity does not enhance the sensitivity.

JHEP09(2025)067

Region	Variable requirement	
	NN score	m_{hh} [GeV]
SR	≥ 0.95	$[100, 900]$
DRa	≥ 0.95	$[100, 250)$
DRb		$[200, 300)$
DRc		$[250, 350)$
DRd		$[300, 400)$
DRe		$[350, 450)$
DRf		$[400, 900)$
DRg		$[500, 900)$

Table 3. Search region event requirements supplementing the preselection defined in table 2.

5.2 Higgs boson reconstruction

The fully visible final state of the dark Higgs boson decay allows its mass to be reconstructed, providing an effective discriminant between the signal process and SM backgrounds. This relies first on selecting the four jets from the two SM Higgs boson decays from which the invariant mass ($m_{4j} = m_{hh}$) can be calculated. If there are at least four b-tagged jets in the event, the four b-tagged jets with the largest transverse momenta are selected. If there are three b-tagged jets, and the mass of one of these is greater than 100 GeV, then it is assumed to be a 'merged' jet formed from two Higgs boson decay products being collimated, and used in addition to the other two b-tagged jets. If the mass threshold is not met by any of the b-tagged jets, then the fourth jet is chosen from the remaining untagged jets. This jet is chosen to minimise the mass of the heaviest possible Higgs boson candidate constructed from any two of the set containing the three b-tagged jets (α, β, γ) and the considered light jets (j):

$$\min_{j} \Big[\max_{\alpha,\beta,\gamma} \Big(m_{\alpha\beta}, m_{\gamma j} \Big) \Big].$$

The kinematic properties of the SM Higgs boson candidates are also useful for discriminating between the signal and backgrounds and are used as input features to the NN. To reconstruct these, the four jets must be paired to form two Higgs bosons. When there is a merged jet present, it is chosen as one Higgs boson candidate, whilst the other two jets form the second Higgs boson candidate. Otherwise, the four jets ($j = 1, 2, 3, 4$) are paired to minimise the greatest angular separation between the Higgs boson candidates decay products (jets i, k, l, m). This is expressed as:

$$\min(\Delta R_{\max}(b, b)) = \min_{i,k,l,m \in j}(\max(\Delta R(i, k), \Delta R(l, m))).$$

The two Higgs boson candidates are then numbered in descending p_{T}.

5.3 Neural network classifier

The supervised NN classifier is trained on events satisfying the preselection requirements defined in table 2. For the signal training set, simulated MC events for all signal models are combined (using the same number of events per model, randomly sampled such that the

JHEP09(2025)067

4.3×10^5 signal training set size is equal to that of the background training set), to maintain sensitivity across the model parameter space of interest. For the background training set, all MC simulated events of the SM background processes were used as they provided a good match to the expected weighted background composition satisfying the analysis preselection. To avoid overtraining and benefit from the full set of available events, orthogonal training and testing/validation datasets are used, through a k-fold splitting procedure with $k = 5$ [102]. The datasets are split randomly into five subsets and five NNs are trained, such that the network trained on four fifths of the events is applied to the other fifth of the events in the analysis, and the full statistical power of the simulated MC datasets can be conserved.

The kinematic input features used in the NN are listed and defined in table 4. These were selected from a wider set as the kinematic variables that provided the best signal-background discrimination and improved the NN performance, either alone or in combination with other variables. The NN can exploit correlations between variables to enhance discrimination power, particularly when the correlations between the variables are different for signal and background events. The impact of each variable was also quantified using Shapley values [103] (a common measure to assess how impactful an input feature is on the classifier output). Variables which had high Shapley values, and led to a reduced NN performance if they were removed from training, were retained. Finally, more complex compound kinematic variables were considered and evaluated, again using their Shapley values. These variables were generated using the Python `featuretools` [104] package, which combines pairs of variables from the existing list using basic arithmetic operations. The compound variables with high Shapley values, and which improved NN performance if they were added, were included in the training. Whilst these variables are correlated with the existing input features, they can help the NN to converge more quickly, focus more on more important properties, and learn finer details in the data sample.

A feed-forward neural network architecture is used. The NN has 8 fully connected hidden layers, with 1024 hidden nodes in the first layer and the number of hidden nodes halving repeatedly in each subsequent layer. Training is performed in batches, with a batch size of 4096. Rectified linear unit (ReLU) activation [105, 106], batch normalisation [107], an Adam [108] optimiser with weight decay, and dropout regularisation [109] (with a dropout rate of 0.2) are used between layers. An initial learning rate of 5×10^{-6} is used, with a learning rate scheduler that halves the learning rate every five epochs. The network is trained for 25 epochs; that with the lowest validation loss is used in the analysis. As the signal regions in the analysis rely on the m_{hh} distribution alongside high NN score values, it is important that the NN does not sculpt or bias the background m_{hh} distribution to a more signal compatible shape. To prevent this, the loss function used contains not only a standard binary cross-entropy term L_{BCE}, but also a distance correlation term $\mathcal{R}$ defined between vectors X and Y as:

$$\mathcal{R}^2(X,Y) = \begin{cases} \frac{\mathcal{V}^2(X,Y)}{\sqrt{\mathcal{V}(X,X)\mathcal{V}(Y,Y)}}, & \text{if } \mathcal{V}^2(X)\mathcal{V}^2(Y) > 0, \\ 0, & \text{otherwise,} \end{cases}$$

where

$$\mathcal{V}^2(X,Y) = \langle |X - X'||Y - Y'| \rangle + \langle |X - X'| \rangle \langle |Y - Y'| \rangle - 2\langle |X - X'||Y - Y''| \rangle,$$

JHEP09(2025)067

Variable	Definition
$p_{\mathrm{T}}^{\mathrm{miss}}$	Missing transverse momentum.
$\mathcal{S}(p_{\mathrm{T}}^{\mathrm{miss}})$	Object-based $p_{\mathrm{T}}^{\mathrm{miss}}$ significance.
$m_{\mathrm{T,min}}^{b}$	Minimum transverse mass of $p_{\mathrm{T}}^{\mathrm{miss}}$ and any of the b-jets in the event.
m_{T}^{4b}	Transverse mass of the di-Higgs system and $p_{\mathrm{T}}^{\mathrm{miss}}$.
m_{h1}	Mass of the higher-p_{T} Higgs boson candidate.
m_{h2}	Mass of the lower-p_{T} Higgs boson candidate.
H_{T}	Scalar sum of p_{T} of `Signal` jets.
p_{T}^{4b}	p_{T} of the reconstructed di-Higgs system.
$p_{\mathrm{T}}(b_1)$	Transverse momentum of the highest p_{T} $b-$jet.
$p_{\mathrm{T}}(b_2)$	Transverse momentum of the second-highest p_{T} $b-$jet.
p_{T}^{j4}	Transverse momentum of the fourth-highest p_{T} jet.
$\Delta R(b_{h1}^1, b_{h1}^2)$	ΔR between the two jets associated with the higher-p_{T} Higgs boson candidate.
$\Delta R(b_{h2}^1, b_{h2}^2)$	ΔR between the two jets associated with the lower-p_{T} Higgs boson candidate.
$\Delta R_{\mathrm{min}}(b,b)$	min $\Delta R(b_i, b_j)$ for all b-jet pairs i and j in the event.
$\Delta\eta_{\mathrm{max}}(b,b)$	max $\Delta\eta(b_i, b_j)$ for all b-jet pairs i and j in the event.
n_{jets}	Number of `Signal` jets in the event.
$n_{b\text{-jets}}$	Number of b-jets in the event.
$p_{\mathrm{T}}^{\mathrm{miss}}/\sqrt{H_{\mathrm{T}}}$	Event-based (rather than object-based) estimate of $\mathcal{S}(p_{\mathrm{T}}^{\mathrm{miss}})$.
$p_{\mathrm{T}}^{\mathrm{miss}}/p_{\mathrm{T}}^{4b}$	The ratio of $p_{\mathrm{T}}^{\mathrm{miss}}$ and p_{T}^{4b}.
$n_{\mathrm{jets}}/n_{b\text{-jets}}$	The ratio of the `Signal` jet and b-jet multiplicities.
$n_{\mathrm{jets}} - n_{b\text{-jets}}$	The number of `Signal` jets in the event not b-tagged.
$p_{\mathrm{T}}(b_1)/n_{\mathrm{jets}}$	The ratio of the p_{T} of the highest p_{T} jet and the event's `Signal` jet multiplicity.
$\mathcal{S}(p_{\mathrm{T}}^{\mathrm{miss}})/n_{b\text{-jets}}$	The ratio of $p_{\mathrm{T}}^{\mathrm{miss}}$ significance and the number of b-jets in the event.
$\mathcal{S}(p_{\mathrm{T}}^{\mathrm{miss}}) \times p_{\mathrm{T}}^{4b}$	The product of $p_{\mathrm{T}}^{\mathrm{miss}}$ significance and the p_{T} of the di-Higgs system.
$\Delta R_{\mathrm{min}}(b,b)/p_{\mathrm{T}}^{\mathrm{miss}}$	The ratio of $\Delta R_{\mathrm{min}}(b,b)$ and $p_{\mathrm{T}}^{\mathrm{miss}}$.
$\Delta\eta_{\mathrm{RMS}}(b,b) \times \Delta\eta_{\mathrm{max}}(b,b)$	The product of RMS $\Delta\eta(b_i, b_j)$ and max $\Delta\eta(b_i, b_j)$ for all b-jet pairs i and j in the event.
$\Delta R_{\mathrm{min}}(b,b) \times p_{\mathrm{T}}(b_2)$	The product of $\Delta R_{\mathrm{min}}(b,b)$ and the second-highest b-tagged jet p_{T}.
`xwt`	min $\sqrt{\left(\frac{m_W^i - 80.4\,\mathrm{GeV}}{0.1 m_W^i}\right)^2 + \left(\frac{m_t^i - 172.5\,\mathrm{GeV}}{0.1 m_t^i}\right)^2}$, for i in the top quark and W-boson candidates in the event. Top quark candidates are defined through a W-boson candidate and b-tagged jet such that each jet from a Higgs boson decay represents the b-jet from the top decay. W-boson candidates are defined from pairs of the event's remaining jets, where at most one is associated with a Higgs boson (as hadronic W decays are likely to produce at least one light jet). The 0.1 approximates the fractional mass resolution for the reconstructed particle candidate hypotheses.

Table 4. Neural network input features and their definitions.

following refs. [110] and [111]. These are combined thus [111]:

$$L_{\mathrm{total}}(\hat{Y}, Y) = \alpha L_{\mathrm{BCE}}(\hat{Y}, Y) + (1 - \alpha)\mathcal{R}(\hat{Y}, m_{hh}),$$

where Y is the vector of true signal or background labels for the events, and $\hat{Y}$ the predictions. The optimal value of α was found to be 0.7, providing successful mass decorrelation and good training and classification performance.

Some example distributions of discriminating kinematic variables important to the NN are shown in figure 2. Figures 2(a) and 2(b) show the $p_{\mathrm{T}}^{\mathrm{miss}}$ and $\mathcal{S}(p_{\mathrm{T}}^{\mathrm{miss}})$ distributions. The illustrated signals demonstrate the large $p_{\mathrm{T}}^{\mathrm{miss}}$ and $\mathcal{S}(p_{\mathrm{T}}^{\mathrm{miss}})$ generated by the dark matter production, in comparison with the rapidly dropping distributions for SM processes,

JHEP09(2025)067

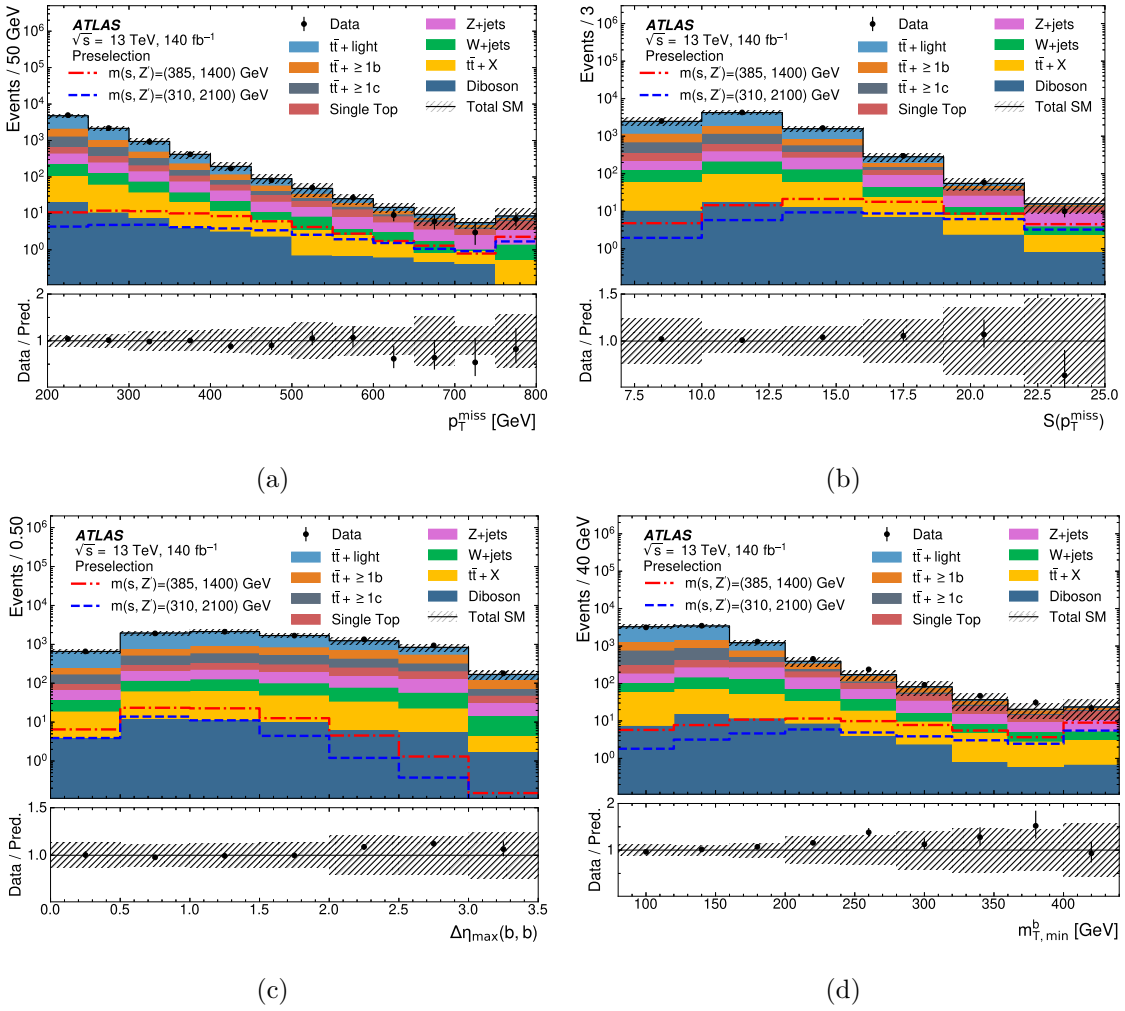

Figure 2. In the top panel of each plot, distributions of important kinematic variables in the NN training are given: (a) $p_{\mathrm{T}}^{\mathrm{miss}}$, (b) $p_{\mathrm{T}}^{\mathrm{miss}}$ significance, (c) $\Delta\eta_{\mathrm{max}}(b,b)$ and (d) $m_{\mathrm{T,min}}^{b}$. The preselection requirements (defined in table 2) are applied and the background, benchmark signals and data distributions are shown, before any fit is performed. The uncertainty band on the background includes all systematic and MC statistical uncertainties. In the bottom panels the ratio of data to background is shown. The final bin in each distribution includes overflow.

particularly $t\bar{t}$ processes. The $\Delta\eta_{\mathrm{max}}(b,b)$ distribution in figure 2(c) demonstrates the discrimination resulting from the closer proximity of the b-tagged jets in the signal process compared with those in the background processes. The $m_{\mathrm{T,min}}^{b}$ distribution (figure 2(d)) connects the $p_{\mathrm{T}}^{\mathrm{miss}}$ and b-tagged jets: for semileptonic top quark decays it is constrained to lie within m_t, whereas at high values processes with additional or independent sources of $p_{\mathrm{T}}^{\mathrm{miss}}$ are increasingly dominant.

6 Background estimation

After the preselection and search region NN score requirements, the dominant SM background processes remaining include $t\bar{t}$ with additional radiation and $Z+$jets production with multiple

JHEP09(2025)067

Variable	CRZ Requirement
n_μ	$= 2$
n_{jets}	$[4, 7]$
$n_{b\text{-jets}}$	≥ 3
$\Delta\phi^{4j}_{\text{min}}$	> 0.4
$p_{\text{T}}^{\text{miss}-\mu}$ [GeV]	> 200
$p_{\text{T}}^{\text{miss}-\mu}/\sqrt{H_{\text{T}}}$ [$\sqrt{\text{GeV}}$]	> 7
$m^{b-\mu}_{\text{T,min}}$ [GeV]	> 80
$p_{\text{T}}^{\text{miss}}$ [GeV]	< 75
$\lvert m_{\mu\mu} - m_Z \rvert$ [GeV]	< 15

Table 5. Selection for $Z+$jets control region.

additional jets. The $t\bar{t}$ backgrounds are divided into distinct processes depending on the flavour of the jets produced in association with the $t\bar{t}$ process: $t\bar{t}+$light, $t\bar{t}+\geq 1b$ (which are both large) and $t\bar{t}+\geq 1c$ (which is smaller). The $Z+$jets, $t\bar{t}+$light and $t\bar{t}+\geq 1b$ backgrounds are estimated by using MC simulated events and dedicated control regions are defined to improve their modelling and provide normalisation factors derived from data. These control regions are designed to be kinematically similar to the search regions, reasonably pure in the relevant background processes and low in signal contamination.[3] Sub-dominant background contributions come from $W+$jets, single top, $t\bar{t}+X$ and diboson production processes. These, and the $t\bar{t}+\geq 1c$ background, are estimated with MC simulated events. The QCD multijet background satisfying the preselection requirements is negligible.

The $Z+$jets process entering the search regions consists primarily of $Z\to\nu\nu$ decays. To obtain a high purity control region, a $Z\to\mu\mu$ selection is used. This event sample is kinematically analogous to the signal process, contains high-p_{T} Z bosons orthogonal to the signal regions, and is treated identically by the $p_{\text{T}}^{\text{miss}}$ triggers, which consider muons to be invisible. So that the $Z\to\mu\mu$ events emulate the $Z\to\nu\nu$ events in the search regions, their missing transverse momentum is calculated treating the muons as invisible, termed $p_{\text{T}}^{\text{miss}-\mu}$. The control region definition starts by altering the standard preselection to require two `Signal` muons, and using $p_{\text{T}}^{\text{miss}-\mu}$ instead of $p_{\text{T}}^{\text{miss}}$ for the 200 GeV selection and $m^{b}_{\text{T,min}}$ calculation ($m^{b-\mu}_{\text{T,min}}$). An event-based proxy of the muon-corrected missing transverse momentum significance is used ($p_{\text{T}}^{\text{miss}-\mu}/\sqrt{H_{\text{T}}}$), with the same lower bound of 7. Events are required to have an unmodified $p_{\text{T}}^{\text{miss}}$ below 75 GeV to reduce top quark backgrounds. High purity in $Z+$jets is ensured by requiring that the muons are consistent with a Z boson decay, with an $m_{\mu\mu}$ invariant mass within 15 GeV of m_Z. This CR has relatively limited yields but the predicted $Z+$jets background was found to reproduce the `SR` kinematics and m_{hh} distribution well, avoiding the need to mirror the NN requirement by developing analogous NN input features based on $p_{\text{T}}^{\text{miss}-\mu}$. The resulting $Z+$jets purity in `CRZ` is $\sim 80\%$, with a sub-leading contribution from $t\bar{t}+Z$. A summary of the `CRZ` definition is given in table 5.

[3] A signal contamination below 10% for dark Higgs models not excluded by other searches is achieved in all control and validation regions.

JHEP09(2025)067

Variable	Region requirement			
	CR3b-low	CR3b-high	CR4b	VR
Preselection	pass			pass
NN score	$[0.35, 0.85)$			$[0.85, 0.95)$
$n_{b\text{-jets}}$	$= 3$	$= 3$	$= 4$	≥ 3
$m^b_{\mathrm{T,min}}$ [GeV]	$[80, 200)$	≥ 200	≥ 80	≥ 80

Table 6. Selections for all single top and $t\bar{t}$ CRs, and the VR.

To estimate the $t\bar{t}$ + light and $t\bar{t}+ \geq 1b$ backgrounds, control regions (summarised in table 6) are defined to fulfil the preselection requirements and have a NN score in the 0.35 to 0.85 range to reduce signal contamination whilst remaining kinematically similar to the search regions. The $t\bar{t}+ \geq 1b$ component is targeted by the CR4b region, requiring exactly four b-tagged jets, which increases its fractional yield to $\sim 45\%$. To target the $t\bar{t}$ + light background, a control region requiring exactly three b-tagged jets is defined. To further increase its purity, an $80\,\mathrm{GeV} < m^b_{\mathrm{T,min}} < 200\,\mathrm{GeV}$ requirement is made, ensuring the $m^b_{\mathrm{T,min}}$ value is compatible with the m_t endpoint. The resulting CR3b-low region, is $\sim 57\%$ pure in $t\bar{t}$ + light, with secondary contributions from other top quark background processes. Its complement, with $m^b_{\mathrm{T,min}}$ above 200 GeV and exactly three b-tagged jets forms the control region CR3b-high. This is used to check the modelling of background components contributing beyond $m^b_{\mathrm{T,min}} = m_t$, and has larger contributions from Z + jets ($\sim 25\%$), single top quark processes ($\sim 20\%$) and $t\bar{t}+ \geq 1b$ events ($\sim 16\%$).

To validate that the normalisation factors derived from the control regions lead to a good agreement between data and the background prediction in a signal-depleted region, a validation region (VR) is defined. This is made kinematically similar to the search regions using the adjacent 0.85 to 0.95 NN score region and the same preselection requirements, as shown in table 6.

7 Systematic uncertainties

Experimental uncertainties in luminosity, pile-up reweighting, jet energy scale and resolution, JVT efficiency, $p_{\mathrm{T}}^{\mathrm{miss}}$ soft term scale and resolution, and b-jet tagging efficiency are considered. The $p_{\mathrm{T}}^{\mathrm{miss}}$ soft term uncertainty is estimated following the procedure described in ref. [101]. Uncertainties in the jet energy scale and resolution and b-jet tagging efficiency are estimated at a per-jet level from calibrations and comparisons between different event simulation models [90, 93, 96]. The uncertainty in the JVT efficiency is estimated following the technique in ref. [94]. Uncertainties related to lepton reconstruction and identification are found to be negligible.

Systematic uncertainties associated with the MC generator choice, parton shower, and the modelling of initial and final state radiation are considered for the $t\bar{t}$ and single top backgrounds. The generator (parton shower) uncertainty is evaluated by comparing the nominal Powheg+Pythia 8 set-up against an alternative sample generated with MadGraph5_aMCNLO+Pythia 8 (Powheg+Herwig 7). The uncertainty due to initial-state radiation is estimated by simultaneously varying the h_{damp} parameter and the μ_{r} and μ_{f}

JHEP09(2025)067

scales, and choosing the Var3c up/down variants of the A14 tune as described in ref. [112]. The final-state radiation uncertainty is evaluated by varying the renormalisation scale up or down by a factor of two. The uncertainty associated with modelling the interference between $t\bar{t}$ and single top processes is evaluated by comparing the nominal diagram removal [113] set-up to an alternative sample with diagram subtraction [113, 114].

Uncertainties related to missing higher-order corrections are assessed by variations of the choice of renormalisation and factorisation scales for the W + jets and Z + jets backgrounds, evaluated as the envelope of a set of seven variations [115]. Uncertainties in the resummation and matching were also assessed and found to be negligible. A conservative 50% uncertainty is used for the $t\bar{t}+ \geq 1c$ and single top backgrounds to account for the uncertainty in their cross-sections in the signal phase space [39], which has negligible impact on the results. For the minor $t\bar{t}+X$ and diboson backgrounds, a 20% uncertainty is used to account for modelling uncertainties in these processes [116]. For the dark Higgs signal model, uncertainties in the renormalisation and factorisation scale choices are evaluated following the same procedure as used for SM backgrounds. The uncertainty in the luminosity is also included and has a negligible impact.

8 Statistical interpretation

The statistical interpretation of the search results is performed via simultaneous likelihood fits to the observed data, using the `HistFitter` framework [117]. The likelihood consists of a product of Poisson probability density functions describing the observed and expected numbers of events in the relevant regions. The systematic uncertainties in the backgrounds and signal processes are included as Gaussian distributed nuisance parameters in the likelihood expression. For the background processes scaled by normalisation factors ($t\bar{t}$ + light, $t\bar{t}+ \geq 1b$, Z + jets), these appear as freely floating parameters multiplying the expected MC yields. MC statistical uncertainties are included as nuisance parameters in the likelihood with Poisson distributions.

A background-only fit is first performed to validate the SM background estimate. For this fit, only the four control region yields are included, and it is assumed that no signal is present. The fit constrains the values of the background normalisation factors, and the results of the fit are applied to the validation region to assess the post-fit agreement between the observed `VR` data and background prediction.

To test the SM-only hypothesis and place limits on the possible number of BSM signal events entering each `DR` at 95% confidence level (CL) without making explicit assumptions about the signal m_{hh} shape, fits are performed. One fit is performed for each `DR` in turn, simultaneously fitting the four control regions and the `DR`. A dummy signal is included in each `DR`, whose signal strength is the parameter of interest for the fit. It is assumed the signal contributions to the control regions are negligible.

To place limits on the dark Higgs models at 95% CL using the CL_s method [118], the four control regions and the binned `SR` are fitted simultaneously. The parameter of interest in the fit is the signal strength μ_{sig}, which multiplies the signal yield nominally predicted by the model.

JHEP09(2025)067

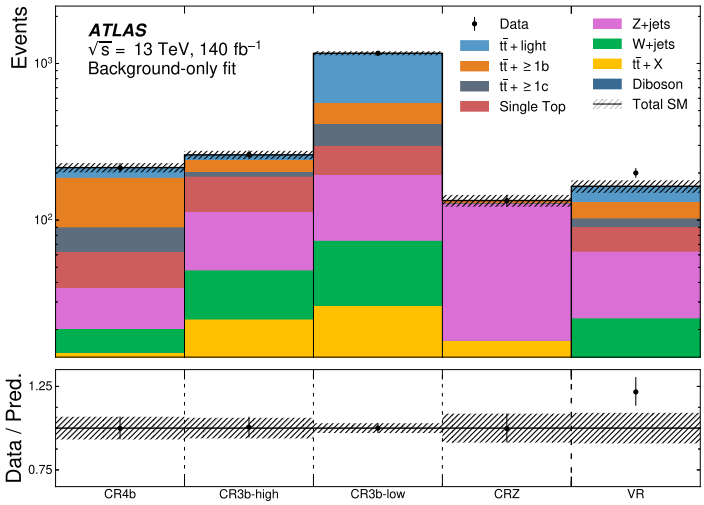

Figure 3. Observed data and expected background yields in each control and validation region after the background-only fit. The hashed band shows the total systematic and MC statistical uncertainty. In the lower panel the ratio of data and background yields is shown.

9 Results

The background normalisation factors obtained in the background-only fit are: $\mu_{Z+\text{jets}} = 1.24 \pm 0.14$, $\mu_{t\bar{t}+\geq 1b} = 1.2 \pm 0.6$ and $\mu_{t\bar{t}+\text{light}} = 0.91 \pm 0.14$. The agreement between the observed data and the SM background prediction after the background-only fit is shown in figure 3. The m_{hh} distribution in the VR after the background-only fit is shown in figure 4, demonstrating no mismodelling trend and a small upward fluctuation ($< 1.7\sigma$). The distribution of the NN score after the background-only fit is shown in figure 5(a), for the range of score values used in the analysis regions. A good agreement between the SM background prediction and data is observed throughout the range. The m_{hh} distribution in the binned signal region after the background-only fit is shown in figure 5(b). The overlaid benchmark signal points highlight the good discrimination power of the NN and m_{hh} distributions. There are no significant excesses or deficits in the data compared with the SM prediction. Additionally, the distribution has a similar shape to that seen in the VR in figure 4, demonstrating that the NN score is not highly correlated with m_{hh}, in line with the NN design.

To place limits on the possible number of BSM events of a similar topology entering each DR, more model-agnostic fits are performed, as described in section 8. The post-fit agreement between the observed data and the expected SM background yields follows from the fitted m_{hh} distribution, and is shown in figure 6, with the derived upper limits detailed in table 7.

In the absence of evidence for a signal, exclusion limits are set on the dark Higgs model in the plane of the masses of the dark Higgs boson (s) and Z' mediator. The impacts of each category of uncertainties in the SR yields in the exclusion fits are assessed in table 8 for a representative signal point with $m_{Z'} = 1400\,\text{GeV}$ and $m_s = 385\,\text{GeV}$. Consistent with the limited yields in the SR, the results are statistically limited, with the statistical uncertainty of the data dominating. The larger systematic uncertainty components are those from the modelling of the predicted backgrounds, such as the normalisation of the

JHEP09(2025)067

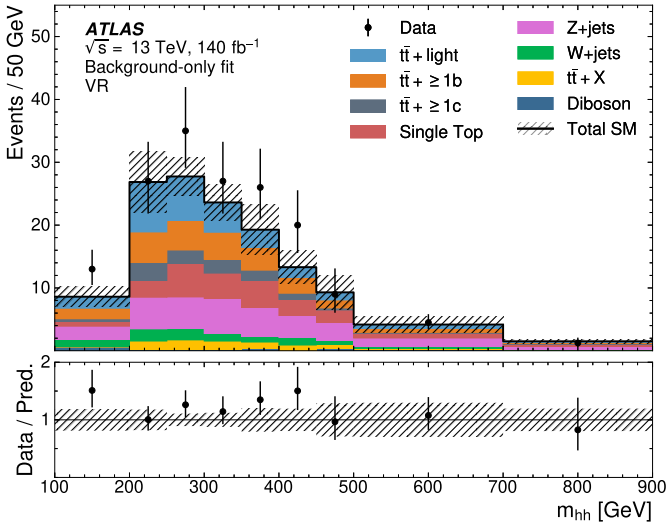

Figure 4. The observed data and expected background m_{hh} distribution in the VR, after the background-only fit. The hashed bands show the total systematic and MC statistical uncertainty. The lower panel shows the ratio of data and predicted background yields.

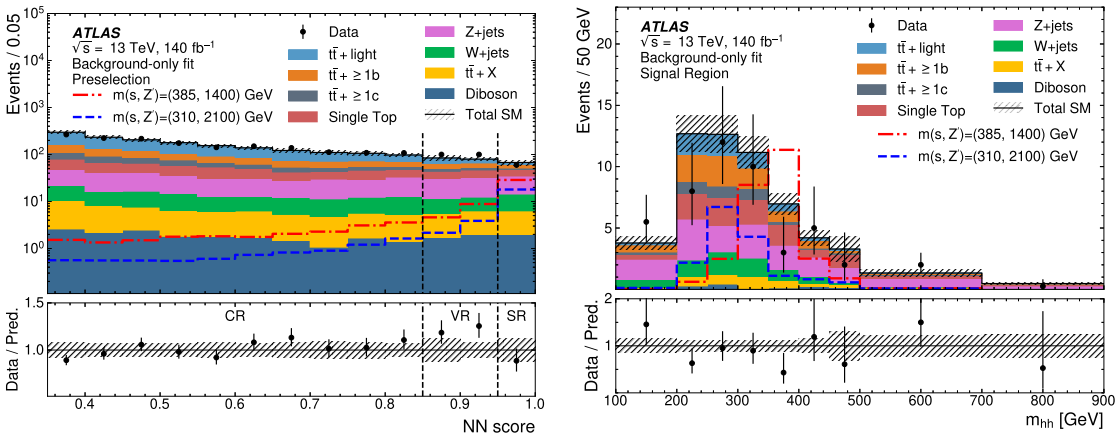

(a) (b)

Figure 5. The observed data and expected background (a) NN score distribution after the preselection requirements and (b) m_{hh} distribution in the SR, after the background-only fit. The hashed bands show the total systematic and MC statistical uncertainty. Benchmark signal distributions are overlaid as dashed lines. The lower panel shows the ratio of data and predicted background yields.

freely floating components and the theoretical modelling and cross-section uncertainties of the other sub-leading components. Smaller contributions come from the limited size of the Monte-Carlo simulations and experimental uncertainties pertaining to the jet and b-jet calibration and identification.

The observed and expected exclusion limits are calculated from the binned signal region, and shown in figure 7. The observed limits follow the expectation closely, and are constrained by the large acceptance changes at the $Z' \to \chi\chi$ threshold of $m_{Z'} \sim 400\,\text{GeV}$ and the s-decay

JHEP09(2025)067

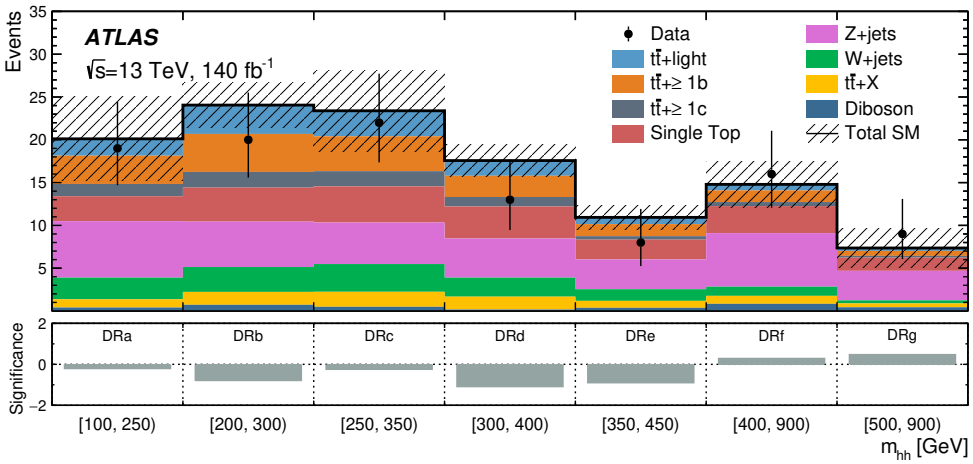

Figure 6. Observed data and fitted background yields in each DR region. The hashed band shows the total systematic and MC statistical uncertainty. In the lower panel the statistical significance (measured using eq. 1 of ref. [119]) of fluctuations between the data and SM expectation is shown.

Region	m_{hh} [GeV]	Data	Fitted background	S^{95}_{exp}	S^{95}_{obs}	$\langle\epsilon\sigma^{95}_{\text{obs}}\rangle$ [fb]	p_0-value
DRa	$[100, 250)$	19	20.1 ± 4.9	$11.1^{+5.1}_{-3.3}$	10	0.072	0.50
DRb	$[200, 300)$	20	24.1 ± 2.7	$12.1^{+5.5}_{-3.6}$	8.8	0.063	0.50
DRc	$[250, 350)$	22	23.4 ± 4.7	$11.9^{+5.5}_{-3.6}$	11	0.076	0.50
DRd	$[300, 400)$	13	17.6 ± 1.9	$10.2^{+4.9}_{-3.1}$	6.9	0.049	0.50
DRe	$[350, 450)$	8	10.9 ± 1.4	$8.2^{+4.1}_{-2.5}$	5.9	0.042	0.50
DRf	$[400, 900)$	16	14.8 ± 2.7	$10.0^{+4.7}_{-3.0}$	11	0.079	0.40
DRg	$[500, 900)$	9	7.4 ± 2.3	$7.2^{+3.6}_{-2.3}$	8.7	0.062	0.33

Table 7. Upper limits on the expected (observed) number of BSM events S^{95}_{exp} (S^{95}_{obs}) at 95% confidence level, the $\pm1\sigma$ variations on the expected upper limit, and the observed limit on the effective visible BSM cross-section ($\langle\epsilon\sigma^{95}_{\text{obs}}\rangle$), for each of DRa-DRg. The discovery p_0-value is also shown, capped at 0.5 if the data yield is smaller than the SM prediction.

thresholds at $m_s \sim 250\,\text{GeV}$ and 400 GeV. At high $m_{Z'}$, the falling cross-section leads to a wider variation in the expected limits, and small fluctuations in the data result in slightly stronger or weaker exclusions than the median expectation accordingly. A comparison of the observed contours with limits placed from other ATLAS dark Higgs boson searches [41–43] is shown in figure 8, highlighting the complementary sensitivities that different dark Higgs boson signatures have to different areas of mass parameter space. The di-Higgs decay of the dark Higgs boson is sensitive to $m_s > 250\,\text{GeV}$ and the high Higgs boson branching ratio to bb provides unique sensitivity in this region, where other dibosonic final states lose sensitivity from their decreased branching fraction and the increasing collimation of the decay products.

JHEP09(2025)067

Source of uncertainty	Percentage of total uncertainty [%]
Signal modelling	<1
b-jet identification	5
Jet calibrations	9
Other experimental	2
$t\bar{t}$ modelling & normalisation	11
Z + jets modelling & normalisation	9
Single top modelling & cross-section	18
Other background modelling & cross-section	13
MC statistical uncertainty	17
Overall systematic error	33
Data statistical	95
Total uncertainty	100

Table 8. Summary of the relative impact of each category of uncertainty in the SR yield, in a signal plus background fit to a $m_{Z'} = 1400\,\text{GeV}$, $m_s = 385\,\text{GeV}$ signal simulation.

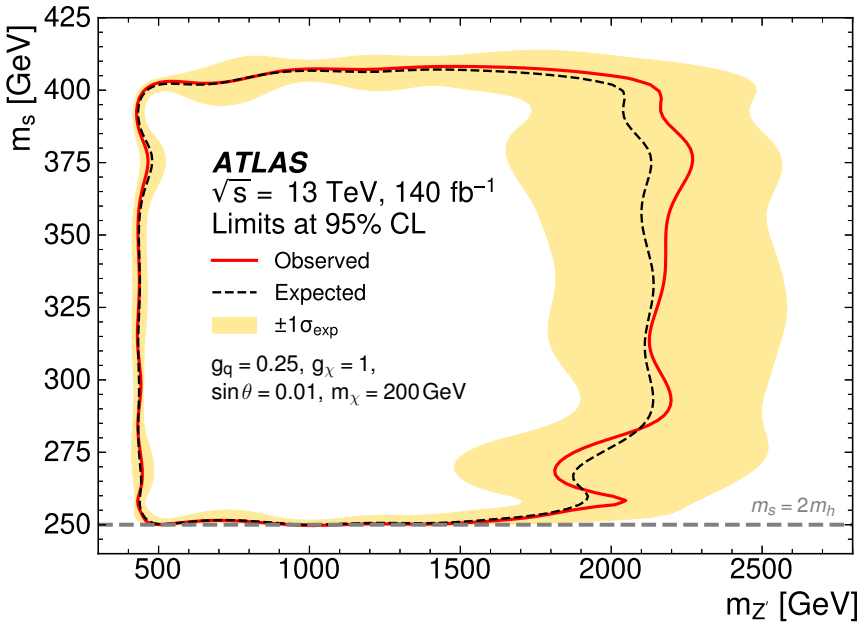

Figure 7. Observed and expected exclusion limits in the $(m_{Z'}, m_s)$ plane at 95% CL, with the excluded part inside the closed contour. The $\pm 1\sigma$ expected exclusion intervals are shown as the filled bands. The horizontal dashed line at $m_s = 2m_h$ indicates the limit where the $s \to hh$ decay mode becomes kinematically accessible.

Also shown in figure 8 is the predicted DM relic density as calculated by MadDM [120]. At $m_s \simeq 2m_\chi = 400\,\text{GeV}$, DM annihilation via a dark Higgs boson is enhanced, strongly depleting the surviving relic abundance of DM. For this benchmark with $m_\chi = 200\,\text{GeV}$, the $s \to \chi\chi$ decay dominates above this m_s value; however these results have generic sensitivity to $m_s > 400\,\text{GeV}$, e.g. in scenarios with larger m_χ.

JHEP09(2025)067

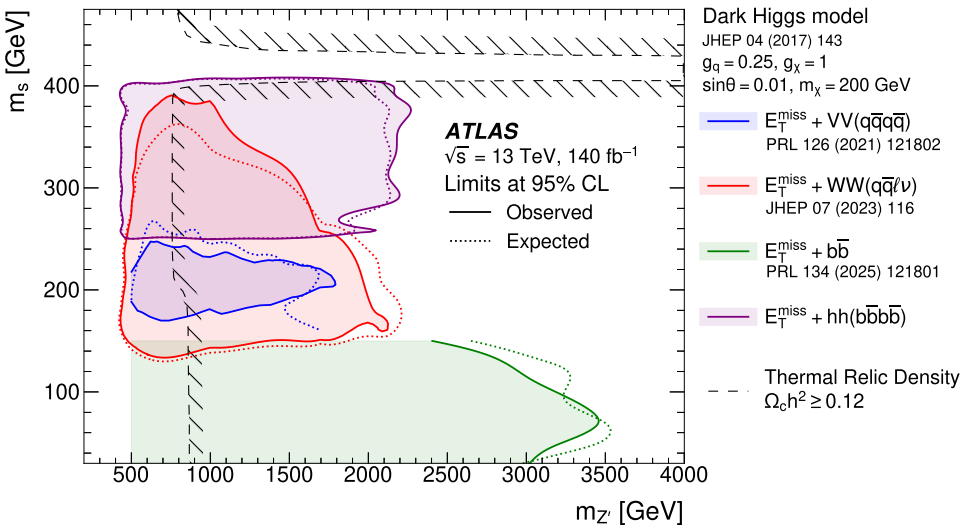

Figure 8. A comparison of this analysis' exclusions with existent ATLAS searches [41–43]. Their observed and expected exclusion limits in the $(m_{Z'}, m_s)$ plane at 95% CL are shown. The observed relic density is indicated with a dashed line, with the diagonal lines indicating an overabundance of DM.

10 Conclusion

A search for dark matter in a final state with significant $p_{\mathrm{T}}^{\mathrm{miss}}$ and a resonantly produced pair of Higgs bosons resulting in at least three b-tagged jets is performed, using the 140 fb^{-1} of Run 2 data recorded by the ATLAS detector at the LHC between 2015 and 2018. The observed data are found to be consistent with Standard Model predictions. Upper limits are placed at 95% confidence level on the effective production cross-section for new particle states with mass greater than 250 GeV decaying into hh in association with $p_{\mathrm{T}}^{\mathrm{miss}}$. The result is interpreted using a dark Higgs model, with a dark Higgs boson s giving rise to massive dark matter, and a Z' mediator. Upper limits are derived on the hypothesised particle masses for $250 < m_s < 400$ GeV, excluding Z' masses up to 2.3 TeV in a recommended model benchmark. This new signature significantly extends the constraints in this mass region existing from previous dark Higgs analyses by the ATLAS and CMS collaborations in different final states. The results complement other lower-mass dark Higgs boson searches, searches for extended Higgs sectors and collider DM searches more generally.

Acknowledgments

We thank CERN for the very successful operation of the LHC and its injectors, as well as the support staff at CERN and at our institutions worldwide without whom ATLAS could not be operated efficiently.

The crucial computing support from all WLCG partners is acknowledged gratefully, in particular from CERN, the ATLAS Tier-1 facilities at TRIUMF/SFU (Canada), NDGF (Denmark, Norway, Sweden), CC-IN2P3 (France), KIT/GridKA (Germany), INFN-CNAF

JHEP09(2025)067

(Italy), NL-T1 (Netherlands), PIC (Spain), RAL (UK) and BNL (USA), the Tier-2 facilities worldwide and large non-WLCG resource providers. Major contributors of computing resources are listed in ref. [121].

We gratefully acknowledge the support of ANPCyT, Argentina; YerPhI, Armenia; ARC, Australia; BMWFW and FWF, Austria; ANAS, Azerbaijan; CNPq and FAPESP, Brazil; NSERC, NRC and CFI, Canada; CERN; ANID, Chile; CAS, MOST and NSFC, China; Minciencias, Colombia; MEYS CR, Czech Republic; DNRF and DNSRC, Denmark; IN2P3-CNRS and CEA-DRF/IRFU, France; SRNSFG, Georgia; BMFTR, HGF and MPG, Germany; GSRI, Greece; RGC and Hong Kong SAR, China; ICHEP and Academy of Sciences and Humanities, Israel; INFN, Italy; MEXT and JSPS, Japan; CNRST, Morocco; NWO, Netherlands; RCN, Norway; MNiSW, Poland; FCT, Portugal; MNE/IFA, Romania; MSTDI, Serbia; MSSR, Slovakia; ARIS and MVZI, Slovenia; DSI/NRF, South Africa; MICIU/AEI, Spain; SRC and Wallenberg Foundation, Sweden; SERI, SNSF and Cantons of Bern and Geneva, Switzerland; NSTC, Taipei; TENMAK, Türkiye; STFC/UKRI, United Kingdom; DOE and NSF, United States of America.

Individual groups and members have received support from BCKDF, CANARIE, CRC and DRAC, Canada; CERN-CZ, FORTE and PRIMUS, Czech Republic; COST, ERC, ERDF, Horizon 2020, ICSC-NextGenerationEU and Marie Skłodowska-Curie Actions, European Union; Investissements d'Avenir Labex, Investissements d'Avenir Idex and ANR, France; DFG and AvH Foundation, Germany; Herakleitos, Thales and Aristeia programmes co-financed by EU-ESF and the Greek NSRF, Greece; BSF-NSF and MINERVA, Israel; NCN and NAWA, Poland; La Caixa Banking Foundation, CERCA Programme Generalitat de Catalunya and PROMETEO and GenT Programmes Generalitat Valenciana, Spain; Göran Gustafssons Stiftelse, Sweden; The Royal Society and Leverhulme Trust, United Kingdom.

In addition, individual members wish to acknowledge support from CERN: European Organization for Nuclear Research (CERN DOCT); Chile: Agencia Nacional de Investigación y Desarrollo (FONDECYT 1230812, FONDECYT 1240864); China: Chinese Ministry of Science and Technology (MOST-2023YFA1605700, MOST-2023YFA1609300), National Natural Science Foundation of China (NSFC - 12175119, NSFC 12275265); Czech Republic: Czech Science Foundation (GACR - 24-11373S), Ministry of Education Youth and Sports (ERC-CZ-LL2327, FORTE CZ.02.01.01/00/22_008/0004632), PRIMUS Research Programme (PRIMUS/21/SCI/017); EU: H2020 European Research Council (ERC - 101002463); European Union: European Research Council (BARD No. 101116429, ERC - 948254, ERC 101089007), European Regional Development Fund (SMASH COFUND 101081355, SLO ERDF), Horizon 2020 Framework Programme (MUCCA - CHIST-ERA-19-XAI-00), European Union, Future Artificial Intelligence Research (FAIR-NextGenerationEU PE00000013), Italian Center for High Performance Computing, Big Data and Quantum Computing (ICSC, NextGenerationEU); France: Agence Nationale de la Recherche (ANR-21-CE31-0022, ANR-22-EDIR-0002); Germany: Baden-Württemberg Stiftung (BW Stiftung-Postdoc Eliteprogramme), Deutsche Forschungsgemeinschaft (DFG - 469666862, DFG - CR 312/5-2); China: Research Grants Council (GRF); Italy: Istituto Nazionale di Fisica Nucleare (ICSC, NextGenerationEU), Ministero dell'Università e della Ricerca (NextGenEU I53D23000820006 M4C2.1.1, SOE2024_0000023); Japan: Japan Society for the Promotion of Science (JSPS KAKENHI

JHEP09(2025)067

JP22H01227, JSPS KAKENHI JP22H04944, JSPS KAKENHI JP22KK0227, JSPS KAKENHI JP24K23939, JSPS KAKENHI JP25H00650, JSPS KAKENHI JP25H01291, JSPS KAKENHI JP25K01023); Norway: Research Council of Norway (RCN-314472); Poland: Ministry of Science and Higher Education (IDUB AGH, POB8, D4 no 9722), Polish National Science Centre (NCN 2021/42/E/ST2/00350, NCN OPUS 2023/51/B/ST2/02507, NCN OPUS nr 2022/47/B/ST2/03059, NCN UMO-2019/34/E/ST2/00393, UMO-2022/47/O/ST2/00148, UMO-2023/49/B/ST2/04085, UMO-2023/51/B/ST2/00920, UMO-2024/53/N/ST2/00869); Portugal: Foundation for Science and Technology (FCT); Spain: Ministry of Science and Innovation (MCIN & NextGenEU PCI2022-135018-2, MICIN & FEDER PID2021-125273NB, RYC2019-028510-I, RYC2020-030254-I, RYC2021-031273-I, RYC2022-038164-I); Sweden: Carl Trygger Foundation (Carl Trygger Foundation CTS 22:2312), Swedish Research Council (Swedish Research Council 2023-04654, VR 2021-03651, VR 2022-03845, VR 2022-04683, VR 2023-03403, VR 2024-05451), Knut and Alice Wallenberg Foundation (KAW 2018.0458, KAW 2022.0358, KAW 2023.0366); Switzerland: Swiss National Science Foundation (SNSF - PCEFP2_194658); United Kingdom: Leverhulme Trust (Leverhulme Trust RPG-2020-004), Royal Society (NIF-R1-231091); United States of America: U.S. Department of Energy (ECA DE-AC02-76SF00515), Neubauer Family Foundation.

Data Availability Statement. This article has no associated data or the data will not be deposited.

Code Availability Statement. This article has no associated code or the code will not be deposited.

Open Access. This article is distributed under the terms of the Creative Commons Attribution License (CC-BY4.0), which permits any use, distribution and reproduction in any medium, provided the original author(s) and source are credited.

References

[1] V. Trimble, *Existence and Nature of Dark Matter in the Universe*, *Ann. Rev. Astron. Astrophys.* **25** (1987) 425 [INSPIRE].

[2] G. Bertone, D. Hooper and J. Silk, *Particle dark matter: Evidence, candidates and constraints*, *Phys. Rept.* **405** (2005) 279 [hep-ph/0404175] [INSPIRE].

[3] J.L. Feng, *Dark Matter Candidates from Particle Physics and Methods of Detection*, *Ann. Rev. Astron. Astrophys.* **48** (2010) 495 [arXiv:1003.0904] [INSPIRE].

[4] T.A. Porter, R.P. Johnson and P.W. Graham, *Dark Matter Searches with Astroparticle Data*, *Ann. Rev. Astron. Astrophys.* **49** (2011) 155 [arXiv:1104.2836] [INSPIRE].

[5] E. Corbelli and P. Salucci, *The Extended Rotation Curve and the Dark Matter Halo of M33*, *Mon. Not. Roy. Astron. Soc.* **311** (2000) 441 [astro-ph/9909252] [INSPIRE].

[6] V.C. Rubin, N. Thonnard and W.K. Ford Jr., *Rotational properties of 21 SC galaxies with a large range of luminosities and radii, from NGC 4605 ($R = 4$ kpc) to UGC 2885 ($R = 122$) kpc*, *Astrophys. J.* **238** (1980) 471 [INSPIRE].

[7] K.G. Begeman, A.H. Broeils and R.H. Sanders, *Extended rotation curves of spiral galaxies: Dark haloes and modified dynamics*, *Mon. Not. Roy. Astron. Soc.* **249** (1991) 523 [INSPIRE].

JHEP09(2025)067

[8] D. Clowe et al., *A direct empirical proof of the existence of dark matter*, *Astrophys. J. Lett.* **648** (2006) L109 [astro-ph/0608407] [INSPIRE].

[9] S.W. Randall et al., *Constraints on the Self-Interaction Cross-Section of Dark Matter from Numerical Simulations of the Merging Galaxy Cluster 1E 0657-56*, *Astrophys. J.* **679** (2008) 1173 [arXiv:0704.0261] [INSPIRE].

[10] M. Bradac et al., *Revealing the properties of dark matter in the merging cluster MACSJ0025.4-1222*, *Astrophys. J.* **687** (2008) 959 [arXiv:0806.2320] [INSPIRE].

[11] WMAP collaboration, *Nine-Year Wilkinson Microwave Anisotropy Probe (WMAP) Observations: Cosmological Parameter Results*, *Astrophys. J. Suppl.* **208** (2013) 19 [arXiv:1212.5226] [INSPIRE].

[12] PLANCK collaboration, *Planck 2018 results. I. Overview and the cosmological legacy of Planck*, *Astron. Astrophys.* **641** (2020) A1 [arXiv:1807.06205] [INSPIRE].

[13] LZ collaboration, *Dark Matter Search Results from 4.2 Tonne-Years of Exposure of the LUX-ZEPLIN (LZ) Experiment*, *Phys. Rev. Lett.* **135** (2025) 011802 [arXiv:2410.17036] [INSPIRE].

[14] LZ collaboration, *First Dark Matter Search Results from the LUX-ZEPLIN (LZ) Experiment*, *Phys. Rev. Lett.* **131** (2023) 041002 [arXiv:2207.03764] [INSPIRE].

[15] XENON collaboration, *Search for Light Dark Matter in Low-Energy Ionization Signals from XENONnT*, *Phys. Rev. Lett.* **134** (2025) 161004 [arXiv:2411.15289] [INSPIRE].

[16] XENON collaboration, *First Dark Matter Search with Nuclear Recoils from the XENONnT Experiment*, *Phys. Rev. Lett.* **131** (2023) 041003 [arXiv:2303.14729] [INSPIRE].

[17] PANDAX collaboration, *Dark Matter Search Results from 1.54 Tonne Year Exposure of PandaX-4T*, *Phys. Rev. Lett.* **134** (2025) 011805 [arXiv:2408.00664] [INSPIRE].

[18] DARKSIDE-50 collaboration, *Search for low-mass dark matter WIMPs with 12 ton-day exposure of DarkSide-50*, *Phys. Rev. D* **107** (2023) 063001 [arXiv:2207.11966] [INSPIRE].

[19] A. Acharyya et al., *Search for Ultraheavy Dark Matter from Observations of Dwarf Spheroidal Galaxies with VERITAS*, *Astrophys. J.* **945** (2023) 101 [arXiv:2302.08784] [INSPIRE].

[20] H.E.S.S. collaboration, *Search for Dark Matter Annihilation Signals in the H.E.S.S. Inner Galaxy Survey*, *Phys. Rev. Lett.* **129** (2022) 111101 [arXiv:2207.10471] [INSPIRE].

[21] CTA collaboration, *Sensitivity of the Cherenkov Telescope Array to a dark matter signal from the Galactic centre*, *JCAP* **01** (2021) 057 [arXiv:2007.16129] [INSPIRE].

[22] FERMI-LAT collaboration, *Searching for Dark Matter Annihilation from Milky Way Dwarf Spheroidal Galaxies with Six Years of Fermi Large Area Telescope Data*, *Phys. Rev. Lett.* **115** (2015) 231301 [arXiv:1503.02641] [INSPIRE].

[23] FERMI-LAT collaboration, *The Fermi Galactic Center GeV Excess and Implications for Dark Matter*, *Astrophys. J.* **840** (2017) 43 [arXiv:1704.03910] [INSPIRE].

[24] C. Pérez de los Heros, *Status, Challenges and Directions in Indirect Dark Matter Searches*, *Symmetry* **12** (2020) 1648 [arXiv:2008.11561] [INSPIRE].

[25] LIGO SCIENTIFIC et al. collaborations, *Constraints on dark photon dark matter using data from LIGO's and Virgo's third observing run*, *Phys. Rev. D* **105** (2022) 063030 [*Erratum ibid.* **109** (2024) 089902] [arXiv:2105.13085] [INSPIRE].

[26] S.M. Vermeulen et al., *Direct limits for scalar field dark matter from a gravitational-wave detector*, arXiv:2103.03783 [DOI:10.1038/s41586-021-04031-y] [INSPIRE].

JHEP09(2025)067

[27] ATLAS collaboration, *Constraints on simplified dark matter models involving an s-channel mediator with the ATLAS detector in pp collisions at $\sqrt{s} = 13$ TeV*, *Eur. Phys. J. C* **84** (2024) 1102 [arXiv:2404.15930] [INSPIRE].

[28] ATLAS collaboration, *Combination and summary of ATLAS dark matter searches interpreted in a 2HDM with a pseudo-scalar mediator using 139 fb^{-1} of $\sqrt{s} = 13$ TeV pp collision data*, *Sci. Bull.* **69** (2024) 3005 [arXiv:2306.00641] [INSPIRE].

[29] CMS collaboration, *Dark sector searches with the CMS experiment*, *Phys. Rept.* **1115** (2025) 448 [arXiv:2405.13778] [INSPIRE].

[30] ATLAS collaboration, *The ATLAS Experiment at the CERN Large Hadron Collider*, 2008 *JINST* **3** S08003 [INSPIRE].

[31] L. Evans and P. Bryant, *LHC Machine*, 2008 *JINST* **3** S08001 [INSPIRE].

[32] PLANCK collaboration, *Planck 2018 results. VI. Cosmological parameters*, *Astron. Astrophys.* **641** (2020) A6 [*Erratum ibid.* **652** (2021) C4] [arXiv:1807.06209] [INSPIRE].

[33] G. Steigman and M.S. Turner, *Cosmological Constraints on the Properties of Weakly Interacting Massive Particles*, *Nucl. Phys. B* **253** (1985) 375 [INSPIRE].

[34] M. Blanke et al., *Spotting hidden sectors with Higgs binoculars*, *JHEP* **04** (2019) 160 [arXiv:1901.07558] [INSPIRE].

[35] S. Argyropoulos, U. Haisch and I. Kalaitzidou, *Novel collider signatures in the type-I 2HDM+a model*, *JHEP* **07** (2024) 263 [arXiv:2404.05704] [INSPIRE].

[36] M. Duerr et al., *Hunting the dark Higgs*, *JHEP* **04** (2017) 143 [arXiv:1701.08780] [INSPIRE].

[37] ATLAS collaboration, *Search for supersymmetry in final states with missing transverse momentum and three or more b-jets in 139 fb^{-1} of proton-proton collisions at $\sqrt{s} = 13$ TeV with the ATLAS detector*, *Eur. Phys. J. C* **83** (2023) 561 [arXiv:2211.08028] [INSPIRE].

[38] CMS collaboration, *Search for top squark production in fully-hadronic final states in proton-proton collisions at $\sqrt{s} = 13$ TeV*, *Phys. Rev. D* **104** (2021) 052001 [arXiv:2103.01290] [INSPIRE].

[39] ATLAS collaboration, *Search for pair production of higgsinos in events with two Higgs bosons and missing transverse momentum in s=13 TeV pp collisions at the ATLAS experiment*, *Phys. Rev. D* **109** (2024) 112011 [arXiv:2401.14922] [INSPIRE].

[40] CMS collaboration, *Search for higgsinos decaying to two Higgs bosons and missing transverse momentum in proton-proton collisions at $\sqrt{s} = 13$ TeV*, *JHEP* **05** (2022) 014 [arXiv:2201.04206] [INSPIRE].

[41] ATLAS collaboration, *Search for Dark Matter Produced in Association with a Dark Higgs Boson in the $b\bar{b}$ Final State Using pp Collisions at $\sqrt{s} = 13$ TeV with the ATLAS Detector*, *Phys. Rev. Lett.* **134** (2025) 121801 [arXiv:2407.10549] [INSPIRE].

[42] ATLAS collaboration, *Search for dark matter produced in association with a dark Higgs boson decaying into W^+W^- in the one-lepton final state at $\sqrt{s} = 13$ TeV using 139 fb^{-1} of pp collisions recorded with the ATLAS detector*, *JHEP* **07** (2023) 116 [arXiv:2211.07175] [INSPIRE].

[43] ATLAS collaboration, *Search for Dark Matter Produced in Association with a Dark Higgs Boson Decaying into $W^{\pm}W^{\mp}$ or ZZ in Fully Hadronic Final States from $\sqrt{s} = 13$ TeV pp Collisions Recorded with the ATLAS Detector*, *Phys. Rev. Lett.* **126** (2021) 121802 [arXiv:2010.06548] [INSPIRE].

JHEP09(2025)067

[44] CMS collaboration, *Search for dark matter particles in W^+W^- events with transverse momentum imbalance in proton-proton collisions at $\sqrt{s} = 13$ TeV*, *JHEP* **03** (2024) 134 [arXiv:2310.12229] [INSPIRE].

[45] G. Avoni et al., *The new LUCID-2 detector for luminosity measurement and monitoring in ATLAS*, 2018 *JINST* **13** P07017 [INSPIRE].

[46] ATLAS collaboration, *Performance of the ATLAS Trigger System in 2015*, *Eur. Phys. J. C* **77** (2017) 317 [arXiv:1611.09661] [INSPIRE].

[47] ATLAS collaboration, *Software and computing for Run 3 of the ATLAS experiment at the LHC*, *Eur. Phys. J. C* **85** (2025) 234 [arXiv:2404.06335] [INSPIRE].

[48] ATLAS collaboration, *Luminosity determination in pp collisions at $\sqrt{s} = 13$ TeV using the ATLAS detector at the LHC*, *Eur. Phys. J. C* **83** (2023) 982 [arXiv:2212.09379] [INSPIRE].

[49] ATLAS collaboration, *ATLAS data quality operations and performance for 2015–2018 data-taking*, 2020 *JINST* **15** P04003 [arXiv:1911.04632] [INSPIRE].

[50] ATLAS collaboration, *Performance of the missing transverse momentum triggers for the ATLAS detector during Run-2 data taking*, *JHEP* **08** (2020) 080 [arXiv:2005.09554] [INSPIRE].

[51] J. Abdallah et al., *Simplified Models for Dark Matter Searches at the LHC*, *Phys. Dark Univ.* **9-10** (2015) 8 [arXiv:1506.03116] [INSPIRE].

[52] D. Abercrombie et al., *Dark Matter benchmark models for early LHC Run-2 Searches: Report of the ATLAS/CMS Dark Matter Forum*, *Phys. Dark Univ.* **27** (2020) 100371 [arXiv:1507.00966] [INSPIRE].

[53] ATLAS collaboration, *The ATLAS Simulation Infrastructure*, *Eur. Phys. J. C* **70** (2010) 823 [arXiv:1005.4568] [INSPIRE].

[54] ATLAS collaboration, *AtlFast3: The Next Generation of Fast Simulation in ATLAS*, *Comput. Softw. Big Sci.* **6** (2022) 7 [arXiv:2109.02551] [INSPIRE].

[55] GEANT4 collaboration, *GEANT4 — A Simulation Toolkit*, *Nucl. Instrum. Meth. A* **506** (2003) 250 [INSPIRE].

[56] ATLAS collaboration, *Improvements in $t\bar{t}$ modelling using NLO+PS Monte Carlo generators for Run2*, ATL-PHYS-PUB-2018-009, CERN, Geneva (2018).

[57] ATLAS collaboration, *Simulation of top quark production for the ATLAS experiment at $\sqrt{s} = 13$ TeV*, ATL-PHYS-PUB-2016-004, CERN, Geneva (2016).

[58] ATLAS collaboration, *Multi-Boson Simulation for 13 TeV ATLAS Analyses*, ATL-PHYS-PUB-2017-005, CERN, Geneva (2017).

[59] ATLAS collaboration, *ATLAS simulation of boson plus jets processes in Run 2*, ATL-PHYS-PUB-2017-006, CERN, Geneva (2017).

[60] ATLAS collaboration, *Modelling and computational improvements to the simulation of single vector-boson plus jet processes for the ATLAS experiment*, *JHEP* **08** (2022) 089 [arXiv:2112.09588] [INSPIRE].

[61] D.J. Lange, *The EvtGen particle decay simulation package*, *Nucl. Instrum. Meth. A* **462** (2001) 152 [INSPIRE].

[62] T. Sjostrand, S. Mrenna and P.Z. Skands, *A Brief Introduction to PYTHIA 8.1*, *Comput. Phys. Commun.* **178** (2008) 852 [arXiv:0710.3820] [INSPIRE].

JHEP09(2025)067

[63] R.D. Ball et al., *Parton distributions with LHC data*, *Nucl. Phys. B* **867** (2013) 244 [arXiv:1207.1303] [INSPIRE].

[64] ATLAS collaboration, *The Pythia 8 A3 tune description of ATLAS minimum bias and inelastic measurements incorporating the Donnachie-Landshoff diffractive model*, ATL-PHYS-PUB-2016-017, CERN, Geneva (2016).

[65] J. Alwall et al., *The automated computation of tree-level and next-to-leading order differential cross sections, and their matching to parton shower simulations*, *JHEP* **07** (2014) 079 [arXiv:1405.0301] [INSPIRE].

[66] C. Bierlich et al., *A comprehensive guide to the physics and usage of PYTHIA 8.3*, *SciPost Phys. Codeb.* **2022** (2022) 8 [arXiv:2203.11601] [INSPIRE].

[67] ATLAS collaboration *ATLAS Pythia 8 tunes to 7 TeV data*, ATL-PHYS-PUB-2014-021, CERN, Geneva (2014).

[68] SHERPA collaboration, *Event Generation with Sherpa 2.2*, *SciPost Phys.* **7** (2019) 034 [arXiv:1905.09127] [INSPIRE].

[69] T. Gleisberg and S. Hoeche, *Comix, a new matrix element generator*, *JHEP* **12** (2008) 039 [arXiv:0808.3674] [INSPIRE].

[70] R. Gavin, Y. Li, F. Petriello and S. Quackenbush, *FEWZ 2.0: A code for hadronic Z production at next-to-next-to-leading order*, *Comput. Phys. Commun.* **182** (2011) 2388 [arXiv:1011.3540] [INSPIRE].

[71] ATLAS collaboration, *Monte Carlo Generators for the Production of a W or Z/γ^* Boson in Association with Jets at ATLAS in Run 2*, ATL-PHYS-PUB-2016-003, CERN, Geneva (2016).

[72] NNPDF collaboration, *Parton distributions for the LHC Run II*, *JHEP* **04** (2015) 040 [arXiv:1410.8849] [INSPIRE].

[73] E. Re, *Single-top Wt-channel production matched with parton showers using the POWHEG method*, *Eur. Phys. J. C* **71** (2011) 1547 [arXiv:1009.2450] [INSPIRE].

[74] P. Nason, *A New method for combining NLO QCD with shower Monte Carlo algorithms*, *JHEP* **11** (2004) 040 [hep-ph/0409146] [INSPIRE].

[75] S. Frixione, P. Nason and C. Oleari, *Matching NLO QCD computations with Parton Shower simulations: the POWHEG method*, *JHEP* **11** (2007) 070 [arXiv:0709.2092] [INSPIRE].

[76] S. Alioli, P. Nason, C. Oleari and E. Re, *A general framework for implementing NLO calculations in shower Monte Carlo programs: the POWHEG BOX*, *JHEP* **06** (2010) 043 [arXiv:1002.2581] [INSPIRE].

[77] T. Sjöstrand et al., *An introduction to PYTHIA 8.2*, *Comput. Phys. Commun.* **191** (2015) 159 [arXiv:1410.3012] [INSPIRE].

[78] M. Czakon and A. Mitov, *Top++: A Program for the Calculation of the Top-Pair Cross-Section at Hadron Colliders*, *Comput. Phys. Commun.* **185** (2014) 2930 [arXiv:1112.5675] [INSPIRE].

[79] M. Aliev et al., *HATHOR: HAdronic Top and Heavy quarks crOss section calculatoR*, *Comput. Phys. Commun.* **182** (2011) 1034 [arXiv:1007.1327] [INSPIRE].

[80] P. Kant et al., *HatHor for single top-quark production: Updated predictions and uncertainty estimates for single top-quark production in hadronic collisions*, *Comput. Phys. Commun.* **191** (2015) 74 [arXiv:1406.4403] [INSPIRE].

JHEP09(2025)067

[81] M.L. Ciccolini, S. Dittmaier and M. Kramer, *Electroweak radiative corrections to associated WH and ZH production at hadron colliders*, *Phys. Rev. D* **68** (2003) 073003 [hep-ph/0306234] [INSPIRE].

[82] O. Brein, A. Djouadi and R. Harlander, *NNLO QCD corrections to the Higgs-strahlung processes at hadron colliders*, *Phys. Lett. B* **579** (2004) 149 [hep-ph/0307206] [INSPIRE].

[83] O. Brein, R. Harlander, M. Wiesemann and T. Zirke, *Top-Quark Mediated Effects in Hadronic Higgs-Strahlung*, *Eur. Phys. J. C* **72** (2012) 1868 [arXiv:1111.0761] [INSPIRE].

[84] L. Altenkamp et al., *Gluon-induced Higgs-strahlung at next-to-leading order QCD*, *JHEP* **02** (2013) 078 [arXiv:1211.5015] [INSPIRE].

[85] A. Denner, S. Dittmaier, S. Kallweit and A. Mück, *HAWK 2.0: A Monte Carlo program for Higgs production in vector-boson fusion and Higgs strahlung at hadron colliders*, *Comput. Phys. Commun.* **195** (2015) 161 [arXiv:1412.5390] [INSPIRE].

[86] O. Brein, R.V. Harlander and T.J.E. Zirke, *vh@nnlo — Higgs Strahlung at hadron colliders*, *Comput. Phys. Commun.* **184** (2013) 998 [arXiv:1210.5347] [INSPIRE].

[87] R.V. Harlander, A. Kulesza, V. Theeuwes and T. Zirke, *Soft gluon resummation for gluon-induced Higgs Strahlung*, *JHEP* **11** (2014) 082 [arXiv:1410.0217] [INSPIRE].

[88] J. Butterworth et al., *PDF4LHC recommendations for LHC Run II*, *J. Phys. G* **43** (2016) 023001 [arXiv:1510.03865] [INSPIRE].

[89] ATLAS collaboration, *Vertex Reconstruction Performance of the ATLAS Detector at* $\sqrt{s} = 13$ *TeV*, ATL-PHYS-PUB-2015-026, CERN, Geneva (2015).

[90] ATLAS collaboration, *Jet reconstruction and performance using particle flow with the ATLAS Detector*, *Eur. Phys. J. C* **77** (2017) 466 [arXiv:1703.10485] [INSPIRE].

[91] M. Cacciari, G.P. Salam and G. Soyez, *FastJet User Manual*, *Eur. Phys. J. C* **72** (2012) 1896 [arXiv:1111.6097] [INSPIRE].

[92] M. Cacciari, G.P. Salam and G. Soyez, *The anti-k_t jet clustering algorithm*, *JHEP* **04** (2008) 063 [arXiv:0802.1189] [INSPIRE].

[93] ATLAS collaboration, *Jet energy scale and resolution measured in proton–proton collisions at* $\sqrt{s} = 13$ *TeV with the ATLAS detector*, *Eur. Phys. J. C* **81** (2021) 689 [arXiv:2007.02645] [INSPIRE].

[94] ATLAS collaboration, *Performance of pile-up mitigation techniques for jets in pp collisions at* $\sqrt{s} = 8$ *TeV using the ATLAS detector*, *Eur. Phys. J. C* **76** (2016) 581 [arXiv:1510.03823] [INSPIRE].

[95] ATLAS collaboration, *ATLAS flavour-tagging algorithms for the LHC Run 2 pp collision dataset*, *Eur. Phys. J. C* **83** (2023) 681 [arXiv:2211.16345] [INSPIRE].

[96] ATLAS collaboration, *ATLAS b-jet identification performance and efficiency measurement with* $t\bar{t}$ *events in pp collisions at* $\sqrt{s} = 13$ *TeV*, *Eur. Phys. J. C* **79** (2019) 970 [arXiv:1907.05120] [INSPIRE].

[97] ATLAS collaboration, *Measurement of the c-jet mistagging efficiency in* $t\bar{t}$ *events using pp collision data at* $\sqrt{s} = 13$ *TeV collected with the ATLAS detector*, *Eur. Phys. J. C* **82** (2022) 95 [arXiv:2109.10627] [INSPIRE].

[98] ATLAS collaboration, *Calibration of the light-flavour jet mistagging efficiency of the b-tagging algorithms with Z+jets events using 139 fb^{-1} of ATLAS proton-proton collision data at* $\sqrt{s} = 13$ *TeV*, *Eur. Phys. J. C* **83** (2023) 728 [arXiv:2301.06319] [INSPIRE].

JHEP09(2025)067

[99] ATLAS collaboration, *Electron and photon performance measurements with the ATLAS detector using the 2015–2017 LHC proton-proton collision data*, 2019 *JINST* **14** P12006 [arXiv:1908.00005] [INSPIRE].

[100] ATLAS collaboration, *Muon reconstruction and identification efficiency in ATLAS using the full Run 2 pp collision data set at* $\sqrt{s} = 13$ *TeV*, *Eur. Phys. J. C* **81** (2021) 578 [arXiv:2012.00578] [INSPIRE].

[101] ATLAS collaboration, *The performance of missing transverse momentum reconstruction and its significance with the ATLAS detector using* 140 fb^{-1} *of* $\sqrt{s} = 13$ *TeV pp collisions*, *Eur. Phys. J. C* **85** (2025) 606 [arXiv:2402.05858] [INSPIRE].

[102] M. Stone, *Cross-Validatory Choice and Assessment of Statistical Predictions*, *J. Roy. Statist. Soc. B* **36** (1974) 111.

[103] B. Rozemberczki et al., *The Shapley Value in Machine Learning*, arXiv:2202.05594.

[104] J.M. Kanter and K. Veeramachaneni, *Deep feature synthesis: Towards automating data science endeavors*, in the proceedings of the *2015 IEEE International Conference on Data Science and Advanced Analytics (DSAA)*, Paris, France (2015) [DOI:10.1109/dsaa.2015.7344858].

[105] K. Fukushima, *Visual Feature Extraction by a Multilayered Network of Analog Threshold Elements*, *IEEE Trans. Syst. Sci. Cybernetics* **5** (1969) 322.

[106] V. Nair and G.E. Hinton, *Rectified linear units improve restricted boltzmann machines*, in the proceedings of the *27th International Conference on International Conference on Machine Learning, ICML'10*, Haifa Israel (2010), pg. 807, [DOI:10.5555/3104322.3104425].

[107] S. Ioffe and C. Szegedy, *Batch Normalization: Accelerating Deep Network Training by Reducing Internal Covariate Shift*, arXiv:1502.03167 [INSPIRE].

[108] D.P. Kingma and J. Ba, *Adam: A Method for Stochastic Optimization*, arXiv:1412.6980 [INSPIRE].

[109] N. Srivastava et al, *Dropout: A Simple Way to Prevent Neural Networks from Overfitting*, *J. Mach. Learn. Res.* **15** (2014) 1929 https://jmlr.org/papers/v15/srivastava14a.html.

[110] G.J. Székely, M.L. Rizzo and N.K. Bakirov, *Measuring and testing dependence by correlation of distances*, *Annals Statist.* **35** (2007) 2769.

[111] G. Kasieczka and D. Shih, *Robust Jet Classifiers through Distance Correlation*, *Phys. Rev. Lett.* **125** (2020) 122001 [arXiv:2001.05310] [INSPIRE].

[112] ATLAS collaboration, *Studies on top-quark Monte Carlo modelling with Sherpa and MG5_aMC@NLO*, ATL-PHYS-PUB-2017-007, CERN, Geneva (2017).

[113] S. Frixione et al., *Single-top hadroproduction in association with a W boson*, *JHEP* **07** (2008) 029 [arXiv:0805.3067] [INSPIRE].

[114] ATLAS collaboration, *Studies on top-quark Monte Carlo modelling for Top2016*, ATL-PHYS-PUB-2016-020, CERN, Geneva (2016).

[115] E. Bothmann, M. Schönherr and S. Schumann, *Reweighting QCD matrix-element and parton-shower calculations*, *Eur. Phys. J. C* **76** (2016) 590 [arXiv:1606.08753] [INSPIRE].

[116] ATLAS collaboration, *Modelling of the* $t\bar{t}H$ *and* $t\bar{t}V$ $(V = W, Z)$ *processes for* $\sqrt{s} = 13$ *TeV ATLAS analyses*, ATL-PHYS-PUB-2016-005, CERN, Geneva (2016).

[117] M. Baak et al., *HistFitter software framework for statistical data analysis*, *Eur. Phys. J. C* **75** (2015) 153 [arXiv:1410.1280] [INSPIRE].

JHEP09(2025)067

[118] A.L. Read, *Presentation of search results: The CL_s technique*, *J. Phys. G* **28** (2002) 2693 [INSPIRE].

[119] ATLAS collaboration, *Formulae for Estimating Significance*, ATL-PHYS-PUB-2020-025, CERN, Geneva (2020).

[120] F. Ambrogi et al., *MadDM v.3.0: a Comprehensive Tool for Dark Matter Studies*, *Phys. Dark Univ.* **24** (2019) 100249 [arXiv:1804.00044] [INSPIRE].

[121] ATLAS collaboration, *ATLAS Computing Acknowledgements*, ATL-SOFT-PUB-2025-001, CERN, Geneva (2025).

JHEP09(2025)067

The ATLAS collaboration

G. Aad[104], E. Aakvaag[17], B. Abbott[123], S. Abdelhameed[119a], K. Abeling[55], N.J. Abicht[49], S.H. Abidi[30], M. Aboelela[45], A. Aboulhorma[36e], H. Abramowicz[157], Y. Abulaiti[120], B.S. Acharya[69a,69b,m], A. Ackermann[63a], C. Adam Bourdarios[4], L. Adamczyk[86a], S.V. Addepalli[149], M.J. Addison[103], J. Adelman[118], A. Adiguzel[22c], T. Adye[137], A.A. Affolder[139], Y. Afik[40], M.N. Agaras[13], A. Aggarwal[102], C. Agheorghiesei[28c], F. Ahmadov[39,ad], S. Ahuja[97], X. Ai[143b], G. Aielli[76a,76b], A. Aikot[169], M. Ait Tamlihat[36e], B. Aitbenchikh[36a], M. Akbiyik[102], T.P.A. Åkesson[100], A.V. Akimov[151], D. Akiyama[174], N.N. Akolkar[25], S. Aktas[172], G.L. Alberghi[24b], J. Albert[171], U. Alberti[20], P. Albicocco[53], G.L. Albouy[60], S. Alderweireldt[52], Z.L. Alegria[124], M. Aleksa[37], I.N. Aleksandrov[39], C. Alexa[28b], T. Alexopoulos[10], F. Alfonsi[24b], M. Algren[56], M. Alhroob[173], B. Ali[135], H.M.J. Ali[93,w], S. Ali[32], S.W. Alibocus[94], M. Aliev[34c], G. Alimonti[71a], W. Alkakhi[55], C. Allaire[66], B.M.M. Allbrooke[152], J.S. Allen[103], J.F. Allen[52], P.P. Allport[21], A. Aloisio[72a,72b], F. Alonso[92], C. Alpigiani[142], Z.M.K. Alsolami[93], A. Alvarez Fernandez[102], M. Alves Cardoso[56], M.G. Alviggi[72a,72b], M. Aly[103], Y. Amaral Coutinho[83b], A. Ambler[106], C. Amelung[37], M. Amerl[103], C.G. Ames[111], T. Amezza[130], D. Amidei[108], B. Amini[54], K. Amirie[161], A. Amirkhanov[39], S.P. Amor Dos Santos[133a], K.R. Amos[169], D. Amperiadou[158], S. An[84], C. Anastopoulos[145], T. Andeen[11], J.K. Anders[94], A.C. Anderson[59], A. Andreazza[71a,71b], S. Angelidakis[9], A. Angerami[42], A.V. Anisenkov[39], A. Annovi[74a], C. Antel[37], E. Antipov[151], M. Antonelli[53], F. Anulli[75a], M. Aoki[84], T. Aoki[159], M.A. Aparo[152], L. Aperio Bella[48], M. Apicella[31], C. Appelt[157], A. Apyan[27], M. Arampatzi[10], S.J. Arbiol Val[87], C. Arcangeletti[53], A.T.H. Arce[51], J-F. Arguin[110], S. Argyropoulos[158], J.-H. Arling[48], O. Arnaez[4], H. Arnold[151], G. Artoni[75a,75b], H. Asada[113], K. Asai[121], S. Asatryan[179], N.A. Asbah[37], R.A. Ashby Pickering[173], A.M. Aslam[97], K. Assamagan[30], R. Astalos[29a], K.S.V. Astrand[100], S. Atashi[165], R.J. Atkin[34a], H. Atmani[36f], P.A. Atmasiddha[131], K. Augsten[135], A.D. Auriol[41], V.A. Austrup[103], G. Avolio[37], K. Axiotis[56], A. Azzam[13], D. Babal[29b], H. Bachacou[138], K. Bachas[158,q], A. Bachiu[35], E. Bachmann[50], M.J. Backes[63a], A. Badea[40], T.M. Baer[108], P. Bagnaia[75a,75b], M. Bahmani[19], D. Bahner[54], K. Bai[126], J.T. Baines[137], L. Baines[96], O.K. Baker[178], E. Bakos[16], D. Bakshi Gupta[8], L.E. Balabram Filho[83b], V. Balakrishnan[123], R. Balasubramanian[4], E.M. Baldin[38], P. Balek[86a], E. Ballabene[24b,24a], F. Balli[138], L.M. Baltes[63a], W.K. Balunas[33], J. Balz[102], I. Bamwidhi[119b], E. Banas[87], M. Bandieramonte[132], A. Bandyopadhyay[25], S. Bansal[25], L. Barak[157], M. Barakat[48], E.L. Barberio[107], D. Barberis[18b], M. Barbero[104], M.Z. Barel[117], T. Barillari[112], M-S. Barisits[37], T. Barklow[149], P. Baron[136], D.A. Baron Moreno[103], A. Baroncelli[62], A.J. Barr[129], J.D. Barr[98], F. Barreiro[101], J. Barreiro Guimarães da Costa[14], M.G. Barros Teixeira[133a], S. Barsov[38], F. Bartels[63a], R. Bartoldus[149], A.E. Barton[93], P. Bartos[29a], A. Basan[102], M. Baselga[49], S. Bashiri[87], A. Bassalat[66,b], M.J. Basso[162a], S. Bataju[45], R. Bate[170], R.L. Bates[59], S. Batlamous[101], M. Battaglia[139], D. Battulga[19], M. Bauce[75a,75b], M. Bauer[79], P. Bauer[25], L.T. Bayer[48], L.T. Bazzano Hurrell[31], J.B. Beacham[112], T. Beau[130], J.Y. Beaucamp[92], P.H. Beauchemin[164], P. Bechtle[25], H.P. Beck[20,p], K. Becker[173], A.J. Beddall[82], V.A. Bednyakov[39], C.P. Bee[151],

JHEP09(2025)067

L.J. Beemster[16], M. Begalli[83d], M. Begel[30], J.K. Behr[48], J.F. Beirer[37], F. Beisiegel[25], M. Belfkir[119b], G. Bella[157], L. Bellagamba[24b], A. Bellerive[35], C.D. Bellgraph[68], P. Bellos[21], K. Beloborodov[38], I. Benaoumeur[21], D. Benchekroun[36a], F. Bendebba[36a], Y. Benhammou[157], K.C. Benkendorfer[61], L. Beresford[48], M. Beretta[53], E. Bergeaas Kuutmann[167], N. Berger[4], B. Bergmann[135], J. Beringer[18a], G. Bernardi[5], C. Bernius[149], F.U. Bernlochner[25], F. Bernon[37], A. Berrocal Guardia[13], T. Berry[97], P. Berta[136], A. Berthold[50], A. Berti[133a], R. Bertrand[104], S. Bethke[112], A. Betti[75a,75b], A.J. Bevan[96], L. Bezio[56], N.K. Bhalla[54], S. Bharthuar[112], S. Bhatta[151], P. Bhattarai[149], Z.M. Bhatti[120], K.D. Bhide[54], V.S. Bhopatkar[124], R.M. Bianchi[132], G. Bianco[24b,24a], O. Biebel[111], M. Biglietti[77a], C.S. Billingsley[45], Y. Bimgdi[36f], M. Bindi[55], A. Bingham[177], A. Bingul[22b], C. Bini[75a,75b], G.A. Bird[33], M. Birman[175], M. Biros[136], S. Biryukov[152], T. Bisanz[49], E. Bisceglie[24b,24a], J.P. Biswal[137], D. Biswas[147], I. Bloch[48], A. Blue[59], U. Blumenschein[96], V.S. Bobrovnikov[39], L. Boccardo[57b,57a], M. Boehler[54], B. Boehm[172], D. Bogavac[13], A.G. Bogdanchikov[38], L.S. Boggia[130], V. Boisvert[97], P. Bokan[37], T. Bold[86a], M. Bomben[5], M. Bona[96], M. Boonekamp[138], A.G. Borbély[59], I.S. Bordulev[38], G. Borissov[93], D. Bortoletto[129], D. Boscherini[24b], M. Bosman[13], K. Bouaouda[36a], N. Bouchhar[169], L. Boudet[4], J. Boudreau[132], E.V. Bouhova-Thacker[93], D. Boumediene[41], R. Bouquet[57b,57a], A. Boveia[122], J. Boyd[37], D. Boye[30], I.R. Boyko[39], L. Bozianu[56], J. Bracinik[21], N. Brahimi[4], G. Brandt[177], O. Brandt[33], B. Brau[105], J.E. Brau[126], R. Brener[175], L. Brenner[117], R. Brenner[167], S. Bressler[175], G. Brianti[78a,78b], D. Britton[59], D. Britzger[112], I. Brock[25], R. Brock[109], G. Brooijmans[42], A.J. Brooks[68], E.M. Brooks[162b], E. Brost[30], L.M. Brown[171,162a], L.E. Bruce[61], T.L. Bruckler[129], P.A. Bruckman de Renstrom[87], B. Brüers[48], A. Bruni[24b], G. Bruni[24b], D. Brunner[47a,47b], M. Bruschi[24b], N. Bruscino[75a,75b], T. Buanes[17], Q. Buat[142], D. Buchin[112], A.G. Buckley[59], O. Bulekov[82], B.A. Bullard[149], S. Burdin[94], C.D. Burgard[49], A.M. Burger[91], B. Burghgrave[8], O. Burlayenko[54], J. Burleson[168], J.C. Burzynski[148], E.L. Busch[42], V. Büscher[102], P.J. Bussey[59], J.M. Butler[26], C.M. Buttar[59], J.M. Butterworth[98], W. Buttinger[137], C.J. Buxo Vazquez[109], A.R. Buzykaev[39], S. Cabrera Urbán[169], L. Cadamuro[66], H. Cai[37], Y. Cai[24b,114c,24a], Y. Cai[114a], V.M.M. Cairo[37], O. Cakir[3a], N. Calace[37], P. Calafiura[18a], G. Calderini[130], P. Calfayan[35], L. Calic[100], G. Callea[59], L.P. Caloba[83b], D. Calvet[41], S. Calvet[41], R. Camacho Toro[130], S. Camarda[37], D. Camarero Munoz[27], P. Camarri[76a,76b], C. Camincher[171], M. Campanelli[98], A. Camplani[43], V. Canale[72a,72b], A.C. Canbay[3a], E. Canonero[97], J. Cantero[169], Y. Cao[168], F. Capocasa[27], M. Capua[44b,44a], A. Carbone[71a,71b], R. Cardarelli[76a], J.C.J. Cardenas[8], M.P. Cardiff[27], G. Carducci[44b,44a], T. Carli[37], G. Carlino[72a], J.I. Carlotto[13], B.T. Carlson[132,r], E.M. Carlson[171], J. Carmignani[94], L. Carminati[71a,71b], A. Carnelli[4], M. Carnesale[37], S. Caron[116], E. Carquin[140g], I.B. Carr[107], S. Carrá[73a,73b], G. Carratta[24b,24a], C. Carrion Martinez[169], A.M. Carroll[126], M.P. Casado[13,h], P. Casolaro[72a,72b], M. Caspar[48], F.L. Castillo[4], L. Castillo Garcia[13], V. Castillo Gimenez[169], N.F. Castro[133a,133e], A. Catinaccio[37], J.R. Catmore[128], T. Cavaliere[4], V. Cavaliere[30], L.J. Caviedes Betancourt[23b], E. Celebi[82], S. Cella[37], V. Cepaitis[56], K. Cerny[125], A.S. Cerqueira[83a], A. Cerri[74a,74b,am], L. Cerrito[76a,76b], F. Cerutti[18a], B. Cervato[71a,71b], A. Cervelli[24b], G. Cesarini[53],

JHEP09(2025)067

S.A. Cetin[82], P.M. Chabrillat[130], R. Chakkappai[66], S. Chakraborty[173], J. Chan[18a], W.Y. Chan[159], J.D. Chapman[33], E. Chapon[138], B. Chargeishvili[155b], D.G. Charlton[21], C. Chauhan[136], Y. Che[114a], S. Chekanov[6], S.V. Chekulaev[162a], G.A. Chelkov[39,a], B. Chen[157], B. Chen[171], H. Chen[114a], H. Chen[30], J. Chen[144a], J. Chen[148], M. Chen[129], S. Chen[89], S.J. Chen[114a], X. Chen[144a], X. Chen[15,ah], Z. Chen[62], C.L. Cheng[176], H.C. Cheng[64a], S. Cheong[149], A. Cheplakov[39], E. Cherepanova[117], R. Cherkaoui El Moursli[36e], E. Cheu[7], K. Cheung[65], L. Chevalier[138], V. Chiarella[53], G. Chiarelli[74a], G. Chiodini[70a], A.S. Chisholm[21], A. Chitan[28b], M. Chitishvili[169], M.V. Chizhov[39,s], K. Choi[11], Y. Chou[142], E.Y.S. Chow[116], K.L. Chu[175], M.C. Chu[64a], X. Chu[14,114c], Z. Chubinidze[53], J. Chudoba[134], J.J. Chwastowski[87], D. Cieri[112], K.M. Ciesla[86a], V. Cindro[95], A. Ciocio[18a], F. Cirotto[72a,72b], Z.H. Citron[175], M. Citterio[71a], D.A. Ciubotaru[28b], A. Clark[56], P.J. Clark[52], N. Clarke Hall[98], C. Clarry[161], S.E. Clawson[48], C. Clement[47a,47b], Y. Coadou[104], M. Cobal[69a,69c], A. Coccaro[57b], R.F. Coelho Barrue[133a], R. Coelho Lopes De Sa[105], S. Coelli[71a], L.S. Colangeli[161], B. Cole[42], P. Collado Soto[101], J. Collot[60], R. Coluccia[70a,70b], P. Conde Muiño[133a,133g], M.P. Connell[34c], S.H. Connell[34c], E.I. Conroy[129], M. Contreras Cossio[11], F. Conventi[72a,aj], A.M. Cooper-Sarkar[129], L. Corazzina[75a,75b], F.A. Corchia[24b,24a], A. Cordeiro Oudot Choi[142], L.D. Corpe[41], M. Corradi[75a,75b], F. Corriveau[106,ab], A. Cortes-Gonzalez[159], M.J. Costa[169], F. Costanza[4], D. Costanzo[145], B.M. Cote[122], J. Couthures[4], G. Cowan[97], K. Cranmer[176], L. Cremer[49], D. Cremonini[24b,24a], S. Crépé-Renaudin[60], F. Crescioli[130], T. Cresta[73a,73b], M. Cristinziani[147], M. Cristoforetti[78a,78b], V. Croft[117], G. Crosetti[44b,44a], A. Cueto[101], H. Cui[98], Z. Cui[7], B.M. Cunnett[152], W.R. Cunningham[59], F. Curcio[169], J.R. Curran[52], M.J. Da Cunha Sargedas De Sousa[57b,57a], J.V. Da Fonseca Pinto[83b], C. Da Via[103], W. Dabrowski[86a], T. Dado[37], S. Dahbi[154], T. Dai[108], D. Dal Santo[20], C. Dallapiccola[105], M. Dam[43], G. D'amen[30], V. D'Amico[111], J. Damp[102], J.R. Dandoy[35], M. D'andrea[57b,57a], D. Dannheim[37], G. D'anniballe[74a,74b], M. Danninger[148], V. Dao[151], G. Darbo[57b], S.J. Das[30], F. Dattola[48], S. D'Auria[71a,71b], A. D'Avanzo[72a,72b], T. Davidek[136], J. Davidson[173], I. Dawson[96], K. De[8], C. De Almeida Rossi[161], R. De Asmundis[72a], N. De Biase[48], S. De Castro[24b,24a], N. De Groot[116], P. de Jong[117], H. De la Torre[118], A. De Maria[114a], A. De Salvo[75a], U. De Sanctis[76a,76b], F. De Santis[70a,70b], A. De Santo[152], J.B. De Vivie De Regie[60], J. Debevc[95], D.V. Dedovich[39], J. Degens[94], A.M. Deiana[45], J. Del Peso[101], L. Delagrange[130], F. Deliot[138], C.M. Delitzsch[49], M. Della Pietra[72a,72b], D. Della Volpe[56], A. Dell'Acqua[37], L. Dell'Asta[71a,71b], M. Delmastro[4], C.C. Delogu[102], P.A. Delsart[60], S. Demers[178], M. Demichev[39], S.P. Denisov[38], H. Denizli[22a,l], L. D'Eramo[41], D. Derendarz[87], F. Derue[130], P. Dervan[94], A.M. Desai[1], K. Desch[25], F.A. Di Bello[57b,57a], A. Di Ciaccio[76a,76b], L. Di Ciaccio[4], A. Di Domenico[75a,75b], C. Di Donato[72a,72b], A. Di Girolamo[37], G. Di Gregorio[37], A. Di Luca[78a,78b], B. Di Micco[77a,77b], R. Di Nardo[77a,77b], K.F. Di Petrillo[40], M. Diamantopoulou[35], F.A. Dias[117], M.A. Diaz[140a,140b], A.R. Didenko[39], M. Didenko[169], S.D. Diefenbacher[18a], E.B. Diehl[108], S. Díez Cornell[48], C. Diez Pardos[147], C. Dimitriadi[150], A. Dimitrievska[21], A. Dimri[151], Y. Ding[62], J. Dingfelder[25], T. Dingley[129], I-M. Dinu[28b], S.J. Dittmeier[63b], F. Dittus[37], M. Divisek[136], B. Dixit[94], F. Djama[104], T. Djobava[155b], C. Doglioni[103,100],

JHEP09(2025)067

A. Dohnalova[29a], Z. Dolezal[136], K. Domijan[86a], K.M. Dona[40], M. Donadelli[83d], B. Dong[109], J. Donini[41], A. D'Onofrio[72a,72b], M. D'Onofrio[94], J. Dopke[137], A. Doria[72a], N. Dos Santos Fernandes[133a], I.A. Dos Santos Luz[83e], P. Dougan[103], M.T. Dova[92], A.T. Doyle[59], M.P. Drescher[55], E. Dreyer[175], I. Drivas-koulouris[10], M. Drnevich[120], D. Du[62], T.A. du Pree[117], Z. Duan[114a], M. Dubau[4], F. Dubinin[39], M. Dubovsky[29a], E. Duchovni[175], G. Duckeck[111], P.K. Duckett[98], O.A. Ducu[28b], D. Duda[52], A. Dudarev[37], M.M. Dudek[87], E.R. Duden[27], M. D'uffizi[103], L. Duflot[66], M. Dührssen[37], I. Duminica[28g], A.E. Dumitriu[28b], M. Dunford[63a], K. Dunne[47a,47b], A. Duperrin[104], H. Duran Yildiz[3a], A. Durglishvili[155b], G.I. Dyckes[18a], M. Dyndal[86a], B.S. Dziedzic[37], Z.O. Earnshaw[152], G.H. Eberwein[129], B. Eckerova[29a], S. Eggebrecht[55], E. Egidio Purcino De Souza[83e], G. Eigen[17], K. Einsweiler[18a], T. Ekelof[167], P.A. Ekman[100], S. El Farkh[36b], Y. El Ghazali[62], H. El Jarrari[37], A. El Moussaouy[36a], D. Elitez[37], M. Ellert[167], F. Ellinghaus[177], T.A. Elliot[97], N. Ellis[37], J. Elmsheuser[30], M. Elsawy[119a], M. Elsing[37], D. Emeliyanov[137], Y. Enari[84], I. Ene[18a], S. Epari[110], D. Ernani Martins Neto[87], F. Ernst[37], M. Errenst[177], M. Escalier[66], C. Escobar[169], E. Etzion[157], G. Evans[133a,133b], H. Evans[68], L.S. Evans[48], A. Ezhilov[38], S. Ezzarqtouni[36a], F. Fabbri[24b,24a], L. Fabbri[24b,24a], G. Facini[98], V. Fadeyev[139], R.M. Fakhrutdinov[38], D. Fakoudis[102], S. Falciano[75a], L.F. Falda Ulhoa Coelho[133a], F. Fallavollita[112], G. Falsetti[44b,44a], J. Faltova[136], C. Fan[168], K.Y. Fan[64b], Y. Fan[14], Y. Fang[14,114c], M. Fanti[71a,71b], M. Faraj[69a,69b], Z. Farazpay[99], A. Farbin[8], A. Farilla[77a], K. Farman[154], T. Farooque[109], J.N. Farr[178], S.M. Farrington[137,52], F. Fassi[36e], D. Fassouliotis[9], L. Fayard[66], P. Federic[136], P. Federicova[134], O.L. Fedin[38,a], M. Feickert[176], L. Feligioni[104], D.E. Fellers[18a], C. Feng[143a], Y. Feng[14], Z. Feng[117], M.J. Fenton[165], L. Ferencz[48], B. Fernandez Barbadillo[93], P. Fernandez Martinez[67], M.J.V. Fernoux[104], J. Ferrando[93], A. Ferrari[167], P. Ferrari[117,116], R. Ferrari[73a], D. Ferrere[56], C. Ferretti[108], M.P. Fewell[1], D. Fiacco[75a,75b], F. Fiedler[102], P. Fiedler[135], S. Filimonov[39], M.S. Filip[28b,t], A. Filipčič[95], E.K. Filmer[162a], F. Filthaut[116], M.C.N. Fiolhais[133a,133c,c], L. Fiorini[169], W.C. Fisher[109], T. Fitschen[103], P.M. Fitzhugh[138], I. Fleck[147], P. Fleischmann[108], T. Flick[177], M. Flores[34d,ag], L.R. Flores Castillo[64a], L. Flores Sanz De Acedo[37], F.M. Follega[78a,78b], N. Fomin[33], J.H. Foo[161], A. Formica[138], A.C. Forti[103], E. Fortin[37], A.W. Fortman[18a], L. Foster[18a], L. Fountas[9,i], D. Fournier[66], H. Fox[93], P. Francavilla[74a,74b], S. Francescato[61], S. Franchellucci[56], M. Franchini[24b,24a], S. Franchino[63a], D. Francis[37], L. Franco[116], L. Franconi[48], M. Franklin[61], G. Frattari[27], Y.Y. Frid[157], J. Friend[59], N. Fritzsche[37], A. Froch[56], D. Froidevaux[37], J.A. Frost[129], Y. Fu[109], S. Fuenzalida Garrido[140g], M. Fujimoto[104], K.Y. Fung[64a], E. Furtado De Simas Filho[83e], M. Furukawa[159], J. Fuster[169], A. Gaa[55], A. Gabrielli[24b,24a], A. Gabrielli[161], P. Gadow[37], G. Gagliardi[57b,57a], L.G. Gagnon[18a], S. Gaid[88b], S. Galantzan[157], J. Gallagher[1], E.J. Gallas[129], A.L. Gallen[167], B.J. Gallop[137], K.K. Gan[122], S. Ganguly[159], Y. Gao[52], A. Garabaglu[142], F.M. Garay Walls[140a,140b], C. García[169], A. Garcia Alonso[117], A.G. Garcia Caffaro[178], J.E. García Navarro[169], M.A. Garcia Ruiz[23b], M. Garcia-Sciveres[18a], G.L. Gardner[131], R.W. Gardner[40], N. Garelli[164], R.B. Garg[149], J.M. Gargan[52], C.A. Garner[161], C.M. Garvey[34a], V.K. Gassmann[164], G. Gaudio[73a], V. Gautam[13], P. Gauzzi[75a,75b], J. Gavranovic[95],

JHEP09(2025)067

I.L. Gavrilenko[133a], A. Gavrilyuk[38], C. Gay[170], G. Gaycken[126], E.N. Gazis[10], A. Gekow[122], C. Gemme[57b], M.H. Genest[60], A.D. Gentry[115], S. George[97], T. Geralis[46], A.A. Gerwin[123], P. Gessinger-Befurt[37], M.E. Geyik[177], M. Ghani[173], K. Ghorbanian[96], A. Ghosal[147], A. Ghosh[165], A. Ghosh[7], B. Giacobbe[24b], S. Giagu[75a,75b], T. Giani[117], A. Giannini[62], S.M. Gibson[97], M. Gignac[139], D.T. Gil[86b], A.K. Gilbert[86a], B.J. Gilbert[42], D. Gillberg[35], G. Gilles[117], D.M. Gingrich[2,ai], M.P. Giordani[69a,69c], P.F. Giraud[138], G. Giugliarelli[69a,69c], D. Giugni[71a], F. Giuli[76a,76b], I. Gkialas[9,i], L.K. Gladilin[38], C. Glasman[101], M. Glazewska[20], R.M. Gleason[165], G. Glemža[48], M. Glisic[126], I. Gnesi[44b], Y. Go[30], M. Goblirsch-Kolb[37], B. Gocke[49], D. Godin[110], B. Gokturk[22a], S. Goldfarb[107], T. Golling[56], M.G.D. Gololo[34c], D. Golubkov[38], J.P. Gombas[109], A. Gomes[133a,133b], G. Gomes Da Silva[147], A.J. Gomez Delegido[37], R. Gonçalo[133a], L. Gonella[21], A. Gongadze[155c], F. Gonnella[21], J.L. Gonski[149], R.Y. González Andana[52], S. González de la Hoz[169], M.V. Gonzalez Rodrigues[48], R. Gonzalez Suarez[167], S. Gonzalez-Sevilla[56], L. Goossens[37], B. Gorini[37], E. Gorini[70a,70b], A. Gorišek[95], T.C. Gosart[131], A.T. Goshaw[51], M.I. Gostkin[39], S. Goswami[124], C.A. Gottardo[37], S.A. Gotz[111], M. Gouighri[36b], A.G. Goussiou[142], N. Govender[34c], R.P. Grabarczyk[129], I. Grabowska-Bold[86a], K. Graham[35], E. Gramstad[128], S. Grancagnolo[70a,70b], C.M. Grant[1], P.M. Gravila[28f], F.G. Gravili[70a,70b], H.M. Gray[18a], M. Greco[112], M.J. Green[1], C. Grefe[25], A.S. Grefsrud[17], I.M. Gregor[48], K.T. Greif[165], P. Grenier[149], S.G. Grewe[112], A.A. Grillo[139], K. Grimm[32], S. Grinstein[13,x], J.-F. Grivaz[66], E. Gross[175], J. Grosse-Knetter[55], L. Guan[108], G. Guerrieri[37], R. Guevara[128], R. Gugel[102], J.A.M. Guhit[108], A. Guida[19], E. Guilloton[173], S. Guindon[37], F. Guo[14,114c], J. Guo[144a], L. Guo[48], L. Guo[114b,v], Y. Guo[108], A. Gupta[49], R. Gupta[132], S. Gupta[27], S. Gurbuz[25], S.S. Gurdasani[48], G. Gustavino[75a,75b], P. Gutierrez[123], L.F. Gutierrez Zagazeta[131], M. Gutsche[50], C. Gutschow[98], C. Gwenlan[129], C.B. Gwilliam[94], E.S. Haaland[128], A. Haas[120], M. Habedank[59], C. Haber[18a], H.K. Hadavand[8], A. Haddad[41], A. Hadef[50], A.I. Hagan[93], J.J. Hahn[147], E.H. Haines[98], M. Haleem[172], J. Haley[124], G.D. Hallewell[104], K. Hamano[171], H. Hamdaoui[167], M. Hamer[25], S.E.D. Hammoud[66], E.J. Hampshire[97], J. Han[143a], L. Han[114a], L. Han[62], S. Han[14], K. Hanagaki[84], M. Hance[139], D.A. Hangal[42], H. Hanif[148], M.D. Hank[131], J.B. Hansen[43], P.H. Hansen[43], D. Harada[56], T. Harenberg[177], S. Harkusha[179], M.L. Harris[105], Y.T. Harris[25], J. Harrison[13], N.M. Harrison[122], P.F. Harrison[173], M.L.E. Hart[98], N.M. Hartman[112], N.M. Hartmann[111], R.Z. Hasan[97,137], Y. Hasegawa[146], F. Haslbeck[129], S. Hassan[17], R. Hauser[109], M. Haviernik[136], C.M. Hawkes[21], R.J. Hawkings[37], Y. Hayashi[159], D. Hayden[109], C. Hayes[108], R.L. Hayes[117], C.P. Hays[129], J.M. Hays[96], H.S. Hayward[94], M. He[14,114c], Y. He[48], Y. He[98], N.B. Heatley[96], V. Hedberg[100], C. Heidegger[54], K.K. Heidegger[54], J. Heilman[35], S. Heim[48], T. Heim[18a], J.G. Heinlein[131], J.J. Heinrich[126], L. Heinrich[112], J. Hejbal[134], M. Helbig[50], A. Held[176], S. Hellesund[17], C.M. Helling[170], S. Hellman[47a,47b], A.M. Henriques Correia[37], H. Herde[100], Y. Hernández Jiménez[151], L.M. Herrmann[25], T. Herrmann[50], G. Herten[54], R. Hertenberger[111], L. Hervas[37], M.E. Hesping[102], N.P. Hessey[162a], J. Hessler[112], M. Hidaoui[36b], N. Hidic[136], E. Hill[161], T.S. Hillersoy[17], S.J. Hillier[21], J.R. Hinds[109], F. Hinterkeuser[25], M. Hirose[127], S. Hirose[163],

JHEP09(2025)067

D. Hirschbuehl[177], T.G. Hitchings[103], B. Hiti[95], J. Hobbs[151], R. Hobincu[28e], N. Hod[175], A.M. Hodges[168], M.C. Hodgkinson[145], B.H. Hodkinson[129], A. Hoecker[37], D.D. Hofer[108], J. Hofer[169], J. Hofner[102], M. Holzbock[37], L.B.A.H. Hommels[33], V. Homsak[129], B.P. Honan[103], J.J. Hong[68], T.M. Hong[132], B.H. Hooberman[168], W.H. Hopkins[6], M.C. Hoppesch[168], Y. Horii[113], M.E. Horstmann[112], S. Hou[154], M.R. Housenga[168], J. Howarth[59], J. Hoya[6], M. Hrabovsky[125], T. Hryn'ova[4], P.J. Hsu[65], S.-C. Hsu[142], T. Hsu[66], M. Hu[18a], Q. Hu[62], S. Huang[33], X. Huang[14,114c], Y. Huang[136], Y. Huang[114b], Y. Huang[14], Z. Huang[66], Z. Hubacek[135], F. Huegging[25], T.B. Huffman[129], M. Hufnagel Maranha De Faria[83a], C.A. Hugli[48], M. Huhtinen[37], S.K. Huiberts[17], R. Hulsken[106], C.E. Hultquist[18a], D.L. Humphreys[105], N. Huseynov[12], J. Huston[109], J. Huth[61], L. Huth[48], R. Hyneman[7], G. Iacobucci[56], G. Iakovidis[30], L. Iconomidou-Fayard[66], J.P. Iddon[37], P. Iengo[72a,72b], R. Iguchi[159], Y. Iiyama[159], T. Iizawa[159], Y. Ikegami[84], D. Iliadis[158], N. Ilic[161], H. Imam[36a], G. Inacio Goncalves[83d], S.A. Infante Cabanas[140c], T. Ingebretsen Carlson[47a,47b], J.M. Inglis[96], G. Introzzi[73a,73b], M. Iodice[77a], V. Ippolito[75a,75b], R.K. Irwin[94], M. Ishino[159], W. Islam[176], C. Issever[19], S. Istin[22a,ao], K. Itabashi[84], H. Ito[174], R. Iuppa[78a,78b], A. Ivina[175], V. Izzo[72a], P. Jacka[135], P. Jackson[1], P. Jain[48], K. Jakobs[54], T. Jakoubek[175], J. Jamieson[59], W. Jang[159], S. Jankovych[136], M. Javurkova[105], P. Jawahar[103], L. Jeanty[126], J. Jejelava[155a,ae], P. Jenni[54,f], C.E. Jessiman[35], C. Jia[143a], H. Jia[170], J. Jia[151], X. Jia[112,114c], Z. Jia[114a], C. Jiang[52], Q. Jiang[64b], S. Jiggins[48], M. Jimenez Ortega[169], J. Jimenez Pena[13], S. Jin[114a], A. Jinaru[28b], O. Jinnouchi[141], P. Johansson[145], K.A. Johns[7], J.W. Johnson[139], F.A. Jolly[48], D.M. Jones[152], E. Jones[48], K.S. Jones[8], P. Jones[33], R.W.L. Jones[93], T.J. Jones[94], H.L. Joos[55], R. Joshi[122], J. Jovicevic[16], X. Ju[18a], J.J. Junggeburth[37], T. Junkermann[63a], A. Juste Rozas[13,x], M.K. Juzek[87], S. Kabana[140f], A. Kaczmarska[87], S.A. Kadir[149], M. Kado[112], H. Kagan[122], M. Kagan[149], A. Kahn[131], C. Kahra[102], T. Kaji[159], E. Kajomovitz[156], N. Kakati[175], N. Kakoty[13], I. Kalaitzidou[54], S. Kandel[8], N.J. Kang[139], D. Kar[34h], E. Karentzos[25], K. Karki[8], O. Karkout[117], S.N. Karpov[39], Z.M. Karpova[39], V. Kartvelishvili[93], A.N. Karyukhin[38], E. Kasimi[158], J. Katzy[48], S. Kaur[35], K. Kawade[146], M.P. Kawale[123], C. Kawamoto[89], T. Kawamoto[62], E.F. Kay[37], F.I. Kaya[164], S. Kazakos[109], V.F. Kazanin[38], J.M. Keaveney[34a], R. Keeler[171], G.V. Kehris[61], J.S. Keller[35], J.M. Kelly[171], J.J. Kempster[152], O. Kepka[134], J. Kerr[162b], B.P. Kerridge[137], B.P. Kerševan[95], L. Keszeghova[29a], R.A. Khan[132], A. Khanov[124], A.G. Kharlamov[38], T. Kharlamova[38], E.E. Khoda[142], M. Kholodenko[133a], T.J. Khoo[19], G. Khoriauli[172], Y. Khoulaki[36a], J. Khubua[155b,*], Y.A.R. Khwaira[130], B. Kibirige[34h], D. Kim[6], D.W. Kim[47a,47b], Y.K. Kim[40], N. Kimura[98], M.K. Kingston[55], A. Kirchhoff[55], C. Kirfel[25], F. Kirfel[25], J. Kirk[137], A.E. Kiryunin[112], S. Kita[163], O. Kivernyk[25], M. Klassen[164], C. Klein[35], L. Klein[172], M.H. Klein[45], S.B. Klein[56], U. Klein[94], A. Klimentov[30], T. Klioutchnikova[37], P. Kluit[117], S. Kluth[112], E. Kneringer[79], T.M. Knight[161], A. Knue[49], M. Kobel[50], D. Kobylianskii[175], S.F. Koch[129], M. Kocian[149], P. Kodyš[136], D.M. Koeck[126], T. Koffas[35], O. Kolay[50], I. Koletsou[4], T. Komarek[87], K. Köneke[55], A.X.Y. Kong[1], T. Kono[121], N. Konstantinidis[98], P. Kontaxakis[56], B. Konya[100], R. Kopeliansky[42], S. Koperny[86a], K. Korcyl[87], K. Kordas[158,d], A. Korn[98], S. Korn[55],

JHEP09(2025)067

I. Korolkov[13], N. Korotkova[38], B. Kortman[117], O. Kortner[112], S. Kortner[112], W.H. Kostecka[118], M. Kostov[29a], V.V. Kostyukhin[147], A. Kotsokechagia[37], A. Kotwal[51], A. Koulouris[37], A. Kourkoumeli-Charalampidi[73a,73b], C. Kourkoumelis[9], E. Kourlitis[112], O. Kovanda[126], R. Kowalewski[171], W. Kozanecki[126], A.S. Kozhin[38], V.A. Kramarenko[38], G. Kramberger[95], P. Kramer[25], M.W. Krasny[130], A. Krasznahorkay[105], A.C. Kraus[118], J.W. Kraus[177], J.A. Kremer[48], N.B. Krengel[147], T. Kresse[50], L. Kretschmann[177], J. Kretzschmar[94], P. Krieger[161], K. Krizka[21], K. Kroeninger[49], H. Kroha[112], J. Kroll[134], J. Kroll[131], K.S. Krowpman[109], U. Kruchonak[39], H. Krüger[25], N. Krumnack[81], M.C. Kruse[51], O. Kuchinskaia[39], S. Kuday[3a], S. Kuehn[37], R. Kuesters[54], T. Kuhl[48], V. Kukhtin[39], Y. Kulchitsky[39], S. Kuleshov[140d,140b], J. Kull[1], E.V. Kumar[111], M. Kumar[34h], N. Kumari[48], P. Kumari[162b], A. Kupco[134], A. Kupich[38], O. Kuprash[54], H. Kurashige[85], L.L. Kurchaninov[162a], O. Kurdysh[4], Y.A. Kurochkin[38], A. Kurova[38], M. Kuze[141], A.K. Kvam[105], J. Kvita[125], N.G. Kyriacou[142], C. Lacasta[169], F. Lacava[75a,75b], H. Lacker[19], D. Lacour[130], N.N. Lad[98], E. Ladygin[39], A. Lafarge[41], B. Laforge[130], T. Lagouri[178], F.Z. Lahbabi[36a], S. Lai[55,37], W.S. Lai[98], J.E. Lambert[171], S. Lammers[68], W. Lampl[7], C. Lampoudis[158,d], G. Lamprinoudis[102], A.N. Lancaster[118], E. Lançon[30], U. Landgraf[54], M.P.J. Landon[96], V.S. Lang[54], O.K.B. Langrekken[128], A.J. Lankford[165], F. Lanni[37], K. Lantzsch[25], A. Lanza[73a], M. Lanzac Berrocal[169], J.F. Laporte[138], T. Lari[71a], D. Larsen[17], L. Larson[11], F. Lasagni Manghi[24b], M. Lassnig[37], S.D. Lawlor[145], R. Lazaridou[165], M. Lazzaroni[71a,71b], E.T.T. Le[165], H.D.M. Le[109], E.M. Le Boulicaut[178], L.T. Le Pottier[18a], B. Leban[24b,24a], F. Ledroit-Guillon[60], T.F. Lee[162b], L.L. Leeuw[34c], M. Lefebvre[171], C. Leggett[18a], G. Lehmann Miotto[37], M. Leigh[56], W.A. Leight[105], W. Leinonen[116], A. Leisos[158,u], M.A.L. Leite[83c], C.E. Leitgeb[19], R. Leitner[136], K.J.C. Leney[45], T. Lenz[25], S. Leone[74a], C. Leonidopoulos[52], A. Leopold[150], J.H. Lepage Bourbonnais[35], R. Les[109], C.G. Lester[33], M. Levchenko[38], J. Levêque[4], L.J. Levinson[175], G. Levrini[24b,24a], M.P. Lewicki[87], C. Lewis[142], D.J. Lewis[4], L. Lewitt[145], A. Li[30], B. Li[143a], C. Li[108], C-Q. Li[112], H. Li[143a], H. Li[103], H. Li[15], H. Li[62], H. Li[143a], J. Li[144a], K. Li[14], L. Li[144a], R. Li[178], S. Li[14,114c], S. Li[144b,144a], T. Li[5], X. Li[106], Y. Li[14], Z. Li[159], Z. Li[14,114c], Z. Li[62], S. Liang[14,114c], Z. Liang[14], M. Liberatore[138], B. Liberti[76a], G.B. Libotte[83d], K. Lie[64c], J. Lieber Marin[83e], H. Lien[68], H. Lin[108], S.F. Lin[151], L. Linden[111], R.E. Lindley[7], J.H. Lindon[37], J. Ling[61], E. Lipeles[131], A. Lipniacka[17], A. Lister[170], J.D. Little[68], B. Liu[14], B.X. Liu[114b], D. Liu[144b,144a], D. Liu[139], E.H.L. Liu[21], J.K.K. Liu[120], K. Liu[144b], K. Liu[144b,144a], M. Liu[62], M.Y. Liu[62], P. Liu[14], Q. Liu[144b,142,144a], S. Liu[151], X. Liu[62], X. Liu[143a], Y. Liu[114b,114c], Y.L. Liu[143a], Y.W. Liu[62], Z. Liu[66,k], S.L. Lloyd[96], E.M. Lobodzinska[48], P. Loch[7], E. Lodhi[161], K. Lohwasser[145], E. Loiacono[48], J.D. Lomas[21], J.D. Long[42], I. Longarini[165], R. Longo[168], A. Lopez Solis[13], N.A. Lopez-canelas[7], N. Lorenzo Martinez[4], A.M. Lory[111], M. Losada[119a], G. Löschcke Centeno[4], X. Lou[47a,47b], X. Lou[14,114c], A. Lounis[66], P.A. Love[93], M. Lu[66], S. Lu[131], Y.J. Lu[154], H.J. Lubatti[142], C. Luci[75a,75b], F.L. Lucio Alves[114a], F. Luehring[68], B.S. Lunday[131], O. Lundberg[150], J. Lunde[37], N.A. Luongo[6], M.S. Lutz[37], A.B. Lux[26], D. Lynn[30], R. Lysak[134], V. Lysenko[135], E. Lytken[100], V. Lyubushkin[39], T. Lyubushkina[39], M.M. Lyukova[151], M.Firdaus M. Soberi[52], H. Ma[30], K. Ma[62],

JHEP09(2025)067

L.L. Ma[143a], W. Ma[62], Y. Ma[124], J.C. MacDonald[102], P.C. Machado De Abreu Farias[83e], D. Macina[37], R. Madar[41], T. Madula[98], J. Maeda[85], T. Maeno[30], P.T. Mafa[34c,j], H. Maguire[145], M. Maheshwari[33], V. Maiboroda[66], A. Maio[133a,133b,133d], K. Maj[86a], O. Majersky[48], S. Majewski[126], R. Makhmanazarov[38], N. Makovec[66], V. Maksimovic[16], B. Malaescu[130], J. Malamant[128], Pa. Malecki[87], V.P. Maleev[38], F. Malek[60,o], M. Mali[95], D. Malito[97], U. Mallik[80,*], A. Maloizel[5], S. Maltezos[10], A. Malvezzi Lopes[83d], S. Malyukov[39], J. Mamuzic[95], G. Mancini[53], M.N. Mancini[27], G. Manco[73a,73b], J.P. Mandalia[96], S.S. Mandarry[152], I. Mandić[95], L. Manhaes de Andrade Filho[83a], I.M. Maniatis[175], J. Manjarres Ramos[91], D.C. Mankad[175], A. Mann[111], T. Manoussos[37], M.N. Mantinan[40], S. Manzoni[37], L. Mao[144a], X. Mapekula[34c], A. Marantis[158], R.R. Marcelo Gregorio[96], G. Marchiori[5], C. Marcon[71a], E. Maricic[16], M. Marinescu[48], S. Marium[48], M. Marjanovic[123], A. Markhoos[54], M. Markovitch[66], M.K. Maroun[105], M.C. Marr[148], G.T. Marsden[103], E.J. Marshall[93], Z. Marshall[18a], S. Marti-Garcia[169], J. Martin[98], T.A. Martin[137], V.J. Martin[52], B. Martin dit Latour[17], L. Martinelli[75a,75b], M. Martinez[13,x], P. Martinez Agullo[169], V.I. Martinez Outschoorn[105], P. Martinez Suarez[37], S. Martin-Haugh[137], G. Martinovicova[136], V.S. Martoiu[28b], A.C. Martyniuk[98], A. Marzin[37], D. Mascione[78a,78b], L. Masetti[102], J. Masik[103], A.L. Maslennikov[39], S.L. Mason[42], P. Massarotti[72a,72b], P. Mastrandrea[74a,74b], A. Mastroberardino[44b,44a], T. Masubuchi[127], T.T. Mathew[126], J. Matousek[136], D.M. Mattern[49], J. Maurer[28b], T. Maurin[59], A.J. Maury[66], B. Maček[95], C. Mavungu Tsava[104], D.A. Maximov[38], A.E. May[103], E. Mayer[41], R. Mazini[34h], I. Maznas[118], S.M. Mazza[139], E. Mazzeo[37], J.P. Mc Gowan[171], S.P. Mc Kee[108], C.A. Mc Lean[6], C.C. McCracken[170], E.F. McDonald[107], A.E. McDougall[117], L.F. Mcelhinney[93], J.A. Mcfayden[152], R.P. McGovern[131], R.P. Mckenzie[34h], T.C. Mclachlan[48], D.J. Mclaughlin[98], S.J. McMahon[137], C.M. Mcpartland[94], R.A. McPherson[171,ab], S. Mehlhase[111], A. Mehta[94], D. Melini[169], B.R. Mellado Garcia[34h], A.H. Melo[55], F. Meloni[48], A.M. Mendes Jacques Da Costa[103], L. Meng[93], S. Menke[112], M. Mentink[37], E. Meoni[44b,44a], G. Mercado[118], S. Merianos[158], C. Merlassino[69a,69c], C. Meroni[71a,71b], J. Metcalfe[6], A.S. Mete[6], E. Meuser[102], C. Meyer[68], J-P. Meyer[138], Y. Miao[114a], R.P. Middleton[137], M. Mihovilovic[66], L. Mijović[52], G. Mikenberg[175], M. Mikestikova[134], M. Mikuž[95], H. Mildner[102], A. Milic[37], D.W. Miller[40], E.H. Miller[149], A. Milov[175], D.A. Milstead[47a,47b], T. Min[114a], A.A. Minaenko[38], I.A. Minashvili[155b], A.I. Mincer[120], B. Mindur[86a], M. Mineev[39], Y. Mino[89], L.M. Mir[13], M. Miralles Lopez[59], M. Mironova[18a], M.C. Missio[116], A. Mitra[173], V.A. Mitsou[169], Y. Mitsumori[113], O. Miu[161], P.S. Miyagawa[96], T. Mkrtchyan[63a], M. Mlinarevic[98], T. Mlinarevic[98], M. Mlynarikova[136], L. Mlynarska[86a], C. Mo[144a], S. Mobius[20], M.H. Mohamed Farook[115], S. Mohapatra[42], S. Mohiuddin[124], G. Mokgatitswane[34h], L. Moleri[175], U. Molinatti[129], L.G. Mollier[20], B. Mondal[134], S. Mondal[135], K. Mönig[48], E. Monnier[104], L. Monsonis Romero[169], J. Montejo Berlingen[13], A. Montella[47a,47b], M. Montella[122], F. Montereali[77a,77b], F. Monticelli[92], S. Monzani[69a,69c], A. Morancho Tarda[43], N. Morange[66], A.L. Moreira De Carvalho[48], M. Moreno Llácer[169], C. Moreno Martinez[56], J.M. Moreno Perez[23b], P. Morettini[57b], S. Morgenstern[37], M. Morii[61], M. Morinaga[159], M. Moritsu[90], F. Morodei[75a,75b], P. Moschovakos[37], B. Moser[54], M. Mosidze[155b],

JHEP09(2025)067

T. Moskalets[45], P. Moskvitina[116], J. Moss[32], P. Moszkowicz[86a], A. Moussa[36d], Y. Moyal[175], H. Moyano Gomez[13], E.J.W. Moyse[105], T.G. Mroz[87], O. Mtintsilana[34h], S. Muanza[104], M. Mucha[25], J. Mueller[132], R. Müller[37], G.A. Mullier[167], A.J. Mullin[33], J.J. Mullin[51], A.C. Mullins[45], A.E. Mulski[61], D.P. Mungo[161], D. Munoz Perez[169], F.J. Munoz Sanchez[103], W.J. Murray[173,137], M. Muškinja[95], C. Mwewa[48], A.G. Myagkov[38,a], A.J. Myers[8], G. Myers[108], M. Myska[135], B.P. Nachman[149], K. Nagai[129], K. Nagano[84], R. Nagasaka[159], J.L. Nagle[30,al], E. Nagy[104], A.M. Nairz[37], Y. Nakahama[84], K. Nakamura[84], K. Nakkalil[5], A. Nandi[63b], H. Nanjo[127], E.A. Narayanan[45], Y. Narukawa[159], I. Naryshkin[38], L. Nasella[71a,71b], S. Nasri[119b], C. Nass[25], G. Navarro[23a], A. Nayaz[19], P.Y. Nechaeva[38], S. Nechaeva[24b,24a], F. Nechansky[134], L. Nedic[129], T.J. Neep[21], A. Negri[73a,73b], M. Negrini[24b], C. Nellist[117], C. Nelson[106], K. Nelson[108], S. Nemecek[134], M. Nessi[37,g], M.S. Neubauer[168], J. Newell[94], P.R. Newman[21], Y.W.Y. Ng[168], B. Ngair[119a], H.D.N. Nguyen[110], J.D. Nichols[123], R.B. Nickerson[129], R. Nicolaidou[138], J. Nielsen[139], M. Niemeyer[55], J. Niermann[37], N. Nikiforou[37], V. Nikolaenko[38,a], I. Nikolic-Audit[130], P. Nilsson[30], I. Ninca[48], G. Ninio[157], A. Nisati[75a], R. Nisius[112], N. Nitika[69a,69c], J-E. Nitschke[50], E.K. Nkadimeng[34b], T. Nobe[159], D. Noll[18a], T. Nommensen[153], M.B. Norfolk[145], B.J. Norman[35], M. Noury[36a], J. Novak[95], T. Novak[95], R. Novotny[135], L. Nozka[125], K. Ntekas[165], N.M.J. Nunes De Moura Junior[83b], J. Ocariz[130], I. Ochoa[133a], S. Oerdek[48,y], J.T. Offermann[40], A. Ogrodnik[136], A. Oh[103], C.C. Ohm[150], H. Oide[84], M.L. Ojeda[37], Y. Okumura[159], L.F. Oleiro Seabra[133a], I. Oleksiyuk[56], G. Oliveira Correa[13], D. Oliveira Damazio[30], J.L. Oliver[165], R. Omar[68], Ö.O. Öncel[54], A.P. O'Neill[20], A. Onofre[133a,133e,e], P.U.E. Onyisi[11], M.J. Oreglia[40], D. Orestano[77a,77b], R. Orlandini[77a,77b], R.S. Orr[161], L.M. Osojnak[42], Y. Osumi[113], G. Otero y Garzon[31], H. Otono[90], M. Ouchrif[36d], F. Ould-Saada[128], T. Ovsiannikova[142], M. Owen[59], R.E. Owen[137], V.E. Ozcan[22a], F. Ozturk[87], N. Ozturk[8], S. Ozturk[82], H.A. Pacey[129], K. Pachal[162a], A. Pacheco Pages[13], C. Padilla Aranda[13], G. Padovano[75a,75b], S. Pagan Griso[18a], G. Palacino[68], A. Palazzo[70a,70b], J. Pampel[25], J. Pan[178], T. Pan[64a], D.K. Panchal[11], C.E. Pandini[60], J.G. Panduro Vazquez[137], H.D. Pandya[1], H. Pang[138], P. Pani[48], G. Panizzo[69a,69c], L. Panwar[130], L. Paolozzi[56], S. Parajuli[168], A. Paramonov[6], C. Paraskevopoulos[53], D. Paredes Hernandez[64b], A. Pareti[73a,73b], K.R. Park[42], T.H. Park[112], F. Parodi[57b,57a], J.A. Parsons[42], U. Parzefall[54], B. Pascual Dias[41], L. Pascual Dominguez[101], E. Pasqualucci[75a], S. Passaggio[57b], F. Pastore[97], P. Patel[87], U.M. Patel[51], J.R. Pater[103], T. Pauly[37], F. Pauwels[136], C.I. Pazos[164], M. Pedersen[128], R. Pedro[133a], S.V. Peleganchuk[38], O. Penc[134], E.A. Pender[52], S. Peng[15], G.D. Penn[178], K.E. Penski[111], M. Penzin[38], B.S. Peralva[83d], A.P. Pereira Peixoto[142], L. Pereira Sanchez[149], D.V. Perepelitsa[30,al], G. Perera[105], E. Perez Codina[37], M. Perganti[10], H. Pernegger[37], S. Perrella[75a,75b], K. Peters[48], R.F.Y. Peters[103], B.A. Petersen[37], T.C. Petersen[43], E. Petit[104], V. Petousis[135], A.R. Petri[71a,71b], C. Petridou[158,d], T. Petru[136], A. Petrukhin[147], M. Pettee[18a], A. Petukhov[82], K. Petukhova[37], R. Pezoa[140g], L. Pezzotti[24b,24a], G. Pezzullo[178], L. Pfaffenbichler[37], A.J. Pfleger[79], T.M. Pham[176], T. Pham[107], P.W. Phillips[137], G. Piacquadio[151], E. Pianori[18a], F. Piazza[126], R. Piegaia[31], D. Pietreanu[28b], A.D. Pilkington[103],

JHEP09(2025)067

M. Pinamonti[69a,69c], J.L. Pinfold[2], B.C. Pinheiro Pereira[133a], J. Pinol Bel[13], A.E. Pinto Pinoargote[130], L. Pintucci[69a,69c], K.M. Piper[152], A. Pirttikoski[56], D.A. Pizzi[35], L. Pizzimento[64b], A. Plebani[33], M.-A. Pleier[30], V. Pleskot[136], E. Plotnikova[39], G. Poddar[96], R. Poettgen[100], L. Poggioli[130], S. Polacek[136], G. Polesello[73a], A. Poley[148], A. Polini[24b], C.S. Pollard[173], Z.B. Pollock[122], E. Pompa Pacchi[123], N.I. Pond[98], D. Ponomarenko[68], L. Pontecorvo[37], S. Popa[28a], G.A. Popeneciu[28d], A. Poreba[37], D.M. Portillo Quintero[162a], S. Pospisil[135], M.A. Postill[145], P. Postolache[28c], K. Potamianos[173], P.A. Potepa[86a], I.N. Potrap[39], C.J. Potter[33], H. Potti[153], J. Poveda[169], M.E. Pozo Astigarraga[37], R. Pozzi[37], A. Prades Ibanez[76a,76b], S.R. Pradhan[145], J. Pretel[171], D. Price[103], M. Primavera[70a], L. Primomo[69a,69c], M.A. Principe Martin[101], R. Privara[125], T. Procter[86b], M.L. Proffitt[142], N. Proklova[131], K. Prokofiev[64c], G. Proto[112], J. Proudfoot[6], M. Przybycien[86a], W.W. Przygoda[86b], A. Psallidas[46], J.E. Puddefoot[145], D. Pudzha[53], H.I. Purnell[1], D. Pyatiizbyantseva[116], J. Qian[108], R. Qian[109], D. Qichen[129], Y. Qin[13], T. Qiu[52], A. Quadt[55], M. Queitsch-Maitland[103], G. Quetant[56], R.P. Quinn[170], G. Rabanal Bolanos[61], D. Rafanoharana[112], F. Raffaeli[76a,76b], F. Ragusa[71a,71b], J.L. Rainbolt[40], S. Rajagopalan[30], E. Ramakoti[39], L. Rambelli[57b,57a], I.A. Ramirez-Berend[35], K. Ran[48,114c], D.S. Rankin[131], N.P. Rapheeha[34h], H. Rasheed[28b], D.F. Rassloff[63a], A. Rastogi[18a], S. Rave[102], S. Ravera[57b,57a], B. Ravina[37], I. Ravinovich[175], M. Raymond[37], A.L. Read[128], N.P. Readioff[145], D.M. Rebuzzi[73a,73b], A.S. Reed[59], K. Reeves[27], J.A. Reidelsturz[177], D. Reikher[37], A. Rej[49], C. Rembser[37], H. Ren[62], M. Renda[28b], F. Renner[48], A.G. Rennie[59], A.L. Rescia[57b,57a], S. Resconi[71a], M. Ressegotti[57b,57a], S. Rettie[117], W.F. Rettie[35], M.M. Revering[33], E. Reynolds[18a], O.L. Rezanova[39], P. Reznicek[136], H. Riani[36d], N. Ribaric[51], B. Ricci[69a,69c], E. Ricci[78a,78b], R. Richter[112], S. Richter[47a,47b], E. Richter-Was[86b], M. Ridel[130], S. Ridouani[36d], P. Rieck[120], P. Riedler[37], E.M. Riefel[47a,47b], J.O. Rieger[117], M. Rijssenbeek[151], M. Rimoldi[37], L. Rinaldi[24b,24a], P. Rincke[167,55], G. Ripellino[167], I. Riu[13], J.C. Rivera Vergara[171], F. Rizatdinova[124], E. Rizvi[96], B.R. Roberts[18a], S.S. Roberts[139], D. Robinson[33], M. Robles Manzano[102], A. Robson[59], A. Rocchi[76a,76b], C. Roda[74a,74b], S. Rodriguez Bosca[37], Y. Rodriguez Garcia[23a], A.M. Rodríguez Vera[118], S. Roe[37], J.T. Roemer[37], O. Røhne[128], R.A. Rojas[37], C.P.A. Roland[130], A. Romaniouk[79], E. Romano[73a,73b], M. Romano[24b], A.C. Romero Hernandez[168], N. Rompotis[94], L. Roos[130], S. Rosati[75a], B.J. Rosser[40], E. Rossi[129], E. Rossi[72a,72b], L.P. Rossi[61], L. Rossini[54], R. Rosten[122], M. Rotaru[28b], B. Rottler[54], D. Rousseau[66], D. Rousso[48], S. Roy-Garand[161], A. Rozanov[104], Z.M.A. Rozario[59], Y. Rozen[156], A. Rubio Jimenez[169], V.H. Ruelas Rivera[19], T.A. Ruggeri[1], A. Ruggiero[129], A. Ruiz-Martinez[169], A. Rummler[37], Z. Rurikova[54], N.A. Rusakovich[39], S. Ruscelli[49], H.L. Russell[171], G. Russo[75a,75b], J.P. Rutherfoord[7], S. Rutherford Colmenares[33], M. Rybar[136], P. Rybczynski[86a], A. Ryzhov[45], J.A. Sabater Iglesias[56], H.F-W. Sadrozinski[139], F. Safai Tehrani[75a], S. Saha[1], M. Sahinsoy[82], B. Sahoo[175], A. Saibel[169], B.T. Saifuddin[123], M. Saimpert[138], G.T. Saito[83c], M. Saito[159], T. Saito[159], A. Sala[71a,71b], A. Salnikov[149], J. Salt[169], A. Salvador Salas[157], F. Salvatore[152], A. Salzburger[37], D. Sammel[54], E. Sampson[93], D. Sampsonidis[158,d], D. Sampsonidou[126], J. Sánchez[169], V. Sanchez Sebastian[169],

JHEP09(2025)067

H. Sandaker[128], C.O. Sander[48], J.A. Sandesara[176], M. Sandhoff[177], C. Sandoval[23b], L. Sanfilippo[63a], D.P.C. Sankey[137], T. Sano[89], A. Sansoni[53], M. Santana Queiroz[18b], L. Santi[37], C. Santoni[41], H. Santos[133a,133b], A. Santra[175], E. Sanzani[24b,24a], K.A. Saoucha[88b], J.G. Saraiva[133a,133d], J. Sardain[7], O. Sasaki[84], K. Sato[163], C. Sauer[37], E. Sauvan[4], P. Savard[161,ai], R. Sawada[159], C. Sawyer[137], L. Sawyer[99], C. Sbarra[24b], A. Sbrizzi[24b,24a], T. Scanlon[98], J. Schaarschmidt[142], U. Schäfer[102], A.C. Schaffer[66,45], D. Schaile[111], R.D. Schamberger[151], C. Scharf[19], M.M. Schefer[20], V.A. Schegelsky[38], D. Scheirich[136], M. Schernau[140f], C. Scheulen[56], C. Schiavi[57b,57a], M. Schioppa[44b,44a], B. Schlag[149], S. Schlenker[37], J. Schmeing[177], E. Schmidt[112], M.A. Schmidt[177], K. Schmieden[102], C. Schmitt[102], N. Schmitt[102], S. Schmitt[48], N.A. Schneider[111], L. Schoeffel[138], A. Schoening[63b], P.G. Scholer[35], E. Schopf[147], M. Schott[25], S. Schramm[56], T. Schroer[56], H-C. Schultz-Coulon[63a], M. Schumacher[54], B.A. Schumm[139], Ph. Schune[138], H.R. Schwartz[7], A. Schwartzman[149], T.A. Schwarz[108], Ph. Schwemling[138], R. Schwienhorst[109], F.G. Sciacca[20], A. Sciandra[30], G. Sciolla[27], F. Scuri[74a], C.D. Sebastiani[37], K. Sedlaczek[118], S.C. Seidel[115], A. Seiden[139], B.D. Seidlitz[42], C. Seitz[48], J.M. Seixas[83b], G. Sekhniaidze[72a], L. Selem[60], N. Semprini-Cesari[24b,24a], A. Semushin[179], D. Sengupta[56], V. Senthilkumar[169], L. Serin[66], M. Sessa[72a,72b], H. Severini[123], F. Sforza[57b,57a], A. Sfyrla[56], Q. Sha[14], E. Shabalina[55], H. Shaddix[118], A.H. Shah[33], R. Shaheen[150], J.D. Shahinian[131], M. Shamim[37], L.Y. Shan[14], M. Shapiro[18a], A. Sharma[37], A.S. Sharma[170], P. Sharma[30], P.B. Shatalov[38], K. Shaw[152], S.M. Shaw[103], Q. Shen[144a], D.J. Sheppard[148], P. Sherwood[98], L. Shi[98], X. Shi[14], S. Shimizu[84], C.O. Shimmin[178], I.P.J. Shipsey[129,*], S. Shirabe[90], M. Shiyakova[39,z], M.J. Shochet[40], D.R. Shope[128], B. Shrestha[123], S. Shrestha[122,an], I. Shreyber[39], M.J. Shroff[171], P. Sicho[134], A.M. Sickles[168], E. Sideras Haddad[34h,166], A.C. Sidley[117], A. Sidoti[24b], F. Siegert[50], Dj. Sijacki[16], F. Sili[92], J.M. Silva[52], I. Silva Ferreira[83b], M.V. Silva Oliveira[30], S.B. Silverstein[47a], S. Simion[66], R. Simoniello[37], E.L. Simpson[103], H. Simpson[152], L.R. Simpson[6], S. Simsek[82], S. Sindhu[55], P. Sinervo[161], S.N. Singh[27], S. Singh[30], S. Sinha[48], S. Sinha[103], M. Sioli[24b,24a], K. Sioulas[9], I. Siral[37], E. Sitnikova[48], J. Sjölin[47a,47b], A. Skaf[55], E. Skorda[21], P. Skubic[123], M. Slawinska[87], I. Slazyk[17], I. Sliusar[128], V. Smakhtin[175], B.H. Smart[137], S.Yu. Smirnov[140b], Y. Smirnov[82], L.N. Smirnova[38,a], O. Smirnova[100], A.C. Smith[42], D.R. Smith[165], J.L. Smith[103], M.B. Smith[35], R. Smith[149], H. Smitmanns[102], M. Smizanska[93], K. Smolek[135], P. Smolyanskiy[135], A.A. Snesarev[39], H.L. Snoek[117], S. Snyder[30], R. Sobie[171,ab], A. Soffer[157], C.A. Solans Sanchez[37], E.Yu. Soldatov[39], U. Soldevila[169], A.A. Solodkov[34h], S. Solomon[27], A. Soloshenko[39], K. Solovieva[54], O.V. Solovyanov[41], P. Sommer[50], A. Sonay[13], A. Sopczak[135], A.L. Sopio[52], F. Sopkova[29b], J.D. Sorenson[115], I.R. Sotarriva Alvarez[141], V. Sothilingam[63a], O.J. Soto Sandoval[140c,140b], S. Sottocornola[68], R. Soualah[88a], Z. Soumaimi[36e], D. South[48], N. Soybelman[175], S. Spagnolo[70a,70b], M. Spalla[112], D. Sperlich[54], B. Spisso[72a,72b], D.P. Spiteri[59], L. Splendori[104], M. Spousta[136], E.J. Staats[35], R. Stamen[63a], E. Stanecka[87], W. Stanek-Maslouska[48], M.V. Stange[50], B. Stanislaus[18a], M.M. Stanitzki[48], B. Stapf[48], E.A. Starchenko[38], G.H. Stark[139], J. Stark[91], P. Staroba[134], P. Starovoitov[88b], R. Staszewski[87], C. Stauch[111], G. Stavropoulos[46], A. Stefl[37], A. Stein[102], P. Steinberg[30],

JHEP09(2025)067

B. Stelzer[148,162a], H.J. Stelzer[132], O. Stelzer-Chilton[162a], H. Stenzel[58], T.J. Stevenson[152], G.A. Stewart[37], J.R. Stewart[124], G. Stoicea[28b], M. Stolarski[133a], S. Stonjek[112], A. Straessner[50], J. Strandberg[150], S. Strandberg[47a,47b], M. Stratmann[177], M. Strauss[123], T. Strebler[104], P. Strizenec[29b], R. Ströhmer[172], D.M. Strom[126], R. Stroynowski[45], A. Strubig[47a,47b], S.A. Stucci[30], B. Stugu[17], J. Stupak[123], N.A. Styles[48], D. Su[149], S. Su[62], X. Su[62], D. Suchy[29a], A.D. Sudhakar Ponnu[55], K. Sugizaki[131], V.V. Sulin[38], D.M.S. Sultan[129], L. Sultanaliyeva[25], S. Sultansoy[3b], S. Sun[176], W. Sun[14], O. Sunneborn Gudnadottir[167], N. Sur[100], M.R. Sutton[152], M. Svatos[134], P.N. Swallow[33], M. Swiatlowski[162a], T. Swirski[172], A. Swoboda[37], I. Sykora[29a], M. Sykora[136], T. Sykora[136], D. Ta[102], K. Tackmann[48,y], A. Taffard[165], R. Tafirout[162a], Y. Takubo[84], M. Talby[104], A.A. Talyshev[38], K.C. Tam[64b], N.M. Tamir[157], A. Tanaka[159], J. Tanaka[159], R. Tanaka[66], M. Tanasini[151], Z. Tao[170], S. Tapia Araya[140g], S. Tapprogge[102], A. Tarek Abouelfadl Mohamed[37], S. Tarem[156], K. Tariq[14], G. Tarna[37], G.F. Tartarelli[71a], M.J. Tartarin[91], P. Tas[136], M. Tasevsky[134], E. Tassi[44b,44a], A.C. Tate[168], Y. Tayalati[36e,aa], G.N. Taylor[107], W. Taylor[162b], R.J. Taylor Vara[169], A.S. Tegetmeier[91], P. Teixeira-Dias[97], J.J. Teoh[161], K. Terashi[159], J. Terron[101], S. Terzo[13], M. Testa[53], R.J. Teuscher[161,ab], A. Thaler[79], O. Theiner[56], T. Theveneaux-Pelzer[104], D.W. Thomas[97], J.P. Thomas[21], E.A. Thompson[18a], P.D. Thompson[21], E. Thomson[131], R.E. Thornberry[45], C. Tian[62], Y. Tian[56], V. Tikhomirov[82], Yu.A. Tikhonov[39], S. Timoshenko[38], D. Timoshyn[136], E.X.L. Ting[1], P. Tipton[178], A. Tishelman-Charny[30], K. Todome[141], S. Todorova-Nova[136], L. Toffolin[69a,69c], M. Togawa[84], J. Tojo[90], S. Tokár[29a], O. Toldaiev[68], G. Tolkachev[104], M. Tomoto[84], L. Tompkins[149,n], E. Torrence[126], H. Torres[91], D.I. Torres Arza[140g], E. Torró Pastor[169], M. Toscani[31], C. Tosciri[40], M. Tost[11], D.R. Tovey[145], T. Trefzger[172], P.M. Tricarico[13], A. Tricoli[30], I.M. Trigger[162a], S. Trincaz-Duvoid[130], D.A. Trischuk[27], A. Tropina[39], L. Truong[34c], M. Trzebinski[87], A. Trzupek[87], F. Tsai[151], M. Tsai[108], A. Tsiamis[158], P.V. Tsiareshka[39], S. Tsigaridas[162a], A. Tsirigotis[158,u], V. Tsiskaridze[155a], E.G. Tskhadadze[155a], Y. Tsujikawa[89], I.I. Tsukerman[38], V. Tsulaia[18a], S. Tsuno[84], K. Tsuri[121], D. Tsybychev[151], Y. Tu[64b], A. Tudorache[28b], V. Tudorache[28b], S.B. Tuncay[129], S. Turchikhin[57b,57a], I. Turk Cakir[3a], R. Turra[71a], T. Turtuvshin[39,ac], P.M. Tuts[42], S. Tzamarias[158,d], Y. Uematsu[84], F. Ukegawa[163], P.A. Ulloa Poblete[140c,140b], E.N. Umaka[30], G. Unal[37], A. Undrus[30], G. Unel[165], J. Urban[29b], P. Urrejola[140e], G. Usai[8], R. Ushioda[160], M. Usman[110], F. Ustuner[52], Z. Uysal[82], V. Vacek[135], B. Vachon[106], T. Vafeiadis[37], A. Vaitkus[98], C. Valderanis[111], E. Valdes Santurio[47a,47b], M. Valente[37], S. Valentinetti[24b,24a], A. Valero[169], E. Valiente Moreno[169], A. Vallier[91], J.A. Valls Ferrer[169], D.R. Van Arneman[117], A. Van Der Graaf[49], H.Z. Van Der Schyf[34h], P. Van Gemmeren[6], M. Van Rijnbach[37], S. Van Stroud[98], I. Van Vulpen[117], P. Vana[136], M. Vanadia[76a,76b], U.M. Vande Voorde[150], W. Vandelli[37], E.R. Vandewall[124], D. Vannicola[157], L. Vannoli[53], R. Vari[75a], M. Varma[178], E.W. Varnes[7], C. Varni[118], D. Varouchas[66], L. Varriale[169], K.E. Varvell[153], M.E. Vasile[28b], L. Vaslin[84], M.D. Vassilev[149], A. Vasyukov[39], L.M. Vaughan[124], R. Vavricka[136], T. Vazquez Schroeder[13], J. Veatch[32], V. Vecchio[103], M.J. Veen[105], I. Veliscek[30], I. Velkovska[95], L.M. Veloce[161], F. Veloso[133a,133c], S. Veneziano[75a], A. Ventura[70a,70b], A. Verbytskyi[112], M. Verducci[74a,74b],

JHEP09(2025)067

C. Vergis[96], M. Verissimo De Araujo[83b], W. Verkerke[117], J.C. Vermeulen[117], C. Vernieri[149], M. Vessella[165], M.C. Vetterli[148,ai], A. Vgenopoulos[102], N. Viaux Maira[140g,af], T. Vickey[145], O.E. Vickey Boeriu[145], G.H.A. Viehhauser[129], L. Vigani[63b], M. Vigl[112], M. Villa[24b,24a], M. Villaplana Perez[169], E.M. Villhauer[40], E. Vilucchi[53], M. Vincent[169], M.G. Vincter[35], A. Visibile[117], A. Visive[117], C. Vittori[37], I. Vivarelli[24b,24a], M.I. Vivas Albornoz[48], E. Voevodina[112], F. Vogel[111], J.C. Voigt[50], P. Vokac[135], Yu. Volkotrub[86b], L. Vomberg[25], E. Von Toerne[25], B. Vormwald[37], K. Vorobev[51], M. Vos[169], K. Voss[147], M. Vozak[37], L. Vozdecky[123], N. Vranjes[16], M. Vranjes Milosavljevic[16], M. Vreeswijk[117], N.K. Vu[144b,144a], R. Vuillermet[37], O. Vujinovic[102], I. Vukotic[40], I.K. Vyas[35], J.F. Wack[33], S. Wada[163], C. Wagner[149], J.M. Wagner[18a], W. Wagner[177], S. Wahdan[177], H. Wahlberg[92], C.H. Waits[123], J. Walder[137], R. Walker[111], K. Walkingshaw Pass[59], W. Walkowiak[147], A. Wall[131], E.J. Wallin[100], T. Wamorkar[18a], K. Wandall-Christensen[169], A. Wang[62], A.Z. Wang[139], C. Wang[102], C. Wang[11], H. Wang[18a], J. Wang[64c], P. Wang[103], P. Wang[98], R. Wang[61], R. Wang[6], S.M. Wang[154], S. Wang[14], T. Wang[116], T. Wang[62], W.T. Wang[129], W. Wang[14], X. Wang[168], X. Wang[144a], X. Wang[48], Y. Wang[114a], Y. Wang[62], Z. Wang[108], Z. Wang[144b], Z. Wang[108], C. Wanotayaroj[84], A. Warburton[106], A.L. Warnerbring[147], S. Waterhouse[97], A.T. Watson[21], H. Watson[52], M.F. Watson[21], E. Watton[59], G. Watts[142], B.M. Waugh[98], J.M. Webb[54], C. Weber[30], H.A. Weber[19], M.S. Weber[20], S.M. Weber[63a], C. Wei[62], Y. Wei[54], A.R. Weidberg[129], E.J. Weik[120], J. Weingarten[49], C. Weiser[54], C.J. Wells[48], T. Wenaus[30], T. Wengler[37], N.S. Wenke[112], N. Wermes[25], M. Wessels[63a], A.M. Wharton[93], A.S. White[61], A. White[8], M.J. White[1], D. Whiteson[165], L. Wickremasinghe[127], W. Wiedenmann[176], M. Wielers[137], R. Wierda[150], C. Wiglesworth[43], H.G. Wilkens[37], J.J.H. Wilkinson[33], D.M. Williams[42], H.H. Williams[131], S. Williams[33], S. Willocq[105], B.J. Wilson[103], D.J. Wilson[103], P.J. Windischhofer[40], F.I. Winkel[31], F. Winklmeier[126], B.T. Winter[54], M. Wittgen[149], M. Wobisch[99], T. Wojtkowski[60], Z. Wolffs[117], J. Wollrath[37], M.W. Wolter[87], H. Wolters[133a,133c], M.C. Wong[139], E.L. Woodward[42], S.D. Worm[48], B.K. Wosiek[87], K.W. Woźniak[87], S. Wozniewski[55], K. Wraight[59], C. Wu[161], C. Wu[21], J. Wu[159], M. Wu[114b], M. Wu[116], S.L. Wu[176], S. Wu[14,ak], X. Wu[62], Y.Q. Wu[161], Y. Wu[62], Z. Wu[4], Z. Wu[114a], J. Wuerzinger[112], T.R. Wyatt[103], B.M. Wynne[52], S. Xella[43], L. Xia[114a], M. Xia[15], M. Xie[62], A. Xiong[126], J. Xiong[18a], D. Xu[14], H. Xu[62], L. Xu[62], R. Xu[131], T. Xu[108], Y. Xu[142], Z. Xu[52], R. Xue[132], B. Yabsley[153], S. Yacoob[34a], Y. Yamaguchi[84], E. Yamashita[159], H. Yamauchi[163], T. Yamazaki[18a], Y. Yamazaki[85], S. Yan[59], Z. Yan[105], H.J. Yang[144a,144b], H.T. Yang[62], S. Yang[62], T. Yang[64c], X. Yang[37], X. Yang[14], Y. Yang[159], Y. Yang[62], W-M. Yao[18a], C.L. Yardley[152], J. Ye[14], S. Ye[30], X. Ye[62], Y. Yeh[98], I. Yeletskikh[39], B. Yeo[18b], M.R. Yexley[98], T.P. Yildirim[129], K. Yorita[174], C.J.S. Young[37], C. Young[149], N.D. Young[126], Y. Yu[62], J. Yuan[14,114c], M. Yuan[108], R. Yuan[144b,144a], L. Yue[98], M. Zaazoua[62], B. Zabinski[87], I. Zahir[36a], A. Zaio[57b,57a], Z.K. Zak[87], T. Zakareishvili[169], S. Zambito[56], J.A. Zamora Saa[140d], J. Zang[159], R. Zanzottera[71a,71b], O. Zaplatilek[135], C. Zeitnitz[177], H. Zeng[14], J.C. Zeng[168], D.T. Zenger Jr[27], O. Zenin[38], T. Ženiš[29a], S. Zenz[96], D. Zerwas[66], M. Zhai[14,114c], D.F. Zhang[145], G. Zhang[14,ak], J. Zhang[143a], J. Zhang[6], K. Zhang[14,114c], L. Zhang[62],

JHEP09(2025)067

L. Zhang[114a], P. Zhang[14,114c], R. Zhang[114a], S. Zhang[91], T. Zhang[159], Y. Zhang[142], Y. Zhang[98], Y. Zhang[62], Y. Zhang[114a], Z. Zhang[18a], Z. Zhang[143a], Z. Zhang[66], H. Zhao[142], T. Zhao[143a], Y. Zhao[35], Z. Zhao[62], Z. Zhao[62], A. Zhemchugov[39], J. Zheng[114a], K. Zheng[168], X. Zheng[62], Z. Zheng[149], D. Zhong[168], B. Zhou[108], H. Zhou[7], N. Zhou[144a], Y. Zhou[15], Y. Zhou[114a], Y. Zhou[7], C.G. Zhu[143a], J. Zhu[108], X. Zhu[144b], Y. Zhu[144a], Y. Zhu[62], X. Zhuang[14], K. Zhukov[68], N.I. Zimine[39], J. Zinsser[63b], M. Ziolkowski[147], L. Živković[16], A. Zoccoli[24b,24a], K. Zoch[61], A. Zografos[37], T.G. Zorbas[145], O. Zormpa[46], L. Zwalinski[37]

[1] *Department of Physics, University of Adelaide, Adelaide; Australia*
[2] *Department of Physics, University of Alberta, Edmonton AB; Canada*
[3] [(a)] *Department of Physics, Ankara University, Ankara;* [(b)] *Division of Physics, TOBB University of Economics and Technology, Ankara; Türkiye*
[4] *LAPP, Université Savoie Mont Blanc, CNRS/IN2P3, Annecy; France*
[5] *APC, Université Paris Cité, CNRS/IN2P3, Paris; France*
[6] *High Energy Physics Division, Argonne National Laboratory, Argonne IL; U.S.A.*
[7] *Department of Physics, University of Arizona, Tucson AZ; U.S.A.*
[8] *Department of Physics, University of Texas at Arlington, Arlington TX; U.S.A.*
[9] *Physics Department, National and Kapodistrian University of Athens, Athens; Greece*
[10] *Physics Department, National Technical University of Athens, Zografou; Greece*
[11] *Department of Physics, University of Texas at Austin, Austin TX; U.S.A.*
[12] *Institute of Physics, Azerbaijan Academy of Sciences, Baku; Azerbaijan*
[13] *Institut de Física d'Altes Energies (IFAE), Barcelona Institute of Science and Technology, Barcelona; Spain*
[14] *Institute of High Energy Physics, Chinese Academy of Sciences, Beijing; China*
[15] *Physics Department, Tsinghua University, Beijing; China*
[16] *Institute of Physics, University of Belgrade, Belgrade; Serbia*
[17] *Department for Physics and Technology, University of Bergen, Bergen; Norway*
[18] [(a)] *Physics Division, Lawrence Berkeley National Laboratory, Berkeley CA;* [(b)] *University of California, Berkeley CA; U.S.A.*
[19] *Institut für Physik, Humboldt Universität zu Berlin, Berlin; Germany*
[20] *Albert Einstein Center for Fundamental Physics and Laboratory for High Energy Physics, University of Bern, Bern; Switzerland*
[21] *School of Physics and Astronomy, University of Birmingham, Birmingham; U.K.*
[22] [(a)] *Department of Physics, Bogazici University, Istanbul;* [(b)] *Department of Physics Engineering, Gaziantep University, Gaziantep;* [(c)] *Department of Physics, Istanbul University, Istanbul; Türkiye*
[23] [(a)] *Facultad de Ciencias y Centro de Investigaciónes, Universidad Antonio Nariño, Bogotá;* [(b)] *Departamento de Física, Universidad Nacional de Colombia, Bogotá; Colombia*
[24] [(a)] *Dipartimento di Fisica e Astronomia A. Righi, Università di Bologna, Bologna;* [(b)] *INFN Sezione di Bologna; Italy*
[25] *Physikalisches Institut, Universität Bonn, Bonn; Germany*
[26] *Department of Physics, Boston University, Boston MA; U.S.A.*
[27] *Department of Physics, Brandeis University, Waltham MA; U.S.A.*
[28] [(a)] *Transilvania University of Brasov, Brasov;* [(b)] *Horia Hulubei National Institute of Physics and Nuclear Engineering, Bucharest;* [(c)] *Department of Physics, Alexandru Ioan Cuza University of Iasi, Iasi;* [(d)] *National Institute for Research and Development of Isotopic and Molecular Technologies, Physics Department, Cluj-Napoca;* [(e)] *National University of Science and Technology Politechnica, Bucharest;* [(f)] *West University in Timisoara, Timisoara;* [(g)] *Faculty of Physics, University of Bucharest, Bucharest; Romania*
[29] [(a)] *Faculty of Mathematics, Physics and Informatics, Comenius University, Bratislava;* [(b)] *Department of Subnuclear Physics, Institute of Experimental Physics of the Slovak Academy of Sciences, Kosice; Slovak Republic*
[30] *Physics Department, Brookhaven National Laboratory, Upton NY; U.S.A.*

JHEP09(2025)067

[31] Universidad de Buenos Aires, Facultad de Ciencias Exactas y Naturales, Departamento de Física, y CONICET, Instituto de Física de Buenos Aires (IFIBA), Buenos Aires; Argentina
[32] California State University, CA; U.S.A.
[33] Cavendish Laboratory, University of Cambridge, Cambridge; U.K.
[34] [(a)] Department of Physics, University of Cape Town, Cape Town;[(b)] iThemba Labs, Western Cape;[(c)] Department of Mechanical Engineering Science, University of Johannesburg, Johannesburg;[(d)] National Institute of Physics, University of the Philippines Diliman (Philippines);[(e)] Department of Physics, Stellenbosch University, Matieland;[(f)] University of South Africa, Department of Physics, Pretoria;[(g)] University of Zululand, KwaDlangezwa;[(h)] School of Physics, University of the Witwatersrand, Johannesburg; South Africa
[35] Department of Physics, Carleton University, Ottawa ON; Canada
[36] [(a)] Faculté des Sciences Ain Chock, Université Hassan II de Casablanca;[(b)] Faculté des Sciences, Université Ibn-Tofail, Kénitra;[(c)] Faculté des Sciences Semlalia, Université Cadi Ayyad, LPHEA-Marrakech;[(d)] LPMR, Faculté des Sciences, Université Mohamed Premier, Oujda;[(e)] Faculté des sciences, Université Mohammed V, Rabat;[(f)] Institute of Applied Physics, Mohammed VI Polytechnic University, Ben Guerir; Morocco
[37] CERN, Geneva; Switzerland
[38] Affiliated with an institute formerly covered by a cooperation agreement with CERN
[39] Affiliated with an international laboratory covered by a cooperation agreement with CERN
[40] Enrico Fermi Institute, University of Chicago, Chicago IL; U.S.A.
[41] LPC, Université Clermont Auvergne, CNRS/IN2P3, Clermont-Ferrand; France
[42] Nevis Laboratory, Columbia University, Irvington NY; U.S.A.
[43] Niels Bohr Institute, University of Copenhagen, Copenhagen; Denmark
[44] [(a)] Dipartimento di Fisica, Università della Calabria, Rende;[(b)] INFN Gruppo Collegato di Cosenza, Laboratori Nazionali di Frascati; Italy
[45] Physics Department, Southern Methodist University, Dallas TX; U.S.A.
[46] National Centre for Scientific Research "Demokritos", Agia Paraskevi; Greece
[47] [(a)] Department of Physics, Stockholm University;[(b)] Oskar Klein Centre, Stockholm; Sweden
[48] Deutsches Elektronen-Synchrotron DESY, Hamburg and Zeuthen; Germany
[49] Fakultät Physik , Technische Universität Dortmund, Dortmund; Germany
[50] Institut für Kern- und Teilchenphysik, Technische Universität Dresden, Dresden; Germany
[51] Department of Physics, Duke University, Durham NC; U.S.A.
[52] SUPA - School of Physics and Astronomy, University of Edinburgh, Edinburgh; U.K.
[53] INFN e Laboratori Nazionali di Frascati, Frascati; Italy
[54] Physikalisches Institut, Albert-Ludwigs-Universität Freiburg, Freiburg; Germany
[55] II. Physikalisches Institut, Georg-August-Universität Göttingen, Göttingen; Germany
[56] Département de Physique Nucléaire et Corpusculaire, Université de Genève, Genève; Switzerland
[57] [(a)] Dipartimento di Fisica, Università di Genova, Genova;[(b)] INFN Sezione di Genova; Italy
[58] II. Physikalisches Institut, Justus-Liebig-Universität Giessen, Giessen; Germany
[59] SUPA - School of Physics and Astronomy, University of Glasgow, Glasgow; U.K.
[60] LPSC, Université Grenoble Alpes, CNRS/IN2P3, Grenoble INP, Grenoble; France
[61] Laboratory for Particle Physics and Cosmology, Harvard University, Cambridge MA; U.S.A.
[62] Department of Modern Physics and State Key Laboratory of Particle Detection and Electronics, University of Science and Technology of China, Hefei; China
[63] [(a)] Kirchhoff-Institut für Physik, Ruprecht-Karls-Universität Heidelberg, Heidelberg;[(b)] Physikalisches Institut, Ruprecht-Karls-Universität Heidelberg, Heidelberg; Germany
[64] [(a)] Department of Physics, Chinese University of Hong Kong, Shatin, N.T., Hong Kong;[(b)] Department of Physics, University of Hong Kong, Hong Kong;[(c)] Department of Physics and Institute for Advanced Study, Hong Kong University of Science and Technology, Clear Water Bay, Kowloon, Hong Kong; China
[65] Department of Physics, National Tsing Hua University, Hsinchu; Taiwan
[66] IJCLab, Université Paris-Saclay, CNRS/IN2P3, 91405, Orsay; France
[67] Centro Nacional de Microelectrónica (IMB-CNM-CSIC), Barcelona; Spain
[68] Department of Physics, Indiana University, Bloomington IN; U.S.A.
[69] [(a)] INFN Gruppo Collegato di Udine, Sezione di Trieste, Udine;[(b)] ICTP, Trieste;[(c)] Dipartimento

JHEP09(2025)067

Politecnico di Ingegneria e Architettura, Università di Udine, Udine; Italy
[70] [(a)] *INFN Sezione di Lecce;* [(b)] *Dipartimento di Matematica e Fisica, Università del Salento, Lecce; Italy*
[71] [(a)] *INFN Sezione di Milano;* [(b)] *Dipartimento di Fisica, Università di Milano, Milano; Italy*
[72] [(a)] *INFN Sezione di Napoli;* [(b)] *Dipartimento di Fisica, Università di Napoli, Napoli; Italy*
[73] [(a)] *INFN Sezione di Pavia;* [(b)] *Dipartimento di Fisica, Università di Pavia, Pavia; Italy*
[74] [(a)] *INFN Sezione di Pisa;* [(b)] *Dipartimento di Fisica E. Fermi, Università di Pisa, Pisa; Italy*
[75] [(a)] *INFN Sezione di Roma;* [(b)] *Dipartimento di Fisica, Sapienza Università di Roma, Roma; Italy*
[76] [(a)] *INFN Sezione di Roma Tor Vergata;* [(b)] *Dipartimento di Fisica, Università di Roma Tor Vergata, Roma; Italy*
[77] [(a)] *INFN Sezione di Roma Tre;* [(b)] *Dipartimento di Matematica e Fisica, Università Roma Tre, Roma; Italy*
[78] [(a)] *INFN-TIFPA;* [(b)] *Università degli Studi di Trento, Trento; Italy*
[79] *Universität Innsbruck, Department of Astro and Particle Physics, Innsbruck; Austria*
[80] *University of Iowa, Iowa City IA; U.S.A.*
[81] *Department of Physics and Astronomy, Iowa State University, Ames IA; U.S.A.*
[82] *Istinye University, Sariyer, Istanbul; Türkiye*
[83] [(a)] *Departamento de Engenharia Elétrica, Universidade Federal de Juiz de Fora (UFJF), Juiz de Fora;* [(b)] *Universidade Federal do Rio De Janeiro COPPE/EE/IF, Rio de Janeiro;* [(c)] *Instituto de Física, Universidade de São Paulo, São Paulo;* [(d)] *Rio de Janeiro State University, Rio de Janeiro;* [(e)] *Federal University of Bahia, Bahia; Brazil*
[84] *KEK, High Energy Accelerator Research Organization, Tsukuba; Japan*
[85] *Graduate School of Science, Kobe University, Kobe; Japan*
[86] [(a)] *AGH University of Krakow, Faculty of Physics and Applied Computer Science, Krakow;* [(b)] *Marian Smoluchowski Institute of Physics, Jagiellonian University, Krakow; Poland*
[87] *Institute of Nuclear Physics Polish Academy of Sciences, Krakow; Poland*
[88] [(a)] *Khalifa University of Science and Technology, Abu Dhabi;* [(b)] *University of Sharjah, Sharjah; United Arab Emirates*
[89] *Faculty of Science, Kyoto University, Kyoto; Japan*
[90] *Research Center for Advanced Particle Physics and Department of Physics, Kyushu University, Fukuoka; Japan*
[91] *L2IT, Université de Toulouse, CNRS/IN2P3, UPS, Toulouse; France*
[92] *Instituto de Física La Plata, Universidad Nacional de La Plata and CONICET, La Plata; Argentina*
[93] *Physics Department, Lancaster University, Lancaster; U.K.*
[94] *Oliver Lodge Laboratory, University of Liverpool, Liverpool; U.K.*
[95] *Department of Experimental Particle Physics, Jožef Stefan Institute and Department of Physics, University of Ljubljana, Ljubljana; Slovenia*
[96] *Department of Physics and Astronomy, Queen Mary University of London, London; U.K.*
[97] *Department of Physics, Royal Holloway University of London, Egham; U.K.*
[98] *Department of Physics and Astronomy, University College London, London; U.K.*
[99] *Louisiana Tech University, Ruston LA; U.S.A.*
[100] *Fysiska institutionen, Lunds universitet, Lund; Sweden*
[101] *Departamento de Física Teorica C-15 and CIAFF, Universidad Autónoma de Madrid, Madrid; Spain*
[102] *Institut für Physik, Universität Mainz, Mainz; Germany*
[103] *School of Physics and Astronomy, University of Manchester, Manchester; U.K.*
[104] *CPPM, Aix-Marseille Université, CNRS/IN2P3, Marseille; France*
[105] *Department of Physics, University of Massachusetts, Amherst MA; U.S.A.*
[106] *Department of Physics, McGill University, Montreal QC; Canada*
[107] *School of Physics, University of Melbourne, Victoria; Australia*
[108] *Department of Physics, University of Michigan, Ann Arbor MI; U.S.A.*
[109] *Department of Physics and Astronomy, Michigan State University, East Lansing MI; U.S.A.*
[110] *Group of Particle Physics, University of Montreal, Montreal QC; Canada*
[111] *Fakultät für Physik, Ludwig-Maximilians-Universität München, München; Germany*
[112] *Max-Planck-Institut für Physik (Werner-Heisenberg-Institut), München; Germany*
[113] *Graduate School of Science and Kobayashi-Maskawa Institute, Nagoya University, Nagoya; Japan*

JHEP09(2025)067

[114] [(a)] Department of Physics, Nanjing University, Nanjing; [(b)] School of Science, Shenzhen Campus of Sun Yat-sen University; [(c)] University of Chinese Academy of Science (UCAS), Beijing; China
[115] Department of Physics and Astronomy, University of New Mexico, Albuquerque NM; U.S.A.
[116] Institute for Mathematics, Astrophysics and Particle Physics, Radboud University/Nikhef, Nijmegen; Netherlands
[117] Nikhef National Institute for Subatomic Physics and University of Amsterdam, Amsterdam; Netherlands
[118] Department of Physics, Northern Illinois University, DeKalb IL; U.S.A.
[119] [(a)] New York University Abu Dhabi, Abu Dhabi; [(b)] United Arab Emirates University, Al Ain; United Arab Emirates
[120] Department of Physics, New York University, New York NY; U.S.A.
[121] Ochanomizu University, Otsuka, Bunkyo-ku, Tokyo; Japan
[122] Ohio State University, Columbus OH; U.S.A.
[123] Homer L. Dodge Department of Physics and Astronomy, University of Oklahoma, Norman OK; U.S.A.
[124] Department of Physics, Oklahoma State University, Stillwater OK; U.S.A.
[125] Palacký University, Joint Laboratory of Optics, Olomouc; Czech Republic
[126] Institute for Fundamental Science, University of Oregon, Eugene, OR; U.S.A.
[127] Graduate School of Science, University of Osaka, Osaka; Japan
[128] Department of Physics, University of Oslo, Oslo; Norway
[129] Department of Physics, Oxford University, Oxford; U.K.
[130] LPNHE, Sorbonne Université, Université Paris Cité, CNRS/IN2P3, Paris; France
[131] Department of Physics, University of Pennsylvania, Philadelphia PA; U.S.A.
[132] Department of Physics and Astronomy, University of Pittsburgh, Pittsburgh PA; U.S.A.
[133] [(a)] Laboratório de Instrumentação e Física Experimental de Partículas - LIP, Lisboa; [(b)] Departamento de Física, Faculdade de Ciências, Universidade de Lisboa, Lisboa; [(c)] Departamento de Física, Universidade de Coimbra, Coimbra; [(d)] Centro de Física Nuclear da Universidade de Lisboa, Lisboa; [(e)] Departamento de Física, Escola de Ciências, Universidade do Minho, Braga; [(f)] Departamento de Física Teórica y del Cosmos, Universidad de Granada, Granada (Spain); [(g)] Departamento de Física, Instituto Superior Técnico, Universidade de Lisboa, Lisboa; Portugal
[134] Institute of Physics of the Czech Academy of Sciences, Prague; Czech Republic
[135] Czech Technical University in Prague, Prague; Czech Republic
[136] Charles University, Faculty of Mathematics and Physics, Prague; Czech Republic
[137] Particle Physics Department, Rutherford Appleton Laboratory, Didcot; U.K.
[138] IRFU, CEA, Université Paris-Saclay, Gif-sur-Yvette; France
[139] Santa Cruz Institute for Particle Physics, University of California Santa Cruz, Santa Cruz CA; U.S.A.
[140] [(a)] Departamento de Física, Pontificia Universidad Católica de Chile, Santiago; [(b)] Millennium Institute for Subatomic physics at high energy frontier (SAPHIR), Santiago; [(c)] Instituto de Investigación Multidisciplinario en Ciencia y Tecnología, y Departamento de Física, Universidad de La Serena; [(d)] Universidad Andres Bello, Department of Physics, Santiago; [(e)] Universidad San Sebastian, Recoleta; [(f)] Instituto de Alta Investigación, Universidad de Tarapacá, Arica; [(g)] Departamento de Física, Universidad Técnica Federico Santa María, Valparaíso; Chile
[141] Department of Physics, Institute of Science, Tokyo; Japan
[142] Department of Physics, University of Washington, Seattle WA; U.S.A.
[143] [(a)] Institute of Frontier and Interdisciplinary Science and Key Laboratory of Particle Physics and Particle Irradiation (MOE), Shandong University, Qingdao; [(b)] School of Physics, Zhengzhou University; China
[144] [(a)] State Key Laboratory of Dark Matter Physics, School of Physics and Astronomy, Shanghai Jiao Tong University, Key Laboratory for Particle Astrophysics and Cosmology (MOE), SKLPPC, Shanghai; [(b)] State Key Laboratory of Dark Matter Physics, Tsung-Dao Lee Institute, Shanghai Jiao Tong University, Shanghai; China
[145] Department of Physics and Astronomy, University of Sheffield, Sheffield; U.K.
[146] Department of Physics, Shinshu University, Nagano; Japan
[147] Department Physik, Universität Siegen, Siegen; Germany
[148] Department of Physics, Simon Fraser University, Burnaby BC; Canada
[149] SLAC National Accelerator Laboratory, Stanford CA; U.S.A.

JHEP09(2025)067

[150] Department of Physics, Royal Institute of Technology, Stockholm; Sweden
[151] Departments of Physics and Astronomy, Stony Brook University, Stony Brook NY; U.S.A.
[152] Department of Physics and Astronomy, University of Sussex, Brighton; U.K.
[153] School of Physics, University of Sydney, Sydney; Australia
[154] Institute of Physics, Academia Sinica, Taipei; Taiwan
[155] [(a)] E. Andronikashvili Institute of Physics, Iv. Javakhishvili Tbilisi State University, Tbilisi;[(b)] High Energy Physics Institute, Tbilisi State University, Tbilisi;[(c)] University of Georgia, Tbilisi; Georgia
[156] Department of Physics, Technion, Israel Institute of Technology, Haifa; Israel
[157] Raymond and Beverly Sackler School of Physics and Astronomy, Tel Aviv University, Tel Aviv; Israel
[158] Department of Physics, Aristotle University of Thessaloniki, Thessaloniki; Greece
[159] International Center for Elementary Particle Physics and Department of Physics, University of Tokyo, Tokyo; Japan
[160] Graduate School of Science and Technology, Tokyo Metropolitan University, Tokyo; Japan
[161] Department of Physics, University of Toronto, Toronto ON; Canada
[162] [(a)] TRIUMF, Vancouver BC;[(b)] Department of Physics and Astronomy, York University, Toronto ON; Canada
[163] Division of Physics and Tomonaga Center for the History of the Universe, Faculty of Pure and Applied Sciences, University of Tsukuba, Tsukuba; Japan
[164] Department of Physics and Astronomy, Tufts University, Medford MA; U.S.A.
[165] Department of Physics and Astronomy, University of California Irvine, Irvine CA; U.S.A.
[166] University of West Attica, Athens; Greece
[167] Department of Physics and Astronomy, University of Uppsala, Uppsala; Sweden
[168] Department of Physics, University of Illinois, Urbana IL; U.S.A.
[169] Instituto de Física Corpuscular (IFIC), Centro Mixto Universidad de Valencia - CSIC, Valencia; Spain
[170] Department of Physics, University of British Columbia, Vancouver BC; Canada
[171] Department of Physics and Astronomy, University of Victoria, Victoria BC; Canada
[172] Fakultät für Physik und Astronomie, Julius-Maximilians-Universität Würzburg, Würzburg; Germany
[173] Department of Physics, University of Warwick, Coventry; U.K.
[174] Waseda University, Tokyo; Japan
[175] Department of Particle Physics and Astrophysics, Weizmann Institute of Science, Rehovot; Israel
[176] Department of Physics, University of Wisconsin, Madison WI; U.S.A.
[177] Fakultät für Mathematik und Naturwissenschaften, Fachgruppe Physik, Bergische Universität Wuppertal, Wuppertal; Germany
[178] Department of Physics, Yale University, New Haven CT; U.S.A.
[179] Yerevan Physics Institute, Yerevan; Armenia

[a] Also at Affiliated with an institute formerly covered by a cooperation agreement with CERN
[b] Also at An-Najah National University, Nablus; Palestine
[c] Also at Borough of Manhattan Community College, City University of New York, New York NY; U.S.A.
[d] Also at Center for Interdisciplinary Research and Innovation (CIRI-AUTH), Thessaloniki; Greece
[e] Also at Centre of Physics of the Universities of Minho and Porto (CF-UM-UP); Portugal
[f] Also at CERN, Geneva; Switzerland
[g] Also at Département de Physique Nucléaire et Corpusculaire, Université de Genève, Genève; Switzerland
[h] Also at Departament de Fisica de la Universitat Autonoma de Barcelona, Barcelona; Spain
[i] Also at Department of Financial and Management Engineering, University of the Aegean, Chios; Greece
[j] Also at Department of Mathematical Sciences, University of South Africa, Johannesburg; South Africa
[k] Also at Department of Modern Physics and State Key Laboratory of Particle Detection and Electronics, University of Science and Technology of China, Hefei; China
[l] Also at Department of Physics, Bolu Abant Izzet Baysal University, Bolu; Türkiye
[m] Also at Department of Physics, King's College London, London; U.K.
[n] Also at Department of Physics, Stanford University, Stanford CA; U.S.A.
[o] Also at Department of Physics, Stellenbosch University; South Africa
[p] Also at Department of Physics, University of Fribourg, Fribourg; Switzerland
[q] Also at Department of Physics, University of Thessaly; Greece

JHEP09(2025)067

[r] Also at Department of Physics, Westmont College, Santa Barbara; U.S.A.
[s] Also at Faculty of Physics, Sofia University, 'St. Kliment Ohridski', Sofia; Bulgaria
[t] Also at Faculty of Physics, University of Bucharest; Romania
[u] Also at Hellenic Open University, Patras; Greece
[v] Also at Henan University; China
[w] Also at Imam Mohammad Ibn Saud Islamic University; Saudi Arabia
[x] Also at Institucio Catalana de Recerca i Estudis Avancats, ICREA, Barcelona; Spain
[y] Also at Institut für Experimentalphysik, Universität Hamburg, Hamburg; Germany
[z] Also at Institute for Nuclear Research and Nuclear Energy (INRNE) of the Bulgarian Academy of Sciences, Sofia; Bulgaria
[aa] Also at Institute of Applied Physics, Mohammed VI Polytechnic University, Ben Guerir; Morocco
[ab] Also at Institute of Particle Physics (IPP); Canada
[ac] Also at Institute of Physics and Technology, Mongolian Academy of Sciences, Ulaanbaatar; Mongolia
[ad] Also at Institute of Physics, Azerbaijan Academy of Sciences, Baku; Azerbaijan
[ae] Also at Institute of Theoretical Physics, Ilia State University, Tbilisi; Georgia
[af] Also at Millennium Institute for Subatomic physics at high energy frontier (SAPHIR), Santiago; Chile
[ag] Also at National Institute of Physics, University of the Philippines Diliman (Philippines); Philippines
[ah] Also at The Collaborative Innovation Center of Quantum Matter (CICQM), Beijing; China
[ai] Also at TRIUMF, Vancouver BC; Canada
[aj] Also at Università di Napoli Parthenope, Napoli; Italy
[ak] Also at University of Chinese Academy of Sciences (UCAS), Beijing; China
[al] Also at University of Colorado Boulder, Department of Physics, Colorado; U.S.A.
[am] Also at University of Sienna; Italy
[an] Also at Washington College, Chestertown, MD; U.S.A.
[ao] Also at Yeditepe University, Physics Department, Istanbul; Türkiye
[*] Deceased

JHEP09(2025)067